

Contents lists available at ScienceDirect

# Acta Materialia

journal homepage: www.elsevier.com/locate/actamat



Full length article

# A simple yet general model of binary diffusion coefficients emerged from a comprehensive assessment of 18 binary systems



Wei Zhong<sup>a</sup>, Qiaofu Zhang<sup>b</sup>, Ji-Cheng Zhao<sup>a,\*</sup>

- <sup>a</sup> Department of Materials Science and Engineering, University of Maryland, 4418 Stadium Drive, College Park, Maryland 20742 USA
- <sup>b</sup> QuesTek Innovations LLC, 1820 Ridge Avenue, Evanston, Illinois 60201 USA

#### ARTICLE INFO

Article history: Received 10 March 2021 Revised 3 June 2021 Accepted 7 June 2021 Available online 12 June 2021

Keywords: Interdiffusion coefficient Tracer diffusion coefficient Intrinsic diffusion coefficient Diffusion model Atomic mobility CALPHAD

#### ABSTRACT

This study is the most comprehensive test to date aiming at defining the optimal number of fitting parameters for a reliable mathematical description of the diffusion behavior of a binary solid solution. Our systematic test of 18 diverse binary systems has yielded a surprisingly simple model with only one fitting parameter/constant which can be evaluated from experimental diffusion data. The rest of the quantities in the model are the self-diffusion and impurity (dilute) diffusion coefficients of the *pure elements* and the thermodynamic factor which can be computed from a CALPHAD thermodynamic assessment of the pertinent binary system. The 1-parameter Z-Z-Z model has been demonstrated to be very reliable and robust since the 18 binary systems tested in this study include very asymmetrical systems such as Co-Pd and Fe-Pd as well as Nb-Ti whose experimental diffusion coefficient data cover ~9 orders of magnitude and over a temperature range spanning ~1200°C (from ~800°C to ~2000°C). The Z-Z-Z model allows both tracer and intrinsic diffusion coefficients to be reliably computed for any composition at any temperature after the sole constant is evaluated from the interdiffusion or all experimental diffusion data. Extension of such a simple and robust model from binary to ternary and higher order systems will lead to a substantial reduction of fitting parameters and an enhancement of the reliability of future multicomponent diffusion (atomic mobility) databases for simulation of kinetic processes in materials.

 $\ensuremath{\mathbb{C}}$  2021 Acta Materialia Inc. Published by Elsevier Ltd. All rights reserved.

### 1. Introduction

Diffusion coefficients are essential materials data to understand and simulate kinetic behaviors in materials such as precipitate growth and creep deformation as well as materials processing such as casting/solidification, homogenization, and surface modification. Mathematical models are required to describe diffusion coefficients as a function of composition and temperature, either within the CALPHAD (CALculation of PHAse Diagrams) framework [1–6] or being used directly in various modeling studies outside the CALPHAD approach. Ågren and Andersson have systematically established such models of the diffusion coefficients in binary and multicomponent systems by systematizing the framework of atomic mobilities [7,8]. Their models are widely adopted by the CALPHAD community and the fitting parameters in their semi-empricial models are evaluated from experimental diffusion coefficients and computed data when reliable experimental values are not available.

Four fitting parameters are often employed to model the diffusion coefficients of a binary solid solution (e.g., fcc, bcc or hcp); i.e., two parameters (a + bT) for each diffusing element for each phase. Up to 6 and 8 fitting parameters are used for many binary systems. Questions remain to date: (1) do we really need four fitting parameters for each binary solid solution and are we over-fitting? and (2) what is the optimal number of fitting parameters? We set out to answer these questions by performing the most comprehensive test of the number of fitting parameters of diffusion coefficient models for binary systems. Ascribing to the Occam's Razor-that the simplest solution/explanation is most likely the right one, we posited that such a systematic test might yield simpler and more robust binary diffusion models with the fewest fitting parameters to avoid overfitting, which will further contribute to more robust models for ternary and multicomponent systems. This article reports the insights gained from our comprehensive model test of diffusion coefficients in 18 binary systems. A surprisingly simple yet general model has emerged from this study which will substantially simplify future assessments of diffusion coefficients and atomic mobilities.

E-mail address: jczhao@umd.edu (J.-C. Zhao).

<sup>\*</sup> Corresponding author.

# 2. Methodology

There are various types of phenomenological diffusion coefficients which can be measured under different experimental settings [9]. Self-diffusion coefficient and impurity (dilute) diffusion coefficient are measured for pure elements. Their temperature dependence can generally be represented by the Arrhenius Eq. (1) or (2):

$$D_i^j = D_{0_i}^{\ j} \exp\left(-\frac{Q_i^j}{RT}\right) \tag{1}$$

$$\ln D_i^j = -\frac{Q_i^j}{RT} + \ln D_{0i}^j \tag{2}$$

Where R is the gas constant, T is the absolute temperature,  $D_0^j$  is the pre-exponential factor and  $Q_i^j$  is the activation energy for element i diffusion in element j.  $D_i^j$  denotes self-diffusion coefficient when i=j and represents impurity diffusion coefficient of i in j when  $i\neq j$ . In addition to the above temperature dependency, tracer, intrinsic and interdiffusion (chemical diffusion) coefficients are also composition dependent. Darken's equations relate these three types of diffusion coefficients of a binary A-B system [10]:

$$D_A^I = D_A^* \varphi, \quad D_B^I = D_B^* \varphi \tag{3}$$

$$\tilde{D} = x_B D_A^I + x_A D_B^I = (x_B D_A^* + x_A D_B^*) \varphi \tag{4}$$

Where  $D_i^*$  represents tracer diffusion coefficient of i (A or B),  $D_i^I$  denotes intrinsic diffusion coefficient of i, and  $\tilde{D}$  is the interdiffusion coefficient.  $x_A$  and  $x_B$  are the mole fractions of elements A and B, respectively.  $\varphi$  is the thermodynamic factor which can be easily computed using CALPHAD software and associated thermodynamic databases/assessments and is defined in a binary system as:

$$\varphi = 1 + \frac{d \ln \gamma_i}{d \ln x_i} = \frac{x_i}{RT} \frac{d\mu_i}{dx_i} = \frac{x_A x_B}{RT} \frac{d^2 G}{dx_R^2}$$
 (5)

Where  $\gamma_i$  is the activity coefficient and  $\mu_i$  is the chemical potential of element i in the alloy. G is the molar Gibbs free energy. The thermodynamic factor is the same for both elements of a binary system due to the Gibbs-Duhem relation. The Darken's equations are an approximation which assumes the vacancy wind factor to be unity. Nevertheless, they are found to be a good approximation through years of assessments and applications in numerous systems. The composition-dependent molar volume can be taken into account in this framework using a more sophisticated treatment [8,11], but its effect is ignored in the current analysis similar to most CALPHAD atomic mobility assessments.

Based on Darken's Eq. (4), the tracer diffusion coefficient of element A (e.g., Fe) becomes either the self-diffusion coefficient of A when the concentration of B (e.g., Ni) approaches 0, or the impurity diffusion coefficient of A in B when the concentration of B reaches 100% in the binary A-B system; and the same holds for the tracer diffusion coefficient of B, as shown in Fig. 1 using the fcc phase of the Fe-Ni system as an example. Therefore, reliable self-diffusion coefficients and impurity diffusion coefficients, as shown on both sides of Fig. 1, are the essential foundation upon which the binary diffusion models can be built. These data serve as a check for the diffusion coefficients measured across the composition – agreement on both sides with the independently measured self-diffusion and impurity diffusion coefficients (often via reliable tracer experiments) is testament for reliability.

It is noted that tracer diffusion coefficients serve as a bridge relating all the other types of diffusion coefficients, as explained above, and as shown in Fig. 1. Hence, modeling tracer diffusion

coefficients is fundamental, and other types of diffusion coefficients can then be computed using Darken's equations. A straightforward model of a binary A-B solid solution, based on the Ågren-Andersson treatment, describes the composition and temperature dependence of tracer diffusion coefficients as:

$$\ln D_i^* = x_A \ln D_i^A + x_B \ln D_i^B + x_A x_B \sum_{r=0.1...} \Phi_i^{A,B} (x_A - x_B)^r / RT$$
 (6)

Where i=A or B. The first two terms on the right side of Eq. (6) are the linear combinations of self-diffusion and impurity diffusion coefficients of the pure elements (A and B) in the composition space while the third term is a Redlich-Kister polynomial [12] that models the non-linear (non-ideal) contributions through the binary interaction parameters,  ${}^{r}\Phi_{i}{}^{A,B}$ . Considering only the zeroth-order interaction r=0, the above equation is simplified into Eq. (7) or (8):

$$\ln D_i^* = x_A \ln D_i^A + x_B \ln D_i^B + \Phi_i^{A,B} x_A x_B / RT \tag{7}$$

$$D_i^* = \exp\left(x_A \ln D_i^A + x_B \ln D_i^B\right) \exp\left(\Phi_i^{A,B} x_A x_B / RT\right) \tag{8}$$

The interaction parameter  $\Phi_i^{A,B}=a_i+b_iT$  with  $a_i$  and  $b_i$  being constants  $(i=A\ or\ B)$ .  $\Phi_i^{A,B}$  is the same as the interaction parameters in the atomic mobility notation according to the Einstein relation  $D_i^*=RTM_i$ , where  $M_i$  is the atomic mobility of i. As a matter of fact, one can multiply both sides of Eqs. (6) and (7) with RT to convert them into the atomic mobility notation that is widely used by the CALPHAD community since the atomic mobility parameter  $\Phi_i=RT\ \ln(RTM_i)=RT\ \ln D_i^*$ . The intrinsic and interdiffusion coefficients can then be derived from tracer diffusion coefficients using Darken's Eqs. (3) and (4) with the thermodynamic factor  $\varphi$  computed using CALPHAD software and thermodynamic databases/assessments.

We set out to perform the most comprehensive test of the binary diffusion models described in Eq. (7) or (8) to determine the optimal number of fitting parameters (from 0 to 4) as listed in Table 1. Completely/mutually soluble binary systems are the best test grounds since they provide the widest composition range (from 0% to 100%) to test the models. Moreover, since the crystal structure is the same for both elements in a completely soluble system at the temperature range of mutual solubility, the impurity diffusion coefficients are much more likely measured and available for the model assessment. In contrast, non-mutually soluble system such as Al-Mg would require the impurity and self-diffusion data of hypothetical (metastable) fcc Mg or hcp Al, which adds uncertainty to the model testing.

After an exhaustive search of the literature, including going through diffusion data compilations such as Landolt-Bornstein [9], Smithells [13], and Neumann and Tuijin [14], we found 18 mutually-soluble binary systems whose self-diffusion and impurity diffusion coefficients of pure elements are reliable and there are sufficient interdiffusion coefficients and tracer (and/or intrinsic) diffusion coefficients across the compositions for a reliable model assessment/test. The 18 binary systems are briefly summarized in Fig. 2, including 11 binary systems with the fcc crystal structure (Ag-Au, Au-Cu, Au-Ni, Co-Fe, Co-Ni, Co-Pd, Cu-Ni, Cu-Pt, Fe-Ni, Fe-Pd, and Ni-Pd), 6 bcc systems (Nb-Ti, Nb-V, Nb-Zr, Ta-Ti, Ti-V, and Ti-Zr), and 1 diamond cubic system (Ge-Si). We did not find any binary hcp systems that satisfy the requirements of having high quality data of both the self-diffusion and impurity diffusion coefficients of the pure elements as well as reliable interdiffusion coefficients and tracer diffusion coefficients across the composition range. Nevertheless, it is our belief that the conclusions drawn from our comprehensive assessment will be equally applicable to hcp systems as well.

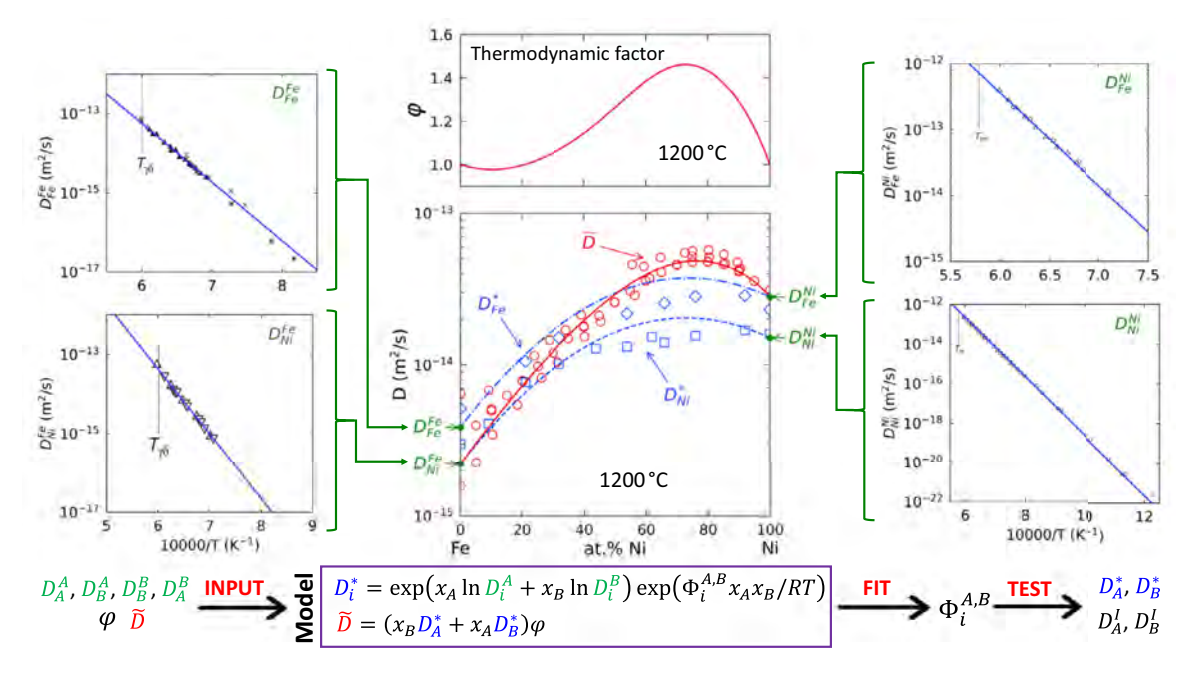
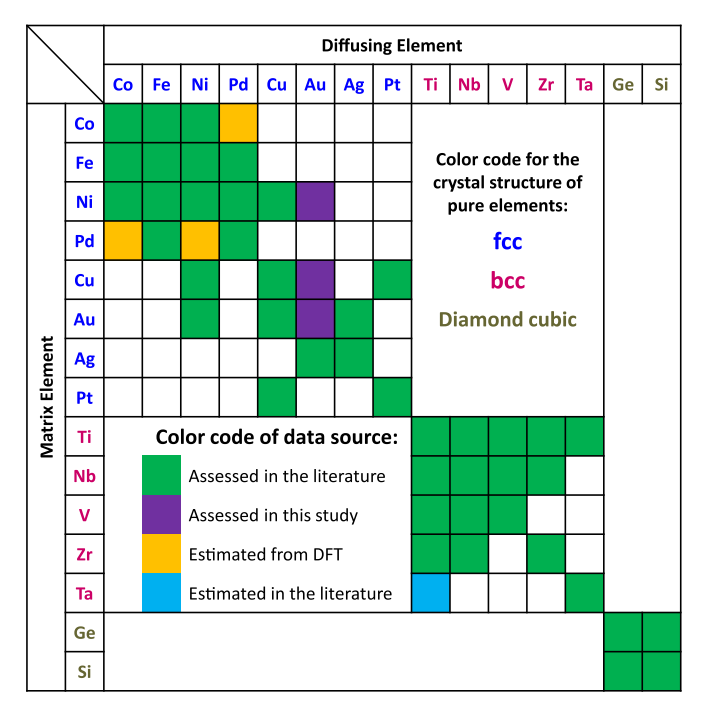


Fig. 1. Diffusion coefficients and thermodynamic factor of the fcc phase of the Fe-Ni binary system (The plots in the center are for 1200°C only).

 Table 1

 Fitting parameters (constants) in the diffusion models explored in this study.

Model	Interaction term of element A	Interaction term of element B
0-parameter model 1-parameter model 2-parameter model 4-parameter model	$\Phi_{A,B}^{A,B} = 0$ $\Phi_{A,B}^{A,B} = a$ $\Phi_{A,B}^{A,B} = a_A$ $\Phi_{A,B}^{A,B} = a_A + b_A T$	$\Phi_{B}^{A,B} = 0$ $\Phi_{B}^{A,B} = a$ $\Phi_{B}^{A,B} = a_{B}$ $\Phi_{B}^{A,B} = a_{B} + b_{B}T$



**Fig. 2.** Summary of assessments of the self-diffusion and impurity diffusion coefficients of pure elements in the 18 binary systems.

The self-diffusion and impurity diffusion coefficients  $D_i^j$  are evaluated first to determine the parameters  $D_0^j$  and  $Q_i^j$ . The

interaction terms  $\Phi_i^{A,B} = a_i + b_i T$  were then evaluated from the composition-dependent interdiffusion coefficients. The interdiffusion coefficients, most often obtained from diffusion couple experiments (e.g. [15]), are employed to optimize different numbers of interaction parameters listed in Table 1 while the tracer and intrinsic diffusion coefficients are used to test the model performance. The objective of the optimization/fitting is to find optimal coefficients of  $\Phi_i^{A,B}$  that minimize the objective function:

$$F = \frac{1}{2} \sum_{i=1}^{n} \left( \ln D_i^{\text{pred}} - \ln D_i^{\text{exp}} \right)^2$$
 (9)

Where n is the number of input data points,  $D_i^{exp}$  and  $D_i^{pred}$  are the experimental diffusion coefficients and predicted diffusion coefficients of the ith data point, respectively. A Python program was coded to perform the whole parameter-optimization and test processes. It is noted that both tracer diffusion coefficients and intrinsic diffusion coefficients were not used to fit the parameters, they are used only for model test/validation. The datasets are separately employed in this manner to investigate whether a diffusion model can be developed only with reliable interdiffusion coefficients as input since they are the most common type of composition-dependent data reported in the literature. The model test process is also summarized at the bottom of Fig. 1. The results of this study are described in the ensuing sections.

# 3. Results and discussion

# 3.1. Self-diffusion and impurity diffusion coefficients

The self-diffusion and impurity diffusion coefficients  $D_i^j$  of the 18 binary systems are mostly evaluated from experimental data

while some of them are determined from first-principles calculations when experimental data are not available, as shown in Fig. 2. For simplicity, most of the optimized  $D_{0i}^{j}$  and  $Q_{i}^{j}$  are taken from the mobility assessments in the literature or the handbook of Neumann and Tuijin [14], depending on which source better reproduces all the available experimental data.  $D_{Au}^{Au}$ ,  $D_{Au}^{Cu}$  and  $D_{Au}^{Ni}$  are reevaluated in this study, while  $D_{Co}^{Pd}$ ,  $D_{Ni}^{Pd}$  and  $D_{Pd}^{Co}$  are estimated from first-principles calculations due to the lack of direct experimental measurements. It is noted that there is neither direct experimental measurement nor first-principles calculations of the impurity diffusion coefficient of Ti in Ta, thus  $D_{Ti}^{Ta}$  is taken from the mobility assessment by Liu et al. [26]. The  $D_i^j$  values of all 18 systems, represented in the form of the Arrhenius Eq. (1), are summarized in Table 2. It should be noted that  $D_{Si}^{Si}$ ,  $D_{Zr}^{Zr}$ , and  $D_{Nb}^{Zr}$  are not expressed as a single Arrhenius Eq. (1) but a combination of two exponentials to describe their abnormal temperature dependence, following the literature practice for these elements. All the evaluated self-diffusion and impurity diffusion coefficients are plotted as a function of temperature in comparison with experimental data (when available) in the Supplementary Information, Fig. S1.

# 3.2. Composition-dependent diffusion coefficients

According to the Darken's Eqs. (3) and (4), the thermodynamic factor  $\varphi$  is essential to derive intrinsic and interdiffusion coefficients from tracer diffusion coefficients. In this study, the  $\varphi$  values of 17 binary systems are obtained using the commercial databases TCNI9 [32], TCFE10 [33], TCTI2 [34], TCSLD3 [35] and TCCU3 [36] from the Thermo-Calc Software [37] while the  $\varphi$  values are obtained from a thermodynamic assessment in the literature for the Ge-Si system [38]. The  $\varphi$  versus composition curves at various temperatures for all 18 binary systems are plotted in Fig. 3.

With the assessed self-diffusion and impurity diffusion coefficients (Table 2 and Fig. S1) as well as the computed thermodynamic factor (Fig. 3) of each system, the diffusion model with different combinations of interaction parameters (Table 1) is fitted using the critically reviewed experimental interdiffusion coefficients. The model performance is then evaluated by comparing the experimental and predicted tracer and intrinsic diffusion coefficients. The experimental information of tracer, intrinsic and interdiffusion coefficients of the 18 binary systems in the literature are summarized in Table S1 in the Supplementary Information file. In this section, four representative examples, the Ag-Au and Fe-Pd systems with the fcc crystal structure, the Ge-Si system with the diamond cubic crystal structure, and the Nb-Ti system with the bcc crystal structure, are presented to illustrate the model testing process. The results of other systems including 9 fcc binaries and 5 bcc binaries are then followed while the corresponding figures are provided in the Supplementary Information, Figs. S2-S15.

# 3.3. The fcc phase of the Ag-Au system

Ag and Au form a continuous solid solution with the fcc crystal structure over the entire composition range. Mead and Birchenall [39] measured the Au tracer diffusion coefficients at 25 and 75 at.% Au with the radioactive Au over a range of temperatures. They also measured interdiffusion coefficients but admitted that the results were of low accuracy due to the porosity formation in the diffusion couples. The Ag and Au tracer diffusion coefficients were also measured by Mallard et al. [40] with radioactive Ag and Au diffusing into a series of Ag-Au alloys at different temperatures. Interdiffusion coefficients and tracer diffusion coefficients of Ag and Au at 49.2 at.% Au at various temperatures were obtained by Johnson [41] with chemical analysis and radioactive isotopes in incremental diffusion couples. The interdiffusion coefficients of Ag-Au system at 900°C were reported by Seith and Kottmann [42] based on a Ag-Au

**Table 2** Summary of the Arrhenius equations for the self-diffusion and impurity diffusion coefficients of the pure elements in the 18 binary systems (TS: This Study).  $R = 8.314 \ J/(mol \cdot K)$ , T in Kelvin, and  $D_i^j$  (diffusion of i in j) in  $m^2/s$ .

Notation   Diffusion equation, $m^2/s$   Ref   $D_{Ag}^{RC}$   1.3 × 10 <sup>-5</sup> exp(-175892/RT)   [16]   $D_{Au}^{RC}$   7.9 × 10 <sup>-6</sup> exp(-169000/RT)   [18]   $D_{Au}^{RC}$   6.2 × 10 <sup>-5</sup> exp(-199000/RT)   [14]   $D_{Au}^{RC}$   6.1 × 10 <sup>-6</sup> exp(-170900/RT)   TS   $D_{Au}^{RC}$   2.2 × 10 <sup>-5</sup> exp(-19943/RT)   TS   $D_{Au}^{RC}$   2.2 × 10 <sup>-6</sup> exp(-219200/RT)   TS   $D_{Au}^{RC}$   2.1 × 10 <sup>-6</sup> exp(-219200/RT)   TS   $D_{Co}^{RC}$   2.2 × 10 <sup>-4</sup> exp(-2301710/RT)   [14]   $D_{Co}^{RC}$   2.4 × 10 <sup>-4</sup> exp(-284724/RT)   [22]   $D_{Co}^{RC}$   2.4 × 10 <sup>-4</sup> exp(-284724/RT)   [23]   $D_{Co}^{RC}$   2.4 × 10 <sup>-4</sup> exp(-255124/RT)   [19]   $D_{Cu}^{RC}$   9.3 × 10 <sup>-6</sup> exp(-255124/RT)   [19]   $D_{Cu}^{RC}$   9.3 × 10 <sup>-5</sup> exp(-205872/RT)   [23]   $D_{Cu}^{RC}$   4.9 × 10 <sup>-5</sup> exp(-205872/RT)   [23]   $D_{Cu}^{RC}$   4.9 × 10 <sup>-5</sup> exp(-265700/RT)   [23]   $D_{Cu}^{RC}$   4.9 × 10 <sup>-5</sup> exp(-265200/RT)   [14]   $D_{Re}^{RC}$   4.6 × 10 <sup>-5</sup> exp(-265200/RT)   [14]   $D_{Re}^{RC}$   4.6 × 10 <sup>-5</sup> exp(-262500/RT)   [14]   $D_{Re}^{RC}$   5.0 × 10 <sup>-5</sup> exp(-272534/RT)   [21]   $D_{Re}^{RC}$   5.0 × 10 <sup>-5</sup> exp(-272534/RT)   [24]   $D_{Re}^{RC}$   5.0 × 10 <sup>-5</sup> exp(-272534/RT)   [24]   $D_{Re}^{RC}$   4.5 × 10 <sup>-1</sup> exp(-478686/RT)   [24]   $D_{Re}^{RC}$   4.5 × 10 <sup>-1</sup> exp(-478686/RT)   [24]   $D_{Re}^{RC}$   4.5 × 10 <sup>-5</sup> exp(-395599/RT)   [30]   $D_{Re}^{RC}$   4.5 × 10 <sup>-5</sup> exp(-2138500/RT)   $D_{Re}^{RC}$   5.0 × 10 <sup>-5</sup> exp(-2138800/RT)   $D_{Re}^{RC}$   5.0 × 10 <sup>-5</sup> exp(-2637000/RT)   $D_{Re}^{RC}$   5.0 × 10 <sup>-5</sup> exp(-2637000/RT)   $D_{Re}^{RC}$   5.0 × 10 <sup>-5</sup> exp(-2637000/RT)   $D_{Re}^{RC}$   5.0 × 10 <sup>-5</sup> exp(-256885/RT)   20]   $D_{Re}^{RC}$   6.6 × 10 <sup>-6</sup> exp(-256800/RT)   14]   $D_{Re}^{RC}$   6.6 × 10 <sup>-6</sup> exp(-256800/RT)   14]   $D_{Re}^{RC}$   6.6 × 10 <sup>-6</sup> exp(-256800/RT)   14]   $D_{Re}^{RC}$	T in Kelvin,	and $D_i^j$ (diffusion of $i$ in $j$ ) in $m^2/s$ .	
$\begin{array}{cccccccccccccccccccccccccccccccccccc$	Notation	<u> </u>	Ref
$\begin{array}{cccccccccccccccccccccccccccccccccccc$	$D_{Ag}^{Ag}$	$1.3 \times 10^{-5} \exp(-175892/RT)$	[16]
$\begin{array}{cccccccccccccccccccccccccccccccccccc$	$D_{Ag}^{Au}$	$7.9 \times 10^{-6} \exp(-169000/RT)$	[18]
$\begin{array}{cccccccccccccccccccccccccccccccccccc$	$D_{Au}^{Ag}$	$6.2 \times 10^{-5} \exp(-199000/RT)$	[14]
$\begin{array}{cccccccccccccccccccccccccccccccccccc$	$D_{Au}^{Au}$	$6.1 \times 10^{-6} \exp(-170900/RT)$	TS
$\begin{array}{cccccccccccccccccccccccccccccccccccc$	$D_{Au}^{Cu}$	$2.2 \times 10^{-5} \exp(-196943/RT)$	TS
$\begin{array}{cccccccccccccccccccccccccccccccccccc$		$2.1 \times 10^{-6} \exp(-219200/RT)$	TS
$\begin{array}{c} D_{Co}^{\text{fe}} & 1.1 \times 10^{-4} \exp(-301710/RT) & [14] \\ D_{Co}^{\text{Ni}} & 2.4 \times 10^{-4} \exp(-284724/RT) & [22] \\ D_{Co}^{\text{Co}} & 6.2 \times 10^{-6} \exp(-255124/RT) & [19] \\ D_{Cu}^{\text{Cu}} & 9.3 \times 10^{-6} \exp(-167950/RT) & [23] \\ D_{Cu}^{\text{Cu}} & 4.9 \times 10^{-5} \exp(-205872/RT) & [16] \\ D_{Ni}^{\text{Ni}} & 3.5 \times 10^{-5} \exp(-250125/RT) & [25] \\ D_{Cu}^{\text{Pt}} & 6.5 \times 10^{-6} \exp(-247994/RT) & [23] \\ D_{Cu}^{\text{Cu}} & 5.5 \times 10^{-6} \exp(-2247994/RT) & [23] \\ D_{Fe}^{\text{Co}} & 2.1 \times 10^{-5} \exp(-226500/RT) & [14] \\ D_{Fe}^{\text{Re}} & 4.6 \times 10^{-5} \exp(-284100/RT) & [14] \\ D_{Fe}^{\text{Re}} & 1.0 \times 10^{-4} \exp(-269400/RT) & [14] \\ D_{Fe}^{\text{Re}} & 5.0 \times 10^{-5} \exp(-272534/RT) & [21] \\ D_{Ge}^{\text{Co}} & 7.8 \times 10^{-3} \exp(-310423/RT) & [24] \\ D_{Nb}^{\text{Co}} & 4.5 \times 10^{-1} \exp(-478686/RT) & [24] \\ D_{Nb}^{\text{Co}} & 4.5 \times 10^{-1} \exp(-478686/RT) & [24] \\ D_{Nb}^{\text{Ni}} & 8.9 \times 10^{-7} \exp(-171238/RT) & [27] \\ D_{Nb}^{\text{Ni}} & 8.9 \times 10^{-7} \exp(-171238/RT) & [27] \\ D_{Nb}^{\text{Ni}} & 3.4 \times 10^{-4} \exp(-330149/RT) & [31] \\ D_{Nb}^{\text{Co}} & 2.7 \times 10^{-9} \exp(-116800/RT) + [14] \\ D_{Ni}^{\text{Ni}} & 2.5 \times 10^{-5} \exp(-238500/RT) & [14] \\ D_{Ni}^{\text{Ni}} & 1.9 \times 10^{-4} \exp(-232788/RT) & [25] \\ D_{Ni}^{\text{Co}} & 2.8 \times 10^{-5} \exp(-270348/RT) & [17] \\ D_{Ni}^{\text{Ni}} & 3.0 \times 10^{-4} \exp(-237948/RT) & [17] \\ D_{Ni}^{\text{Ni}} & 3.0 \times 10^{-4} \exp(-242479/RT) & [19] \\ D_{Ni}^{\text{Co}} & 6.6 \times 10^{-6} \exp(-255685/RT) & [20] \\ D_{Ni}^{\text{Pi}} & 6.6 \times 10^{-6} \exp(-255685/RT) & [20] \\ D_{Pd}^{\text{Pi}} & 6.6 \times 10^{-6} \exp(-255685/RT) & [21] \\ D_{Pd}^{\text{Pi}} & 6.6 \times 10^{-6} \exp(-255685/RT) & [24] \\ D_{Pd}^{\text{Pi}} & 6.6 \times 10^{-6} \exp(-255685/RT) & [24] \\ D_{Pd}^{\text{Pi}} & 3.6 \times 10^{-5} \exp(-266300/RT) & [14] \\ D_{Pd}^{\text{Pi}} & 3.6 \times 10^{-5} \exp(-266300/RT) & [14] \\ D_{Pd}^{\text{Pi}} & 6.6 \times 10^{-6} \exp(-255685/RT) & [24] \\ D_{Pd}^{\text{Pi}} & 6.6 \times 10^{-6} \exp(-256903/RT) & [24] \\ D_{Pd}^{\text{Pi}} & 6.6 \times 10^{-6} \exp(-256903/RT) & [24] \\ D_{Pd}^{\text{Pi}} & 2.5 \times 10^{-5} \exp(-369003/RT) & [24] \\ D_{Pd}^{\text{Pi}} & 2.5 \times 10^{-5} \exp(-348281/RT) & [26] \\ D_{Pd}^{\text{Pi}} & 2.5 \times 10^{-5} \exp(-359003/RT) & [28] \\ D_{Pd}^{\text{Pi}} & 2.5 \times 10^{-5} \exp(-359003$	$D_{Co}^{Co}$	$2.2 \times 10^{-4} \exp(-301654/RT)$	[22]
$\begin{array}{c} D_{Co}^{Ni} & 2.4 \times 10^{-4} \exp(-284724/RT) & [22] \\ D_{Co}^{Ni} & 6.2 \times 10^{-6} \exp(-255124/RT) & [19] \\ D_{Cu}^{Cu} & 9.3 \times 10^{-6} \exp(-255124/RT) & [23] \\ D_{Cu}^{Cu} & 9.3 \times 10^{-5} \exp(-25572/RT) & [16] \\ D_{Cu}^{Ni} & 3.5 \times 10^{-5} \exp(-250125/RT) & [25] \\ D_{Cu}^{Cu} & 6.5 \times 10^{-6} \exp(-247994/RT) & [23] \\ D_{Cu}^{Co} & 2.1 \times 10^{-5} \exp(-262500/RT) & [14] \\ D_{Fe}^{Re} & 4.6 \times 10^{-5} \exp(-284100/RT) & [14] \\ D_{Fe}^{Re} & 4.6 \times 10^{-5} \exp(-284100/RT) & [14] \\ D_{Re}^{Ni} & 1.0 \times 10^{-4} \exp(-269400/RT) & [14] \\ D_{Re}^{Ni} & 5.0 \times 10^{-5} \exp(-272534/RT) & [21] \\ D_{Ge}^{Ge} & 7.8 \times 10^{-3} \exp(-310423/RT) & [24] \\ D_{Nb}^{Si} & 4.5 \times 10^{-1} \exp(-478686/RT) & [24] \\ D_{Nb}^{Si} & 8.9 \times 10^{-3} \exp(-330149/RT) & [30] \\ D_{Nb}^{Ti} & 8.9 \times 10^{-7} \exp(-171238/RT) & [27] \\ D_{Nb}^{Ni} & 3.4 \times 10^{-4} \exp(-330149/RT) & [31] \\ D_{Nb}^{Ge} & 2.7 \times 10^{-9} \exp(-116800/RT) + [14] \\ D_{Nb}^{Gi} & 1.9 \times 10^{-4} \exp(-232788/RT) & [25] \\ D_{Nb}^{Gi} & 2.8 \times 10^{-5} \exp(-188400/RT). & [14] \\ D_{Ni}^{Gi} & 1.9 \times 10^{-4} \exp(-232788/RT) & [25] \\ D_{Ni}^{Gi} & 3.0 \times 10^{-4} \exp(-287000/RT) & [14] \\ D_{Ni}^{Ni} & 2.3 \times 10^{-4} \exp(-2242479/RT) & [19] \\ D_{Ni}^{Ge} & 3.0 \times 10^{-6} \exp(-242479/RT) & [19] \\ D_{Pe}^{Gi} & 4.0 \times 10^{-6} \exp(-255685/RT) & [20] \\ D_{Pe}^{Pi} & 6.6 \times 10^{-6} \exp(-255685/RT) & [20] \\ D_{Pe}^{Pi} & 6.6 \times 10^{-6} \exp(-255685/RT) & [20] \\ D_{Pe}^{Pi} & 6.6 \times 10^{-6} \exp(-255700/RT) & [14] \\ D_{Ni}^{Di} & 3.7 \times 10^{-1} \exp(-485572/RT) & [23] \\ D_{Pi}^{Gi} & 3.0 \times 10^{-5} \exp(-319954/RT) & [24] \\ D_{Si}^{Si} & 3.7 \times 10^{-1} \exp(-485572/RT) & [24] \\ D_{Si}^{Si} & 3.7 \times 10^{-5} \exp(-345476/RT) & [26] \\ D_{Ti}^{Di} & 2.8 \times 10^{-5} \exp(-3459003/RT) & [24] \\ D_{Ti}^{Di} & 2.5 \times 10^{-5} \exp(-3459003/RT) & [24] \\ D_{Ti}^{Di} & 2.5 \times 10^{-5} \exp(-345476/RT) & [26] \\ D_{Ti}^{Di} & 2.5 \times 10^{-5} \exp(-3459003/RT) & [27] \\ D_{Ti}^{Di} & 2.5 \times 10^{-5} \exp(-3459003/RT) & [28] \\ D_{V}^{V} & 1.4 \times 10^{-4} \exp(-332508/RT) & [28] \\ D_{V}^{V} & 1.4 \times 10^{-4} \exp(-31671/RT) & [29] \\ D_{V}^{Nib} & 4.4 \times 10^{-5} \exp(-355000/RT) & [28] \\ D_{V}^{V} & 1.4 \times 10^{-4} \exp(-325008/RT) & [28] \\ D$	$D_{Co}^{Fe}$	$1.1 \times 10^{-4} \exp(-301710/RT)$	[14]
$\begin{array}{cccccccccccccccccccccccccccccccccccc$	$D_{Co}^{Ni}$	$2.4 \times 10^{-4} \exp(-284724/RT)$	[22]
$\begin{array}{cccccccccccccccccccccccccccccccccccc$	$D_{Co}^{\widetilde{Pd}}$	$6.2 \times 10^{-6} \exp(-255124/RT)$	[19]
$\begin{array}{cccccccccccccccccccccccccccccccccccc$	$D_{Cu}^{Au}$	$9.3 \times 10^{-6} \exp(-167950/RT)$	[23]
$\begin{array}{cccccccccccccccccccccccccccccccccccc$	$D_{Cu}^{\tilde{Cu}}$	$4.9 \times 10^{-5} \exp(-205872/RT)$	[16]
$\begin{array}{cccccccccccccccccccccccccccccccccccc$	$D_{Cu}^{Ni}$	$3.5 \times 10^{-5} \exp(-250125/RT)$	[25]
$\begin{array}{cccccccccccccccccccccccccccccccccccc$	$D_{Cu}^{Pt}$	$6.5 \times 10^{-6} \exp(-247994/RT)$	[23]
$\begin{array}{cccccccccccccccccccccccccccccccccccc$	$D_{E_0}^{C_0}$	$2.1 \times 10^{-5} \exp(-262500/RT)$	[14]
$\begin{array}{c} D_{Re}^{Ni} & 1.0 \times 10^{-4} \exp(-269400/RT) & [14] \\ D_{Re}^{Pid} & 5.0 \times 10^{-5} \exp(-272534/RT) & [21] \\ D_{Ge}^{Ce} & 7.8 \times 10^{-3} \exp(-310423/RT) & [24] \\ D_{Ge}^{Se} & 4.5 \times 10^{-1} \exp(-478686/RT) & [24] \\ D_{Nb}^{Si} & 5.2 \times 10^{-5} \exp(-395599/RT) & [30] \\ D_{Nb}^{Ni} & 8.9 \times 10^{-7} \exp(-171238/RT) & [27] \\ D_{Nb}^{V} & 3.4 \times 10^{-4} \exp(-330149/RT) & [31] \\ D_{Nb}^{Air} & 2.7 \times 10^{-9} \exp(-116800/RT) + & [14] \\ 2.6 \times 10^{-5} \exp(-238500/RT) & [25] \\ D_{Ni}^{Cii} & 1.9 \times 10^{-4} \exp(-232788/RT) & [25] \\ D_{Ni}^{Cii} & 2.8 \times 10^{-5} \exp(-188400/RT) & [17] \\ D_{Ni}^{Cii} & 2.8 \times 10^{-5} \exp(-232788/RT) & [17] \\ D_{Ni}^{Cii} & 3.0 \times 10^{-4} \exp(-232788/RT) & [17] \\ D_{Ni}^{Cii} & 3.0 \times 10^{-4} \exp(-232788/RT) & [17] \\ D_{Ni}^{Cii} & 3.0 \times 10^{-6} \exp(-242479/RT) & [19] \\ D_{Ni}^{Cii} & 5.3 \times 10^{-6} \exp(-242479/RT) & [19] \\ D_{Ni}^{Cii} & 5.3 \times 10^{-6} \exp(-255685/RT) & [20] \\ D_{Pd}^{Pd} & 4.0 \times 10^{-6} \exp(-255685/RT) & [20] \\ D_{Pd}^{Pd} & 4.0 \times 10^{-6} \exp(-253148/RT) & [21] \\ D_{Ni}^{Pid} & 6.9 \times 10^{-5} \exp(-266700/RT) & [14] \\ D_{Pd}^{Pid} & 2.0 \times 10^{-5} \exp(-266300/RT) & [14] \\ D_{Pd}^{Cii} & 3.6 \times 10^{-5} \exp(-266300/RT) & [14] \\ D_{Pd}^{Cii} & 3.6 \times 10^{-5} \exp(-264127/RT) & [23] \\ D_{Pd}^{Pir} & 6.6 \times 10^{-6} \exp(-261427/RT) & [23] \\ D_{Pd}^{Pir} & 3.7 \times 10^{-1} \exp(-485572/RT) & [24] \\ D_{Si}^{Si} & 3.7 \times 10^{-1} \exp(-485572/RT) & [24] \\ D_{Si}^{Si} & 3.7 \times 10^{-5} \exp(-345476/RT) & [26] \\ D_{II}^{Tii} & 1.0 \times 10^{-7} \exp(-155731/RT) & [26] \\ D_{II}^{Tii} & 2.2 \times 10^{-7} \exp(-155731/RT) & [26] \\ D_{II}^{Di} & 2.5 \times 10^{-5} \exp(-3458281/RT) & [26] \\ D_{II}^{Di} & 2.5 \times 10^{-5} \exp(-3458281/RT) & [26] \\ D_{II}^{Di} & 2.5 \times 10^{-5} \exp(-3458281/RT) & [28] \\ D_{V}^{V} & 1.4 \times 10^{-4} \exp(-325008/RT) & [28] \\ D_{V}^{V} & 1.4 \times 10^{-4} \exp(-325008/RT) & [28] \\ D_{V}^{V} & 1.4 \times 10^{-4} \exp(-325008/RT) & [28] \\ D_{V}^{V} & 1.4 \times 10^{-4} \exp(-325008/RT) & [28] \\ D_{V}^{Di} & 2.8 \times 10^{-5} \exp(-36700/RT) & [14] \\ D_{Zr}^{Di} & 2.8 \times 10^{-5} \exp(-36700/RT) & [14] \\ D_{Zr}^{Di} & 2.8 \times 10^{-5} \exp(-36700/RT) & [24] \\ D_{Zr}^{Di} & 2.8 \times 10^{-5} \exp(-3100/RT) & [29] \\ D_{Zr$		$4.6 \times 10^{-5} \exp(-284100/RT)$	[14]
$\begin{array}{cccccccccccccccccccccccccccccccccccc$	$D_{Fa}^{Ni}$	$1.0 \times 10^{-4} \exp(-269400/RT)$	[14]
$\begin{array}{cccccccccccccccccccccccccccccccccccc$	$D_{Fe}^{Pd}$	$5.0 \times 10^{-5} \exp(-272534/RT)$	
$\begin{array}{cccccccccccccccccccccccccccccccccccc$	$D_{Ge}^{re}$	$7.8 \times 10^{-3} \exp(-310423/RT)$	
$\begin{array}{cccccccccccccccccccccccccccccccccccc$	o.	$4.5 \times 10^{-1} \exp(-478686/RT)$	
$\begin{array}{cccccccccccccccccccccccccccccccccccc$	$D_{\cdot \cdot \cdot \cdot}^{Nb}$	$5.2 \times 10^{-5} \exp(-395599/RT)$	
$\begin{array}{cccccccccccccccccccccccccccccccccccc$	$D_{NL}^{ND}$	$8.9 \times 10^{-7} \exp(-171238/RT)$	
$\begin{array}{cccccccccccccccccccccccccccccccccccc$	$D_{\cdots}^{V}$		
$\begin{array}{cccccccccccccccccccccccccccccccccccc$	$D_{r}^{Zr}$	$2.7 \times 10^{-9} \exp(-116800/RT) +$	
$\begin{array}{cccccccccccccccccccccccccccccccccccc$	- Nb	$2.6 \times 10^{-5} \exp(-238500/RT)$	[1
$\begin{array}{cccccccccccccccccccccccccccccccccccc$	$D_{N}^{Au}$	$2.5 \times 10^{-5} \exp(-188400/RT)$ .	[14]
$\begin{array}{cccccccccccccccccccccccccccccccccccc$	$D_{\cdots}^{Nl}$	$1.9 \times 10^{-4} \exp(-232788/RT)$	
$\begin{array}{cccccccccccccccccccccccccccccccccccc$	$D_{co}^{Ni}$	$2.8 \times 10^{-5} \exp(-270348/RT)$	
$\begin{array}{cccccccccccccccccccccccccccccccccccc$	D <sub>Fe</sub>	$3.0 \times 10^{-4} \exp(-314000/RT)$	
$\begin{array}{cccccccccccccccccccccccccccccccccccc$	177	$2.3 \times 10^{-4} \exp(-287000/RT)$	
$\begin{array}{cccccccccccccccccccccccccccccccccccc$	$D_{N_i}^{N_l}$	$5.3 \times 10^{-6} \exp(-242479/RT)$	
$\begin{array}{cccccccccccccccccccccccccccccccccccc$	$D_{co}^{Ni}$	$6.6 \times 10^{-6} \exp(-255685/RT)$	
$\begin{array}{cccccccccccccccccccccccccccccccccccc$	$D_{P}^{Pa}$ .	$4.0 \times 10^{-6} \exp(-251348/RT)$	
$\begin{array}{cccccccccccccccccccccccccccccccccccc$	$D_{\rm p,i}^{\rm Pa}$		
$\begin{array}{cccccccccccccccccccccccccccccccccccc$	$D_{p,l}^{Pd}$	$2.0 \times 10^{-5} \exp(-266300/RT)$	
$\begin{array}{cccccccccccccccccccccccccccccccccccc$	$D_{cu}^{Cu}$	$3.6 \times 10^{-5} \exp(-227726/RT)$	
$\begin{array}{cccccccccccccccccccccccccccccccccccc$		$6.6 \times 10^{-6} \exp(-261427/RT)$	
$\begin{array}{cccccccccccccccccccccccccccccccccccc$	$D_{c}^{Pt}$	$3.2 \times 10^{-3} \exp(-319954/RT)$	
$\begin{array}{cccccccccccccccccccccccccccccccccccc$	$D_{-}^{Si}$	$3.7 \times 10^{-1} \exp(-485572/RT) +$	
$\begin{array}{cccccccccccccccccccccccccccccccccccc$	- Si	$2.5 \times 10^{-7} \exp(-345476/RT)$	[1
$\begin{array}{cccccccccccccccccccccccccccccccccccc$	$D_{T-}^{Ta}$	$2.3 \times 10^{-5} \exp(-426474/RT)$	[26]
$\begin{array}{cccccccccccccccccccccccccccccccccccc$	$D_{T_a}^{Ia}$	$1.0 \times 10^{-7} \exp(-155731/RT)$	
$\begin{array}{cccccccccccccccccccccccccccccccccccc$	$D_{T_i}^{Nb}$	$2.8 \times 10^{-5} \exp(-369003/RT)$	
$\begin{array}{cccccccccccccccccccccccccccccccccccc$	$D_{Ti}^{Ii}$	$2.5 \times 10^{-5} \exp(-438281/RT)$	
$\begin{array}{llll} D_{TI}^{V} & 3.9 \times 10^{-4} \exp(-329984/RT) & [28] \\ D_{TI}^{ZT} & 6.1 \times 10^{-8} \exp(-140357/RT) & [29] \\ D_{V}^{ND} & 4.4 \times 10^{-5} \exp(-375659/RT) & [31] \\ D_{V}^{TI} & 2.7 \times 10^{-6} \exp(-179393/RT) & [28] \\ D_{V}^{ND} & 1.4 \times 10^{-4} \exp(-325008/RT) & [28] \\ D_{ZT}^{ND} & 2.8 \times 10^{-5} \exp(-357000/RT) & [14] \\ D_{TI}^{TI} & 1.1 \times 10^{-7} \exp(-131671/RT) & [29] \\ D_{ZT}^{DT} & 2.8 \times 10^{-10} \exp(-81100/RT) + & [14] \\ \end{array}$	$D_{m}^{H}$	$2.2 \times 10^{-7} \exp(-151990/RT)$	
$\begin{array}{lll} D_{Ti}^{Zr} & 6.1 \times 10^{-8} \exp(-140357/RT) & [29] \\ D_{V}^{Nb} & 4.4 \times 10^{-5} \exp(-375659/RT) & [31] \\ D_{V}^{Ti} & 2.7 \times 10^{-6} \exp(-179393/RT) & [28] \\ D_{V}^{V} & 1.4 \times 10^{-4} \exp(-325008/RT) & [28] \\ D_{Zr}^{Nb} & 2.8 \times 10^{-5} \exp(-357000/RT) & [14] \\ D_{Zr}^{Ti} & 1.1 \times 10^{-7} \exp(-131671/RT) & [29] \\ D_{Zr}^{Ti} & 2.8 \times 10^{-10} \exp(-81100/RT) + & [14] \end{array}$	$D_{T_i}^{I_1}$	$3.9 \times 10^{-4} \exp(-329984/RT)$	
$\begin{array}{lll} D_V^{hb} & 4.4 \times 10^{-5} \exp(-375659/RT) & [31] \\ D_V^{ti} & 2.7 \times 10^{-6} \exp(-179393/RT) & [28] \\ D_V^{ti} & 1.4 \times 10^{-4} \exp(-325008/RT) & [28] \\ D_{Zr}^{hb} & 2.8 \times 10^{-5} \exp(-357000/RT) & [14] \\ D_{Zr}^{hb} & 1.1 \times 10^{-7} \exp(-131671/RT) & [29] \\ D_{Zr}^{ho} & 2.8 \times 10^{-10} \exp(-81100/RT) + & [14] \end{array}$		$6.1 \times 10^{-8} \exp(-140357/RT)$	
$\begin{array}{lll} D_V^{TI} & 2.7 \times 10^{-6} \exp(-179393/RT) & [28] \\ D_V^{V} & 1.4 \times 10^{-4} \exp(-325008/RT) & [28] \\ D_{Zr}^{Nb} & 2.8 \times 10^{-5} \exp(-357000/RT) & [14] \\ D_{Zr}^{TI} & 1.1 \times 10^{-7} \exp(-131671/RT) & [29] \\ D_{Zr}^{TI} & 2.8 \times 10^{-10} \exp(-81100/RT) + & [14] \\ \end{array}$	$D_{V}^{Nb}$	$4.4 \times 10^{-5} \exp(-375659/RT)$	
$\begin{array}{lll} D_V^V & 1.4 \times 10^{-4} \exp(-325008/RT) & [28] \\ D_{Zr}^{Nb} & 2.8 \times 10^{-5} \exp(-357000/RT) & [14] \\ D_{Zr}^{Ti} & 1.1 \times 10^{-7} \exp(-131671/RT) & [29] \\ D_{Zr}^{Ti} & 2.8 \times 10^{-10} \exp(-81100/RT) + & [14] \end{array}$		$2.7 \times 10^{-6} \exp(-179393/RT)$	
$D_{Zr}^{Nb}$ 2.8 × 10 <sup>-5</sup> exp(-357000/RT) [14] $D_{Zr}^{Ti}$ 1.1 × 10 <sup>-7</sup> exp(-131671/RT) [29] $D_{Zr}^{Ti}$ 2.8 × 10 <sup>-10</sup> exp(-81100/RT)+ [14]	V.	$1.4 \times 10^{-4} \exp(-325008/RT)$	
$D_{2r}^{Ti}$ 1.1 × 10 <sup>-7</sup> exp(-131671/RT) [29] $D_{2r}^{Zr}$ 2.8 × 10 <sup>-10</sup> exp(-81100/RT)+ [14]		$2.8 \times 10^{-5} \exp(-357000/RT)$	
$D_{7r}^{Zr}$ 2.8 × 10 <sup>-10</sup> exp(-81100/RT)+ [14]	$D_{Zr}^{Ti}$	$1.1 \times 10^{-7} \exp(-131671/RT)$	
$1.7 \times 10^{-6} \exp(-194100/RT)$		$2.8 \times 10^{-10} \exp(-81100/RT) +$	
	ZΓ	$1.7 \times 10^{-6} \exp(-194100/RT)$	[]

diffusion couple. Balluffi and Seigle [43] investigated the interdiffusion using Ag-Au vapor-solid diffusion couple at 940°C, and determined the intrinsic diffusion coefficients with the help of inert markers in the diffusion couple. Ebert and Trommsdorf [44] determined the temperature-dependent interdiffusion coefficients at 91.23 at.% Au by means of incremental diffusion couples.

The collected interdiffusion coefficients from the literature are all employed to fit the diffusion model with 0, 1, 2, and 4 interaction parameters, respectively. The intrinsic and tracer diffusion coefficients are predicted accordingly using Eqs. (3), (4) and (8). The experimental data are compared with the modelled values in Fig. 4, showing that the model with no interaction parameter (i.e.,

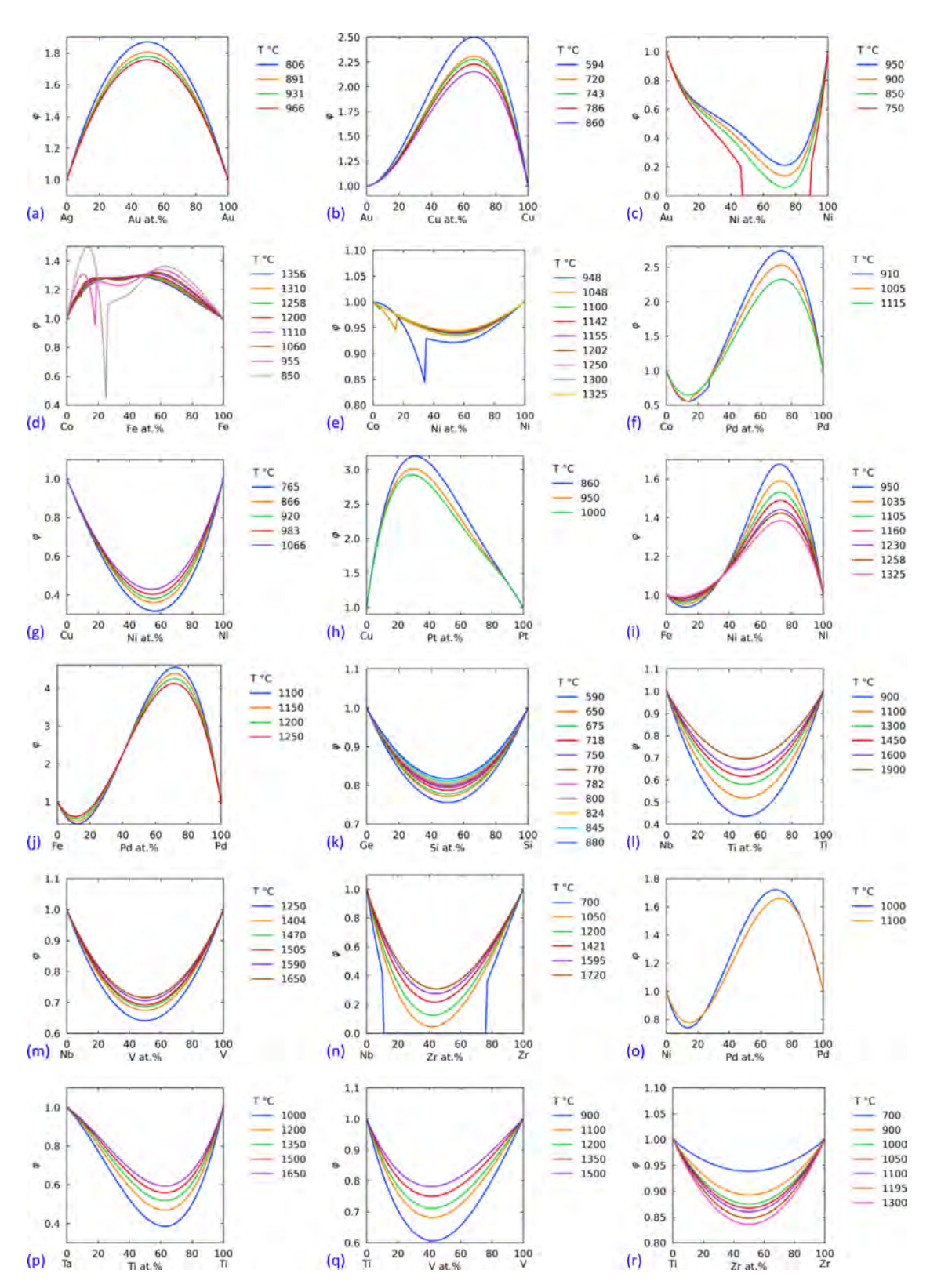


**Fig. 3.** Thermodynamic factor  $\varphi$  of the 18 binary systems analyzed in this study showing the diversity of behaviors including very asymmetrical systems such as Au-Cu, Au-Ni, Co-Pd, Cu-Pt, Fe-Ni, Fe-Pd, and Ni-Pd. Some of the abrupt changes in the thermodynamic factor plots are due to magnetic transitions, ordering transitions, or other effects.

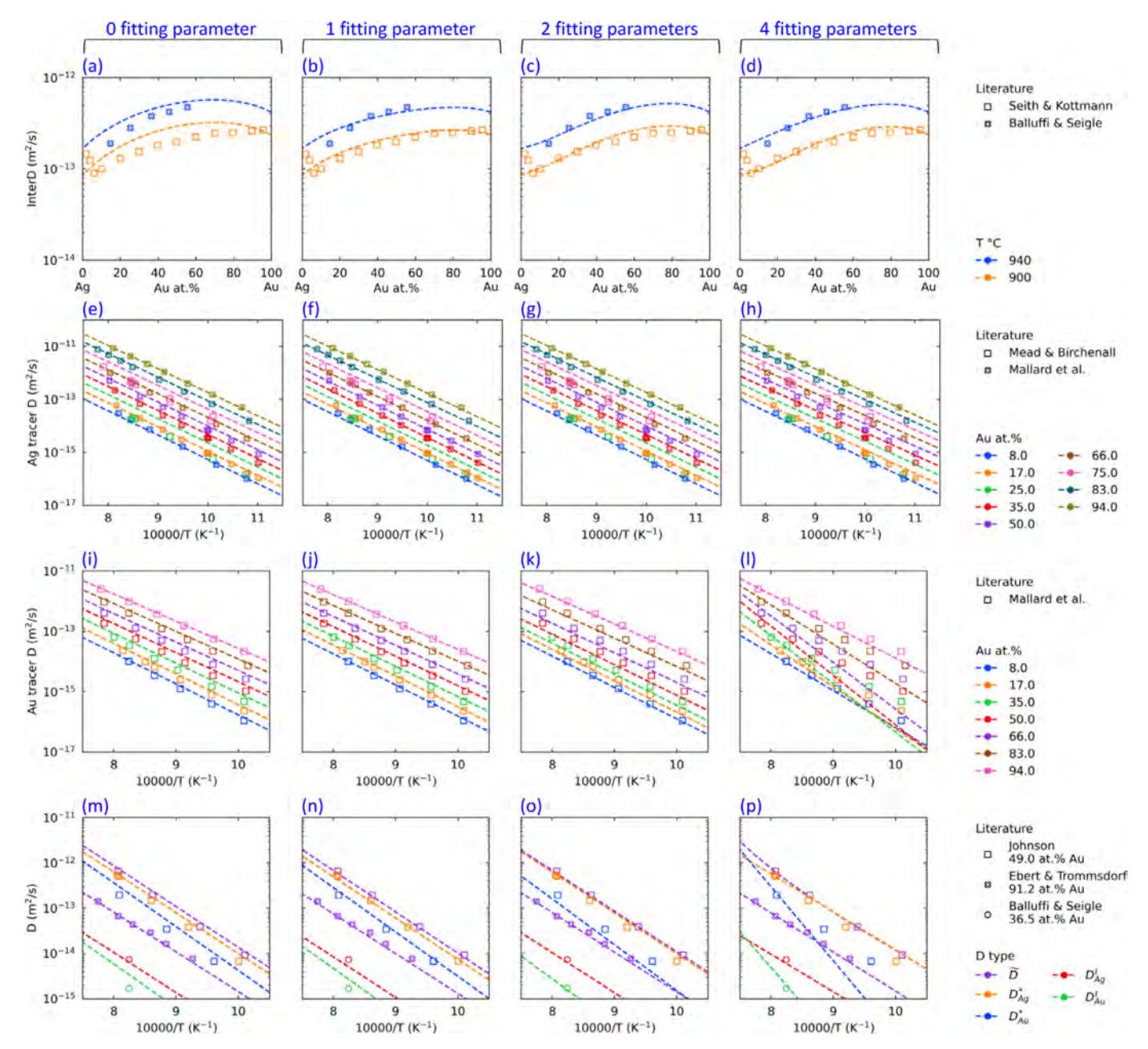


Fig. 4. Comparison of the performance of diffusion models with 0, 1, 2 or 4 parameters for the fcc solid solution of the Ag-Au binary system.

"ideal" diffusion behavior) can predict both the tracer and intrinsic diffusion coefficients reasonably well. It should be noted that the diffusion coefficients at different compositions were shifted by different factors to separate the data for visualization in the plots of subfigures (e) to (p). The 1-parameter model further enhance the model performance, especially in terms of interdiffusion coefficients. The 2-parameter and 4-parameter models do not show much improvement; and as a matter of fact, the two subfigures (l) and (p) of Fig. 4 clearly show signs of over-fitting with the 4-parameter model.

# 3.4. The fcc phase of the Fe-Pd system

Fe and Pd form a complete solid solution of the fcc phase over a wide temperature range. Gomez et al. [45] measured the interdiffusion coefficients at 4 temperatures between 1100°C and 1250°C using diffusion couples. Fillon and Calais [46] determined

the tracer diffusion coefficients of the Fe-Pd system using radioisotopes Fe and Pd at the same temperatures. Intrinsic and interdiffusion coefficients were obtained by van Dal et al. [47] via regular diffusion couples and multi-foil couples at 1100°C.

All the above interdiffusion coefficients are fed to the model with different number of interaction parameters. The comparisons between computed data and experimental data are plotted in Fig. 5, showing that the 0-parameter model does not work for this binary system and the 1-parameter model drastically improve the model performance. Additional fitting parameters (2 and 4) do not lead to improved model performance, and the 4-parameter model has led to reduced agreement with the Pd tracer diffusion coefficients (See subfigures (j) to (l) in Fig. 5).

One can see from subfigures (e) to (l) of Fig. 5 that the tracer diffusion coefficients of both Fe and Pd behave quite "regularly/symmetrically", and the very asymmetrical behavior of both the interdiffusion coefficients (subfigures (a) to (d) in Fig. 5) and

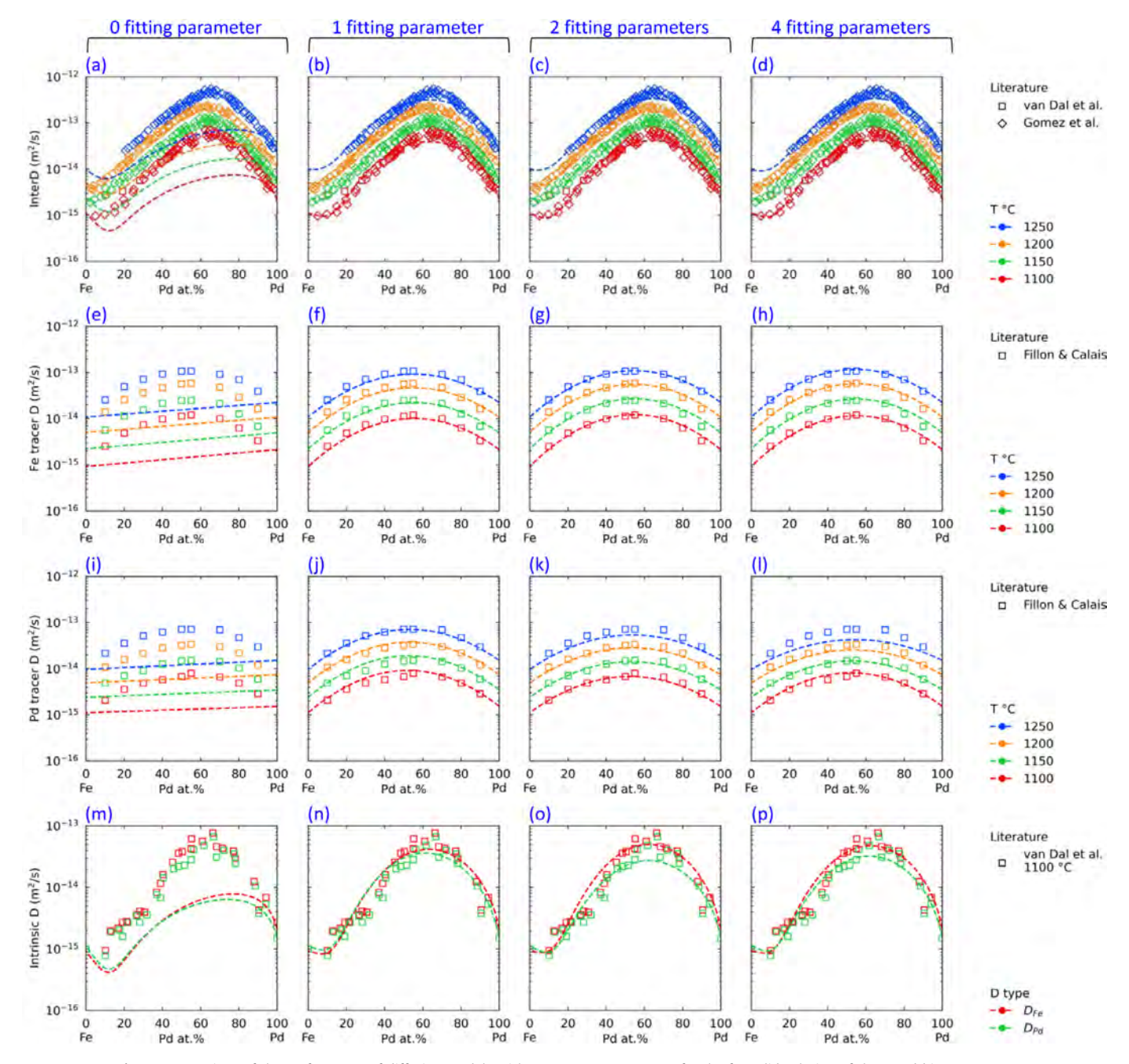


Fig. 5. Comparison of the performance of diffusion models with 0, 1, 2 or 4 parameters for the fcc solid solution of the Fe-Pd binary system.

the intrinsic diffusion coefficients (subfigures (m) to (p) in Fig. 5) is predominately the result of the very asymmetrical thermodynamic factor,  $\varphi$ , showing in subfigure (j) of Fig. 3.

# 3.5. The diamond cubic phase of the Ge-Si system

The Ge-Si system forms a continuous solid solution with a diamond cubic crystal structure. Kube et al. [48] determined the Si and Ge tracer diffusion coefficients in Si-Ge isotope heterostructures at several compositions in the temperature range of 690 – 1270°C using secondary ion mass spectrometry (SIMS). Zangenberg et al. [49] also employed SIMS to measure the Ge isotope concentration profiles and calculated its tracer diffusion coefficients at various compositions over the temperature range of 850°C to 1050°C. Strohm et al. [50,51] conducted tracer experiments in various SiGe wafers or epilayers and obtained the Ge tracer diffu-

sion coefficients between 653 and 1263°C and Si tracer diffusion coefficients between 861 and 1047°C. The Si and Ge tracer diffusion coefficients in  $\rm Si_{0.2}Ge_{0.8}$  layers were extracted by Latinen et al. [52] via tracer experiments.

Xia et al. [53] studied the interdiffusion in Si-Ge heterostructures with Ge composition between 0 and 56 at.% over the temperature range of 770 – 920°C from the diffusion profiles measured using SIMS. The interdiffusion coefficients over the full composition range over a wide range of temperatures were extracted by Gavelle et al. [54] using SIMS. Aubertine and McIntyre [55] obtained the interdiffusion coefficients over the composition range of 7.5 – 19.2 at.% Ge between 770 and 870°C from SiGe superlattices over a small concentration gradient. Ozguven and McIntyre [56] also employed a similar approach and reported the interdiffusion coefficients at 91 at.% Ge at four temperatures from 600°C to 700°C.

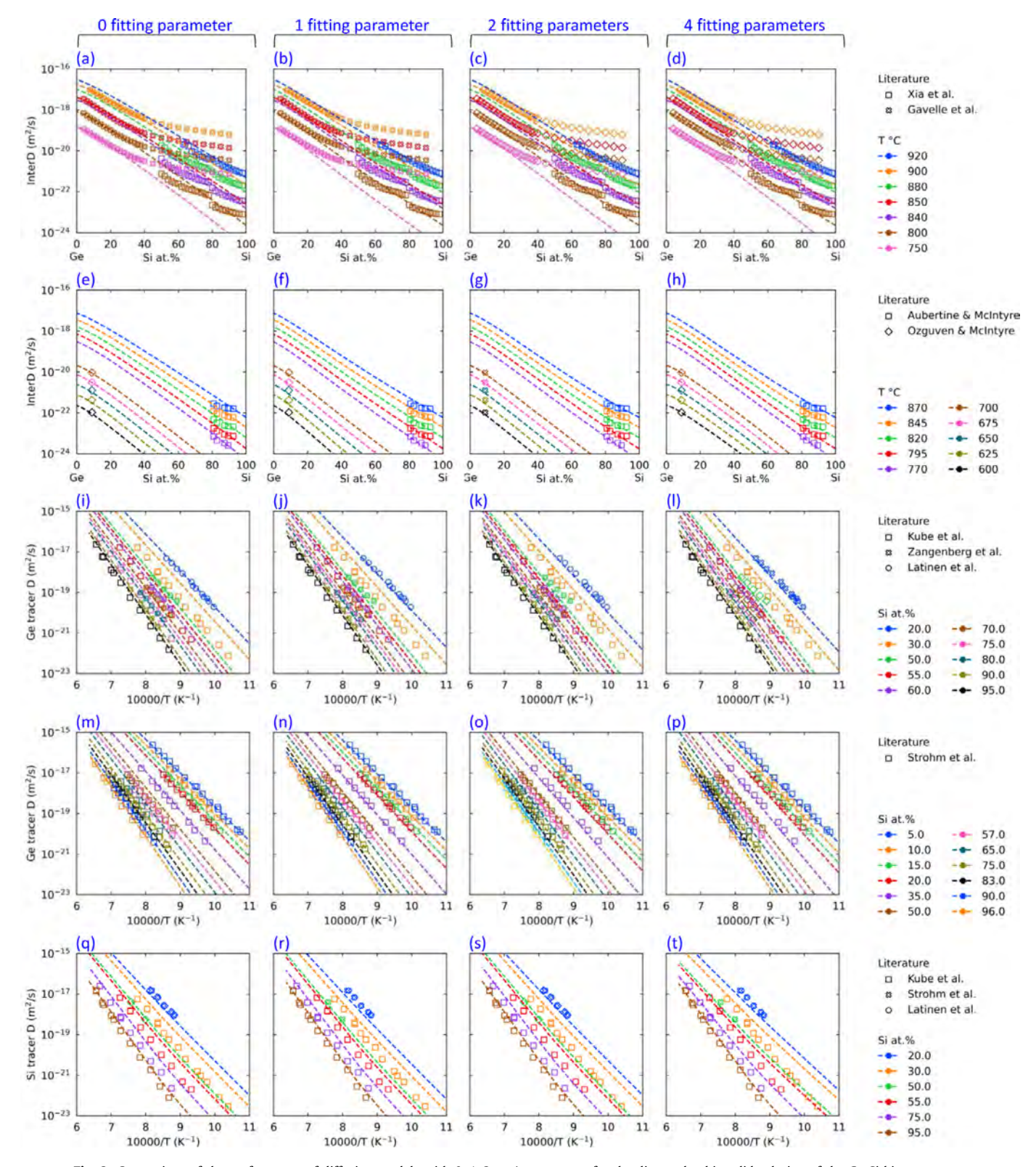


Fig. 6. Comparison of the performance of diffusion models with 0, 1, 2 or 4 parameters for the diamond cubic solid solution of the Ge-Si binary system.

It is noted that the interdiffusion coefficients decrease dramatically as the Si concentration increases, varying by  $\sim$ 6 orders of magnitude ( $\sim$ 10<sup>-17</sup> to  $\sim$ 10<sup>-23</sup>). The data reported by Gavelle et al. [54] show a characteristic "bend-over" (subfigure (a) to (d) in Fig. 6), leading to disagreement with the highly reliable impurity diffusion coefficient of Ge in Si. Such a "bend-over" of interdiffusion

sion coefficients as a function of composition is the result of insufficient spatial resolution of the composition measurement in relation to the sharp concentration gradient, as explained in detail by Chen and Zhao [57]. Such a "bend-over" situation has been observed in other systems such as Au-Ni, Nb-Ti, Nb-Zr, Ta-Ti, and Ti-V. Hence, the data points of Gavelle et al. in the high Si concentration

range are excluded from being used for the fitting of the diffusion model. Fig. 6 shows the comparisons between the model results and experimental data. The 0-parameter model ("ideal" diffusion behavior) already predicts the experimental interdiffusion coefficients and the tracer diffusion coefficients well. Additional fitting parameters do not improve the model performance much.

# 3.6. The bcc phase of the Nb-Ti system

A completely soluble bcc phase is formed between Nb and Ti over a wide temperature range. Peart and Tomlin [58] obtained the Nb tracer diffusion coefficients in a series of Nb-Ti alloys as a function of temperature. The Nb tracer diffusion coefficients in Nb-Ti alloys with less than 15 at.% Nb at various temperatures were also determined by Gibbs et al. [59]. Pontau and Lazarus [60] measured the Nb and Ti tracer diffusion coefficients at 3 compositions in a temperature range of 950 – 1511°C.

Diffusion couple experiments were conducted to obtain the interdiffusion coefficients of the Nb-Ti system. The data were reported in temperature ranges of 1450 – 2075°C by Roux and Vignes [61], 1000 – 1400°C by Ugaste and Zajkin [62], 1000 – 1200°C by Polyanskii et al. [63], 900 – 1000°C by Fedotov et al. [64], 800 – 1200°C by Gryzunov et al. [65], 1100 – 1300°C by Vergasova et al. [66], 900 – 1100°C by Zhu et al. [67], and 800 – 1200°C by Chen et al. [68].

The interdiffusion coefficients drop remarkably as Nb composition increases. Zhu et al. [67] and Chen et al. [68] reported the interdiffusion coefficients in the Ti-rich side compositions. The data measured by Roux and Vignes [61] and Ugaste and Zajkin [62] have good agreement with the Ti impurity diffusion coefficients in Nb. These data sets are used to fit the diffusion model. The modeled diffusion coefficients are compared with the experimental data in Fig. 7. While 1, 2 and 4 interaction parameters reproduce the interdiffusion coefficients in similar agreements, the 1-parameter model performs best in predicting the tracer diffusion coefficients. In fact, the predicted Nb tracer diffusion coefficients from the model with 4 interaction parameters are not in good agreement with the experimental data, and show a clear sign of over-fitting - See subfigure (1) of Fig. 7. It is noted that the 1parameter model shows a good overall fit for this binary system whose experimental diffusion coefficient data cover ~ 9 orders of magnitude ( $\sim 10^{-11}$  to  $\sim 10^{-20}$  m<sup>2</sup>/s) and over a temperature range spanning ~1200°C (from ~800°C to ~2000°C), Fig. 7.

# $3.7.\ The\ fcc\ phase\ of\ the\ Au-Cu\ system$

The tracer diffusion coefficients of Au in disordered Cu<sub>3</sub>Au alloy were determined by Benci et al. [69], as well as Alexander [70] with radioactive Au over a range of temperatures. Heumann and Rottwinkel [71] measured the interdiffusion, intrinsic and tracer diffusion coefficients in Cu-rich Au-Cu solid solutions at 860°C with various diffusion couples and radioactive Au and Cu. Badia and Vignes [72], Borovskii [73], Pinnel and Bennett [74] and Ravi and Paul [75] obtained the interdiffusion coefficients of Au-Cu system from diffusion couples at various temperatures, respectively. Interdiffusion coefficients at 725°C were reported by Ziebold and Ogilvie [76] based on diffusion couple experiments. The lattice interdiffusion coefficients at 750°C were reported by Austin and Richard [77] along with grain boundary diffusion coefficients using electroplated Au onto Cu bicrystals. The diffusion model is fitted with different number of interaction parameters using the interdiffusion coefficients reported by Badia and Vignes [72], Pinnel and Bennett [74], Ziebold and Ogilvie [76] and Heumann and Rottwinkel [71]. The interdiffusion coefficients reported by Ravi and Paul [75], Austin and Richard [77], and Borovskii [73] are less reliable because they do not agree well with the impurity diffusion coefficients of Au in Cu or Cu in Au. The 0-parameter diffusion model does not work as shown in the left-hand column (subfigures (a), (e), (i), (m), (q), (u)) of Fig. S2 in the Supplementary Information. The 1-parameter model works well as shown in the second column (subfigures (b), (f), (j), (n), (r), (v)) in Fig. S2. Additional fitting parameters (2 and 4) do not improve the fitting, as shown in Fig. S2.

# 3.8. The fcc phase of the Au-Ni system

Kurtz et al. [78] used the radioactive Au to extract the Au tracer diffusion coefficients in various Au-Ni alloys at different temperatures. Reynolds et al. [79] employed tracer method to determine the Ni tracer diffusion coefficients in Au-Ni solid solutions as well as diffusion couples to extract the interdiffusion coefficients at various temperatures, respectively. The interdiffusion coefficients of Au-Ni were determined with regular diffusion couples at four temperatures while the intrinsic diffusion was analyzed via multifoil couple experiment at 900°C by van Dal et al. [80]. Iijima and Yamazaki [81] studied the interdiffusion of the Au-Ni system by means of diffusion couple at three temperatures. The collected interdiffusion coefficients from the studies by Iijima and Yamazaki [81], Reynolds et al. [79] and van Dal et al. [80] were used to fit the diffusion model with various number of interaction parameters, except for the data at high Ni concentrations from the study of Reynolds et al. [79]. The problem with the Ni-rich data has been explained by Chen and Zhao [57]. The modeling results are presented in Fig. S3 in the Supplementary Information. One can clearly see that the 0-parameter model does not work (the left column - subfigures (a), (e), (i), (m), (q)); the 1-parameter model works well (the second column - subfigures (b), (f), (j), (n), (r)) and additional fitting parameters lead to no improvement.

# 3.9. The fcc phase of the Co-Fe system

Radioactive Fe and Co were used to determine the tracer diffusion coefficients in Co-Fe alloys in the composition range of 49-68 at.% Fe at 1200°C by Kohn et al. [82]. Ugaste et al. [83] also extracted the tracer diffusion coefficients of the Co-Fe system while Fishman et al. [84] determined the values at equiatomic Co-Fe alloy as a function of temperature. Hirano and Cohen [85] extracted the Co tracer diffusion coefficients as a function of composition from 1060°C to 1310°C. Badia and Vignes [72], Ustad and Sorum [86] and Hirano et al. [87] employed diffusion couples to extract interdiffusion coefficients at various temperatures, respectively. However, the interdiffusion coefficients reported by Ustad and Sorum [86] and Hirano et al. [87] are not in good agreement with the impurity diffusion coefficients. Consequently, only the dataset from Badia and Vignes [72] is fed to the diffusion model with different numbers of interaction parameters. Fig. S4 in the Supplementary Information shows that the 0-parameter model shows a reasonable agreement; the 1-parameter model leads to slightly better performance; and additional parameters slightly degrade the model performance.

# 3.10. The fcc phase of the Co-Ni system

Million and Kucera measured the Co tracer diffusion coefficients in the composition range of 0-80 at.% Ni between 1057°C and 1306°C [88] as well as the Ni tracer diffusion coefficients in the full composition space of the Co-Ni system in the temperature range of 1065-1290°C [89]. Hirano et al. [90] obtained the Co and Ni tracer diffusion coefficients in 4 Co-Ni alloys as a function of temperature. Hirai et al. [91] and Ugaste et al. [83] determined the interdiffusion coefficients at 1100°C using diffusion couples. The interdiffusion coefficients of the Co-Ni system at various temperatures were

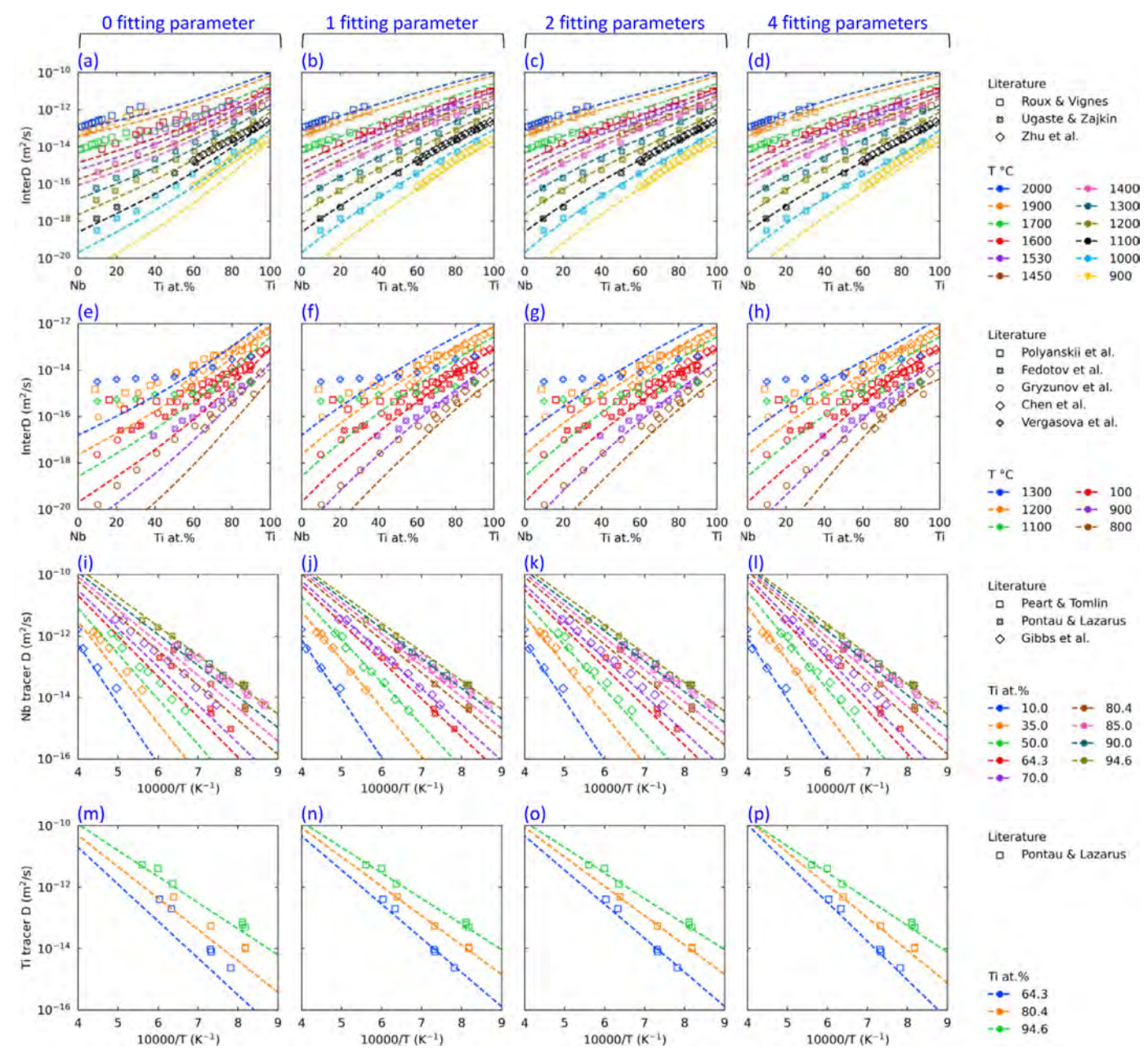


Fig. 7. Comparison of the performance of diffusion models with 0, 1, 2 or 4 parameters for the bcc solid solution of the Nb-Ti binary system.

extracted from diffusion couples in several studies by Zhang and Zhao [92], Heumann and Kottmann [93], Borovskiy et al. [94], Ustad and Sorum [86], Kucera et al. [95], and Iijima and Hirano [96], respectively. The model with 0, 1, 2 and 4 interaction parameters is fitted respectively with all the interdiffusion coefficients reported in the above literature except the data obtained under the magnetic transition condition. Fig. S5 in the Supplementary Information shows the model test results. The tracer diffusion coefficients at different compositions were shifted by different factors to separate them for better visualization in subfigures (i) to (l) and (q) to (x). The 0-parameter ("ideal" diffusion behavior) model works well; the 1-parameter model leads to slightly better performance; and the 2-parameter and 4-parameter models lead to worse agreement of the Ni tracer diffusion coefficients (the bottom row - subfigures (u) to (x) of Fig. S5). Clear sign of over-fitting is seen for the 4-parameter model for the Ni tracer diffusion coefficients in subfigure (x) of Fig. S5.

# 3.11. The fcc phase of the Co-Pd system

lijima and Hirano [97] determined the intrinsic diffusion coefficients of Co and Pd at the Kirkendall marker composition of 22.5 at.% Pd at 1149°C in a Co-Pd diffusion couple. They also studied the interdiffusion in the Co-Pd binary system using a series of diffusion couples in the temperature range of 880 – 1193°C. Only this set of interdiffusion coefficients is used to fit the diffusion model with various number of interaction parameters. It is noted that the data obtained in the ferromagnetic region are not used to feed the model. Only two data points of intrinsic diffusion coefficients were reported so there is insufficient data to make a sound judgement on the model performance. However, one can clearly see from Fig. S6 in the Supplementary Information that the 0-parameter model does not work, the 1-parameter model fits the interdiffusion coefficients really well, and the additional fitting parameters do not lead to any appreciable improvement.

# 3.12. The fcc phase of the Cu-Ni system

Monma et al. [98] reported the Cu and Ni tracer diffusion coefficients in three Cu-Ni alloys at various temperatures. The Cu and Ni tracer diffusion coefficients as a function of temperature in three other Cu-Ni alloys were also determined by Ausavice and Dehoff [99]. Damkohler and Heumann [100] obtained the Cu and Ni tracer and intrinsic diffusion coefficients in Cu-rich Cu-Ni solid solution compositions (up to 20 at.% Ni) at 1000°C using radioactive tracers and diffusion couples. Levasseur and Philibert [101] and lijima et al. [102] studied the interdiffusion and intrinsic diffusion coefficients with the Kirkendall markers in diffusion couples at 1000°C. In addition, foil method was employed to obtain diffusion data at the same temperature by Heumann and Grundoff [103]. Thomas and Birchenall [104] investigated the interdiffusion in Cu-Ni diffusion couples annealed at temperatures from 923°C to 1049°C. Marchukova and Miroshkina [105] obtained interdiffusion coefficients at 920°C and 1000°C from diffusion couples while Brunel et al. [106] measured the interdiffusion coefficients between 710°C and 1066°C. It is noted that the interdiffusion coefficients at 1000°C reported by various groups are in good agreement, but the data at other temperatures show considerable disagreement and some datasets do not agree with the well-established impurity diffusion coefficients, as shown in Fig. S7 in the Supplementary Information. Only the data at 1000°C were employed to fit the diffusion model with various numbers of interaction parameters. The 0-parameter ("ideal" diffusion behavior) model already show good agreement and additional fitting parameters do not lead to improvements, Fig. S7.

#### 3.13. The fcc phase of the Cu-Pt system

Johnson and Faulkenberry [107] determined the Cu and Pt tracer diffusion coefficients in four Cu-Pt alloys at various temperatures. Kubaschewski and Ebert [108] reported interdiffusion coefficients at 13.9 at.% Cu as a function of temperature from diffusion couple experiments while Mishra et al. [109] measured the interdiffusion coefficients over the full composition range at 4 temperatures. However, the data from Mishra et al. do not agree with the impurity diffusion coefficients. Therefore, only the interdiffusion coefficients determined by Kubaschewski and Ebert [108] were used to fit the diffusion model. With such limited interdiffusion coefficient data, the diffusion model is vulnerable to overfitting, as shown in Fig. S8 in the Supplementary Information. The models with 2 or 4 interaction parameters predict unrealistic Pt tracer diffusion coefficients, pushing the predicted lines below the data range in subfigures (k) and (l) of Fig. S8. The 0-parameter model works for this binary system, but the 1-parameter model yields better agreement and is the best choice for this binary system.

# 3.14. The fcc phase in the Fe-Ni system

Interdiffusion coefficients of Fe-Ni were obtained via diffusion couples at temperatures between 1136°C and 1356°C by Badia and Vignes [72], between 1100°C and 1300°C by Borovskiy et al. [94], between 950°C and 1100°C by Ganeshan et al. [110], and between 705 and 1426°C by Ustad and Sorum [86], respectively. Million et al. [111] determined the Fe and Ni tracer diffusion coefficients between 985°C and 1305°C using radioisotopes and measured the interdiffusion coefficients from diffusion couples in the temperature range of 950 – 1250°C at the full composition range. The intrinsic and interdiffusion coefficients at 1200°C were reported by Levasseur and Philibert [112] using diffusion couples. Kohn et al. [82] used radioactive Fe and Ni to determine the tracer diffusion coefficients of the Fe-Ni system and employed diffusion couples to determine the interdiffusion and intrinsic diffusion coefficients at

1200°C. The diffusion model with different interaction parameters was fed with the collected interdiffusion coefficients except some datasets which disagree with the impurity diffusion coefficients. The model test results are compared in Fig. S9 in the Supplementary Information, showing that the 0-parameter model serves as a rough approximation, the 1-parameter model improve the model performance, and additional fitting parameters do not lead to improvement.

# 3.15. The fcc phase of the Ni-Pd system

van Dal et al. [47] measured the intrinsic and interdiffusion coefficients of the Ni-Pd binary system between 900°C and 1200°C with incremental and multi-foil diffusion couples. Those interdiffusion coefficients are fed to the diffusion model with various interaction parameters and the results were summarized in Fig. S10 in the Supplementary Information, showing that the 0-parameter model does not work for this binary system, the 1-parameter model substantially improves the model performance, and additional fitting parameters do not lead to too much improvement.

# 3.16. The bcc phase of the Nb-V system

Interdiffusion coefficients of the Nb-V system at various temperatures have been determined using diffusion couples. Vergasova et al. [66] measured the values at 1300 - 1500°C while Babkin et al. [113] and Ugaste et al. [114] conducted experiments at 1500°C and 1200°C, respectively. A temperature range of 1450 - 2075°C was investigated by Roux and Vignes [61]. In addition to interdiffusion coefficients, Geiss et al. [115] and Mokrov and Zharkov [116] also determined the intrinsic diffusion coefficients over the temperatures of 1404 - 1750°C and 1250 - 1710°C, respectively. Overall, all the datasets of interdiffusion coefficients have a similar trend of composition dependence. The data from Babkin et al. [113], Geiss et al. [115] and Mokrov and Zharkov [116] were chosen among them to feed the diffusion model since they are more consistent with one another. The results are summarized in Fig. S11 in the Supplementary Information, showing that the 0-parameter model does not work, the 1-parameter model works really well, and additional fitting parameters do not lead to too much improvement. As a matter of fact, subfigure (1) of Fig. S11 shows sign of over-fitting of the Nb intrinsic diffusion coefficients.

# 3.17. The bcc phase of the Nb-Zr system

Both Nb and Zr tracer diffusion coefficients were determined by Herzig et al. [117] at 5.5 at.%, 16.3 at.% and 28.1 at.% Nb over a temperature range of 762 - 1598°C, and by Tiwari et al. [118] at 1 wt.% and 2 wt.% Nb over a temperature range of 900 - 1200°C. Zou et al. [119] measured the Nb diffusion coefficients in a Zr-19 at.% Nb alloy between 647°C and 894°C. Interdiffusion between Nb and Zr has been investigated extensively by several research groups using diffusion couples. Patil et al. [120] determined the interdiffusion coefficients over the full composition range from 1320°C to 1720°C while Balakir et al. [121] measured at 4 temperatures between 700°C and 1500°C and Vergasova et al. [66] measured at 1100°C and 1300°C. On the other hand, Chen et al. [68] and Prasad and Paul [122] only reported the interdiffusion coefficients at the Zr rich side at temperature range of 800 - 1200°C and 1000 -1200°C, respectively. It is because the steep concentration gradients in the Nb-rich side of the diffusion couples is beyond the spatial resolution of the measurement and thus the interdiffusion coefficients could not be determined reliably from such steep-gradient part of the concentration profiles. Consequently, only the interdiffusion coefficients at the Zr-rich side are considered as input to the

diffusion model. Fig. S12 in the Supplementary Information summarizes the results and shows that the 0-parameter model does not work, the 1-parameter model substantially improves the fit to both the interdiffusion and tracer diffusion coefficients, and additional fitting parameters do not lead to further improvement. It is noted that the tracer diffusion coefficients at different compositions in subfigures (m) to (f) were shifted by differnt factors to separate them for visualization purpose.

# 3.18. The bcc phase of the Ta-Ti system

Fedotov et al. [64] employed diffusion couples to determine the interdiffusion coefficients at both 900°C and 1000°C. Ansel et al. [123] investigated the interdiffusion of the Ta-Ti system from 1000°C to 1900°C using various diffusion couples and measured the intrinsic diffusion coefficient at 12.25 at.% Ta of the Kirkendall marker plane. The interdiffusion coefficients in the Ti-rich region were reported by Chen et al. [68] since they realized the problem associated with the steep concentration gradients in the Ta-rich part of the diffusion profiles as explained earlier [57]. The "bendover" region of the interdiffusion coefficients in the Ta-rich compositions obtained by Ansel et al. [123] are not reliable and were excluded from being used to fitting the diffusion model. Fig. S13 in the Supplementary Information shows that the model with 1 interaction parameter performs better than the others in predicting the intrinsic diffusion coefficients. The 0-parameter model does not fit the interdiffusion coefficients well for this binary system.

# 3.19. The bcc phase of the Ti-V system

Murdock et al. [124] measured the tracer diffusion coefficients of the Ti-V systems at 10 wt.% increments over the entire composition range from 900°C to about 50°C below the melting points. Diffusion couples were employed by various groups to obtain the interdiffusion coefficients. Carlson [125] reported the interdiffusion coefficients and determined the intrinsic diffusion coefficients of the marker plane compositions at 1350°C. Interdiffusion coefficients at several temperatures from 1000°C to 1400°C were measured over the full composition range by Ugaste and Zajkin [62]. Zhu et al. [67] reported the interdiffusion coefficients in the temperature range of 800 - 1200°C while Fedotov et al. [64] obtained the data in the range of 900 - 1500°C but their data seem to be problematic since their datasets at 900°C and 1000°C overlap each other and the data overlap again at 1350°C and 1500°C. Interdiffusion coefficients from 900 to 1200°C was reported by Kale et al. [126] but their data show the characteristic "bend-over" at high V concentrations, leading to orders of magnitude disagreement with the reliable impurity diffusion coefficient of Ti in V, as shown in Fig. S14 in the Supplementary Information. Thus, only the interdiffusion coefficients at the Ti-rich side were fed to the diffusion model. The results in Fig. S14 show that 0-parameter model does not work, the model with 1 interaction parameter has comparable performance with models with 2 or 4 fitting parameters.

#### 3.20. The bcc phase of the Ti-Zr system

Herzig et al. [127] measured the Ti and Zr tracer diffusion coefficients in a Ti-49 at.% Zr alloy at various temperatures. Thibon et al. [128] determined the interdiffusion coefficients using diffusion couples over a wide temperature range from 830 to 1730°C while Bhanumurthy et al. [129] reported data at 900°C. The temperature range investigated by Brunsch and Steeb [130] is 650 – 1050°C and Raghunathan et al. [131] conducted diffusion couple experiments from 901 to 1068°C. Chen et al. [68] and Zhu et al. [67] employed diffusion multiples to obtain the interdiffusion coefficients in the temperature range of 800 – 1200°C and

900 – 1100°C, respectively. Most of the collected interdiffusion coefficients were used to fit the diffusion model, except for the data from Bhanumurthy et al. [129], which deviate from the composition dependence of other datasets. The modeling results are shown in Fig. S15 in the Supplementary Information and are very similar to the other bcc systems: the 0-parameter model does not work, the 1-parameter model works well, and additional fitting parameters add no benefits.

# 3.21. Quantitative evaluation of the models

The assessed self-diffusion and impurity diffusion coefficients of the pure elements and the computed thermodynamic factors are the foundation upon which diffusion models of the 18 binary systems are built. The critically reviewed interdiffusion coefficients are then employed to optimize the 1, 2, and 4 interaction parameters in the diffusion models; and the models are tested using the experimental tracer and intrinsic diffusion coefficients. Qualitative comparisons between the modelled and experimental diffusion data as functions of composition and temperature are shown and discussed system by system in the previous sections and in the Supplementary Information. For a few systems such as the Ag-Au, Co-Fe, Co-Ni, Cu-Ni, Cu-Pt, Fe-Ni, Ge-Si, and Nb-Ti systems, the 0parameter "ideal"-behavior model can serve as the first-order approximation. Generally, the 1-parameter model performs well in comparison with the 0-parameter model. Further increase of the number of fitting parameters does not lead to better prediction of the tracer and intrinsic diffusion coefficients; and as a matter of fact, has led to overfitting in a number of systems.

This section provides a more quantitative evaluation of the quality of the models with 0, 1, 2 and 4 fitting parameters. Here, the mean absolute error (*MAE*) is defined to quantify the model performance on the test datasets (tracer and intrinsic diffusion coefficients):

$$MAE = \frac{1}{n} \sum_{i=1}^{n} \left| \log_{10} D_i^{\text{exp}} - \log_{10} D_i^{\text{pred}} \right|$$
 (10)

Where n is the number of data points,  $D_i^{exp}$  and  $D_i^{pred}$  are the experimental diffusion coefficients and predicted diffusion coefficients of the ith data point, respectively.

Fig. 8 shows the  $D^{exp}$  versus  $D^{pred}$  calculated by the models with 0, 1, 2 and 4 interaction parameters for the various binary systems examined in this study. The diagonal black dashed line represent a perfect agreement while the dotted lines represent a deviation with a factor of 3 or 1/3. The calculated MAE are also presented on the subfigures. The first row (subfigures (a) to (d)) in Fig. 8 shows that for the 11 fcc binary systems, the MAE drops from 0.308 to 0.154 as the first fitting parameter is introduced. The 2-parameter and 4-parameters models have worse MAE, 0.335 and 0.276, respectively. For the 6 bcc binary systems, the 1-parameter and 2-parameter models have a very similar MAE, 0.126 and 0.124, respectively; thus the 1-parameter model is highly preferred without the burden of fitting the second parameter, as shown in the second row (subfigures (f) to (i)) of Fig. 8. For the diamond cubic phase of the Ge-Si binary system, the 1-parameter model has the lowest MAE and thus the best performance, as shown in the third row (subfigures (k) to (n)) in Fig. 8. For the entire 18 binary systems, the 1-parameter model also has the lowest MAE, as shown in the bottom row (subfigures (p) to (s)) of Fig. 8. It is clear that the 1-parameter is the best and most robust model in consideration of all the 18 binary systems. The extracted binary fitting parameters of the 18 systems coupled with Thermo-Calc Software databases are summarized in Table 3. For the readers without access to the CALPHAD software, the interaction parameters coupled with the thermodynamic assessments in the open literature are also listed

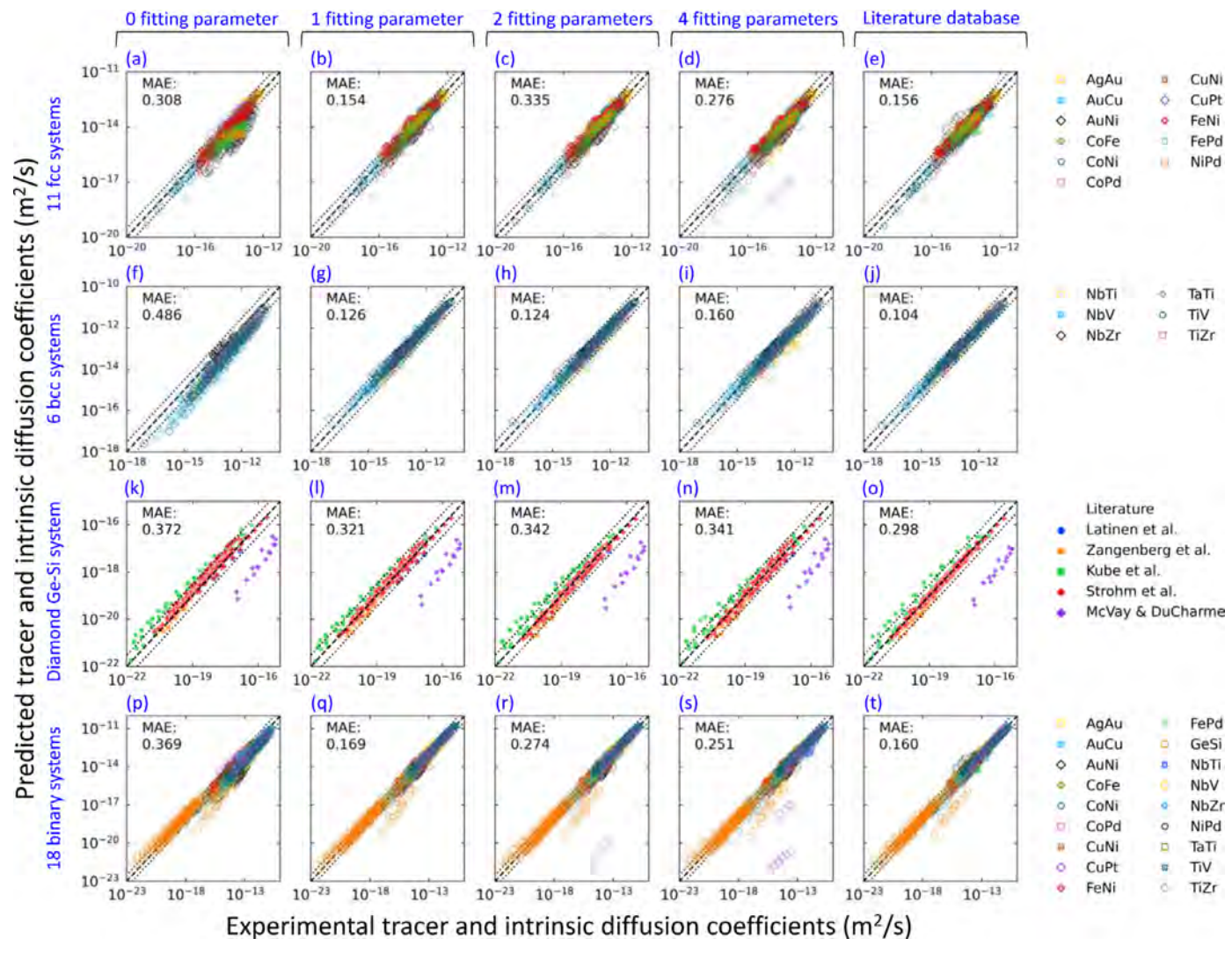


Fig. 8. Comparison of the mean absolute error (MAE) between experimental and predicted tracer and intrinsic diffusion coefficients of the 18 binary systems modeled with 0, 1, 2 and 4 fitting parameters as well as the mobility assessments in the literature.

**Table 3**The assessed binary interaction parameter  $\Phi^{A,B}$  in  $(m^2 \cdot J)/(mol \cdot s)$  of the 18 binary systems by fitting the most reliable tracer, intrinsic and interdiffusion data, coupled with the Thermo-Calc Software databases and thermodynamic assessments in the literature, respectively, and the number of interaction parameters used in the mobility assessments in the literature.

System	Interaction parameter $\Phi^{A,B}$ obtained in this study and the coupled thermodynamic databases				Number of interaction parameters used in the mobility assessments in the literature		
	$\overline{\Phi^{A,B}}$	Thermodynamic database	$\Phi^{A,B}$	Thermodynamic assessment			
Ag-Au, fcc	-15021	TCCU3	-15021	[132]	6	[18]	
Au-Cu, fcc	43282	TCCU3	43282	[133]	4	[23]	
Au-Ni, fcc	97519	TCSLD3	97519	[134]	5	[135]	
Co-Fe, fcc	7120	TCFE10	7120	[136]	4	[22]	
Co-Ni, fcc	15096	TCNI9	15096	[137]	2	[22]	
Co-Pd, fcc	146463	TCNI9	152325	[138]	6	[139]	
Cu-Ni, fcc	1083	TCNI9	1089	[140]	4	[25]	
Cu-Pt, fcc	-39856	TCNI9	-39856	[141]	6	[23]	
Fe-Ni, fcc	49942	TCFE10	49942	[142]	8	[143]	
Fe-Pd, fcc	92766	TCNI9	92766	[138]	4	[21]	
Ge-Si, dia. cubic	-29367	[38]	-29367	[38]	7	[24]	
Nb-Ti, bcc	77831	TCTI2	82692	[144]	4	[27]	
Nb-V, bcc	132825	TCTI2	132825	[145]	6	[31]	
Nb-Zr, bcc	127691	TCTI2	127690	[146]	6	[30]	
Ni-Pd, fcc	115134	TCNI9	115134	[138]	4	[147]	
Ta-Ti, bcc	102859	TCTI2	102858	[148]	4	[26]	
Ti-V, bcc	79863	TCTI2	87171	[145]	6	[28]	
Ti-Zr, bcc	35125	TCTI2	45835	[149]	6	[29]	

in Table 3. In addition, one can easily implement the 1-parameter model without the use of a CALPHAD software by following the guide in the next section.

The tracer and intrinsic diffusion coefficients calculated using the mobility parameters assessed in the literature (references listed in Table 3) are also compared in Fig. 8 as subfigures (e), (j), (o) and (t) - the right-hand side column. It is noted that the mobility assessments in the literature employed all the diffusion data including the tracer and intrinsic diffusion coefficients. In contrast, only interdiffusion coefficients were used to optimize the fitting parameters in the model in the results reported in Figs. 4-8 while both the tracer and intrinsic diffusion coefficients served as test datasets only. Consequently, the mobility assessments in the literature are supposed to give smaller error or MAE since both the tracer and intrinsic diffusion coefficients were also used to optimize their mobility parameters. When the most reliable experimental tracer, intrinsic and interdiffusion coefficients were employed together to optimize the sole constant  $\Phi^{A,B}$  as reported in Table 3, the MAE for the 1-parameter model drops from 0.169 to 0.161 for the 18 binary systems together, comparable to the MAE value of 0.160 of the literature mobility assessments. Therefore, the 1-parameter model in current study shows comparable performance to the literature atomic mobility assessments in predicting the tracer and intrinsic diffusion coefficients, as shown in Fig. 8; yet, the number of interaction parameters used in the literature mobility assessments (summarized in Table 3) is way more than the 1-parameter model: except for the Co-Ni binary system where 2 parameters were used, all the other 17 binary systems used 4 to 8 parameters. To the authors' knowledge, no literature assessments used a single parameter model as emerged from the current study. This comparison suggests that too many parameters were used in most of the literature atomic mobility assessments/databases (except for Co-Ni), leading to risk of overfitting. The 1-parameter model revealed in this study is very simple yet robust.

#### 4. Further discussion

It is straightforward to implement the 1-parameter diffusion model for a binary A-B system. The first step is to collect the self-diffusion coefficients of both pure A  $(D_A^A)$  and pure B  $(D_B^B)$  and the impurity diffusion coefficient of A in pure B  $(D_A^B)$  and B in pure A  $(D_B^A)$  from the literature similar to those listed in Table 2 (and shown in Fig. S1 in the Supplementary Information).

The thermodynamic factor  $\varphi$  then needs to be computed using a CALPHAD software package or through the following process directly from a thermodynamic assessment of the A-B binary system. The molar Gibbs free energy G of a simple solution phase (fcc, bcc, hcp, diamond cubic, etc.) is usually modelled as the following in the CALPHAD approach:

$$G = x_A G_A^0 + x_B G_B^0 + RT(x_A \ln x_A + x_B \ln x_B) + x_A x_B \sum_{k=0,1,\dots} L_k (x_A - x_B)^k$$
(11)

Where  $G_A^0$  and  $G_B^0$  are the molar Gibbs energies of the pure elements or the so-called lattice stabilities, and thus the first two terms on the right hand side of Eq. (11) is the contribution from the Gibbs energy of the constituents of the phase based on the rule of mixture. The third term is the contribution of the ideal entropy of mixing. The last term is the excess Gibbs energy, which is expressed as the Redlich-Kister polynomial where the  $L_k$  values are the related coefficients.

It is straightforward to calculate the thermodynamic factors according to Eq. (5). Combining Eq. (5) and the above Eq. (11), the

thermodynamic factor is computed as:

$$\varphi = 1 - \frac{2x_A x_B}{RT} \left[ \sum_{k=0,1,\dots} (2k+1) L_k (x_A - x_B)^k - 2x_A x_B \sum_{k=2,3,\dots} k(k-1) L_k (x_A - x_B)^{k-2} \right]$$
(12)

Only the parameters  $L_k$  of the molar Gibbs free energy G are needed while other terms disappear due to the derivatives (The ideal mixing term becomes 1). The  $L_k$  values can be directly read from the published thermodynamic assessments in the literature (It is noted that thermodynamic assessments are available in the open literature for most binary systems). Generally, the order of k is up to 2 for most binary systems; and thus the thermodynamic factor is simplified to:

$$\varphi = 1 - \frac{2x_A x_B L_0}{RT}$$
 for  $k = 0$  (13.1)

$$\varphi = 1 - \frac{2x_A x_B}{RT} [L_0 + 3L_1 (x_A - x_B)] \quad \text{for } k = 1$$
 (13.2)

$$\varphi = 1 - \frac{2x_A x_B}{RT} \left[ L_0 + 3L_1 (x_A - x_B) + 5L_2 (x_A - x_B)^2 - 4L_2 x_A x_B \right]$$
for  $k = 2$  (13.3)

For example, the thermodynamic factor of the Ge-Si system can be calculated with the parameters in the thermodynamic assessment by Berche et al. [38] who reported  $L_0=3500\ J/mol$  and the higher order  $L_k$  values were all zero. Therefore, the thermodynamic factor of the Ge-Si system is simply:

$$\varphi^{Ge-Si} = 1 - \frac{2x_{Ge}x_{Si}L_0}{RT}$$

It is noted that the magnetic contribution to the molar Gibbs free energy is ignored in the above Eqs. (11–13), but its effect on the thermodynamic factor is usually negligible except for compositions very close to the Curie temperature or the Néel temperature. One can also add the equation of the magnetic contribution, available from the pertinent binary thermodynamic assessments in the literature, to Eq. (11) and take a second derivative against composition ( $x_B$ ) to include the magnetic contribution directly.

With the self-diffusion coefficients  $(D_A^B \text{ and } D_B^B)$  and the impurity diffusion coefficients  $(D_A^B \text{ and } D_B^A)$  of both pure elements known and the thermodynamic factor  $\varphi$  computed as described above, experimental composition-dependent interdiffusion coefficient  $\tilde{D}$  values are then employed to fit/optimize a single unknown parameter  $\Phi^{A,B}$  which is a constant (not a+bT) in Eq. (14):

$$\tilde{D} = \left[ x_B \exp\left( x_A \ln D_A^A + x_B \ln D_A^B \right) + x_A \exp\left( x_A \ln D_B^A + x_B \ln D_B^B \right) \right] \cdot \varphi \exp\left( \Phi^{A,B} x_A x_B / RT \right)$$
(14)

After the constant  $\Phi^{A,B}$  is obtained (such as the values in Table 3), the interdiffusion coefficients at any composition and temperature can be computed from Eq. (14). The tracer diffusion coefficient  $D_i^*$  (i = A or B) of any composition at any temperature can be computed via Eq. (15):

$$D_i^* = \exp\left(x_A \ln D_i^A + x_B \ln D_i^B\right) \exp\left(\Phi^{A,B} x_A x_B / RT\right)$$
 (15)

The intrinsic diffusion coefficient  $D_i^l = D_i^* \varphi$  is simply the tracer diffusion coefficient multiplied by the thermodynamic factor. In this way, all the diffusion coefficients in the binary A-B system can be computed. For the convenience of future reference to this 1-parameter model, it is hereby called Z-Z-Z binary diffusion model.

In practical assessments, all the experimental data for a binary solid solution, including tracer, intrinsic and interdiffusion coefficients, should be used *together* to optimize the constant  $\Phi^{A,B}$  using both Eq. (14) and (15) as well as  $D_i^I = D_i^* \varphi$ . In this way, the optimized  $\Phi^{A,B}$  value represents the best description of the diffusion behavior of the solid solution. It is noted that the  $\Phi^{A,B}$  values reported in Table 3 are obtained by fitting the most reliable experimental tracer, intrinsic and interdiffusion coefficients for each binary system.

For those who use a CALPHAD software package such as Thermo-Calc for atomic mobility (diffusion coefficient) assessments, the implementation of the Z-Z-Z model is even simpler since the thermodynamic factor can be computed within the software. The mobility interaction parameters are usually set to be:  $\Phi_A^{A,B} = V_1 + V_2 * T$  and  $\Phi_B^{A,B} = V_3 + V_4 * T$ , where  $V_1,\ V_2,\ V_3$  and  $V_4$  are variables/constants to be optimized from experimental diffusion coefficients. To implement the Z-Z-Z model, one simply sets both  $V_2$  and  $V_4$  to be zero, and  $V_1$  and  $V_3$  to be equal. In other words, one can simply set  $\Phi_A^{A,B} = V_1$  and  $\Phi_B^{A,B} = V_1$ , and optimize only one parameter,  $V_1$ . The optimized  $V_1$  should be the same as the  $\Phi^{A,B}$  obtained without using a CALPHAD package.

Our systematic test of the model parameters clearly shows that the temperature dependent terms  $V_2 * T$  and  $V_4 * T$  are completely unnecessary for all the 18 systems tested in this study. Even for the Nb-Ti binary system whose experimental diffusion coefficient data cover ~9 orders of magnitude (~10<sup>-11</sup> to ~10<sup>-20</sup> m²/s) and over a temperature range spanning ~ 1200°C (from ~800°C to ~2000°C), the temperature-dependent fitting terms are not needed to model this system, Fig. 7. In other words, the temperature dependence of diffusion coefficients of *alloys* is well described by the temperature-dependence of the self-diffusion and impurity diffusion coefficients of the *pure elements* as well as the thermodynamic factor. One can see from Fig. 3 that the thermodynamic factor is temperature dependent.

When the single constant  $\Phi^{A,B}$  in the Z-Z-Z model as represented by Eqs. (14) and (15) is zero, the Z-Z-Z model becomes the zeroth-order zero-parameter (Z-Z) model of Eqs. (16) and (17), which represents a kinetically ideal-behaving system (it still includes the thermodynamic factor, thus not a thermodynamically ideal-behaving system).

$$\tilde{D} = \left[ x_B \exp\left( x_A \ln D_A^A + x_B \ln D_A^B \right) + x_A \exp\left( x_A \ln D_B^A + x_B \ln D_B^B \right) \right] \cdot \varphi$$
(16)

$$D_i^* = \exp\left(x_A \ln D_i^A + x_B \ln D_i^B\right) \tag{17}$$

As a matter of fact, the Z-Z model does a reasonable job in describing the behavior of several systems as shown in the left-hand side column of Fig. 4 (Ag-Au), Fig. 6 (Ge-Si), Fig. 7 (Nb-Ti), Fig. S4 (Co-Fe), Fig. S5 (Co-Ni), Fig. S7 (Cu-Ni), Fig. S8 (Cu-Pt), Fig. S9 (Fe-Ni), Fig. S13 (Ta-Ti), Fig. S14 (Ti-V), and Fig. S15 (Ti-Zr) [The figures whose numbers have an "S" are in the Supplementary Information]. When no interdiffusion coefficient or other diffusion data are available for a particular binary system, it is recommended that the Z-Z model which contains only diffusion coefficients of the *pure elements* and the thermodynamic factor, be employed to estimate the diffusion coefficients of *alloys* in the binary system. The Z-Z model estimate will be much better than no data at all or using any of the single diffusion (either self-diffusion or impurity diffusion) coefficient of the *pure elements* as an estimate for the *alloys*.

The surprisingly excellent performance of the Z-Z-Z model for all 18 diverse binary systems implies that the "excess" behavior (i.e., deviation from the kinetically ideal behavior) for both elements in a binary solid solution is similar. It is noted that the atomic mobility of each element can be orders of magnitude different, yet the deviation of each element from its ideal atomic mo-

bility behavior is similar. This in a sense is similar to the fact that the molar Gibbs free energy of the pure elements in a binary system is very different, yet the thermodynamic factor for diffusion, which describes the deviation from the ideal mixing behavior, of both elements are the same based on the Gibbs-Duhem relation. Future theoretical analysis may reveal if an equivalent Gibbs-Duhem relation may hold to some extent for atomic mobilities of binary solid solutions.

When more and more binary systems are assessed in the future using the Z-Z-Z model, the values of the single constant  $\Phi^{A,B}$  (as those listed in Table 3) may be correlated with some other parameters of the binary systems, e.g., the degree of deviation of composition-dependent lattice parameters or/and elastic constants from the Vegard's law. Such correlations may be revealed through either simple data analyses or the use of machine learning tools; and they will be very useful in estimating the diffusion coefficients of *alloys* using the Z-Z-Z model for binary systems whose experimental diffusion coefficients of *alloys* are unavailable.

# 5. Conclusions and Concluding Remarks

Four fitting parameters are often employed to model the diffusion coefficients (atomic mobilities) of a binary solid solution in the widely used framework established by Ågren and Andersson; i.e., two parameters (a+bT) for each diffusing element for each phase [7,8]. Up to 6 and 8 fitting parameters are used for several binary systems, as shown in Table 3. Our study is the most comprehensive test to date aiming at defining the optimal number of fitting parameters for a reliable mathematical description of the diffusion behavior of a binary solid solution.

After an exhaustive search of the literature, 18 completely soluble binary systems were identified that satisfy the following conditions: (1) reliable self-diffusion coefficients and impurity diffusion coefficients of both pure elements are available, (2) reliable composition-dependent interdiffusion coefficients are available, and (3) there are experimental measurements of tracer diffusion and/or intrinsic diffusion coefficients to be used to check the predictions from the diffusion coefficient models with various number of fitting parameters. These 18 binaries cover a very wide range of thermodynamic behavior as shown by the diverse thermodynamic factor in Fig. 3, including very asymmetrical systems such as Au-Cu, Au-Ni, Co-Pd, Cu-Pt, Fe-Ni, Fe-Pd, and Ni-Pd. The experimental diffusion coefficients (self-diffusion, impurity diffusion, tracer diffusion, intrinsic diffusion and interdiffusion coefficients) in these 18 binary systems were collected and reviewed. A systematic test of the CALPHAD diffusion coefficient (atomic mobility) models with 0, 1, 2 and 4 fitting parameters was then performed on these 18 binary systems.

Our systematic testing of the 18 diverse binary systems has yielded a surprisingly simple model with only one fitting parameter. The Z-Z-Z model is described by Eqs. (14) and (15), and the single constant  $\Phi^{A,B}$  in these equations can be evaluated from experimental diffusion data. The rest of the quantities in these equations are the properties (self-diffusion and impurity diffusion coefficients) of the pure elements and the thermodynamic factor that can be computed from a CALPHAD thermodynamic assessment of the pertinent binary system.

The 1-parameter Z-Z-Z model has been demonstrated to be very reliable and robust since the 18 binary systems tested in our study include very asymmetrical systems such as Co-Pd and Fe-Pd (Fig. 3) as well as Nb-Ti whose experimental diffusion coefficient data cover ~9 orders of magnitude (~10<sup>-11</sup> to ~10<sup>-20</sup> m²/s) and over a temperature range spanning ~ 1200°C (from ~800°C to ~2000°C). For all of them, the Z-Z-Z model works well. Additional fitting parameters do not lead to appreciable improvement of model performance and as a matter of fact sometimes lead to over-fitting.

The Z-Z-Z model allows both tracer and intrinsic diffusion coefficients to be reliably computed for any composition at any temperature after the  $\Phi^{A,B}$  parameter/constant is evaluated/fitted from the interdiffusion data. This has been demonstrated for all 18 binary systems tested in this study. This conclusion is already embedded in the CALPHAD atomic mobility treatment/framework, but might be less apparent to those who are not familiar with the atomic mobility notation.

When no interdiffusion or other (tracer and intrinsic) diffusion coefficient data of *alloys* are available for a particular binary system, it is recommended that the zeroth-order zero-parameter (Z-Z) model, as represented in Eqs. (16) and (17) that contain only diffusion coefficients of the *pure elements* and the thermodynamic factor, be employed to estimate the diffusion coefficients of *alloys*.

Our next step is to extend the Z-Z-Z model into ternary systems to help reduce the number of fitting parameters for ternary and higher-order solid solutions. When the number of fitting parameters in each binary is reduced from 4 to 1, the total number from the three binaries is reduced from 12 to 3. Even when the number for each binary is reduced from 2 to 1, the binary-related parameters are reduced from 6 to 3. A systematic test of ternary systems will reveal how many additional ternary related interaction parameters will need to be introduced to reliably describe the diffusion behavior of ternary solid solutions. The reduction in the number of fitting parameters for binary and ternary systems will substantially reduce the total number of parameters for multicomponent systems and yet improve the robustness of the resultant diffusion (atomic mobility) databases.

# **Declaration of Competing Interest**

The authors declare that they have no known competing financial interests or personal relationships that could have appeared to influence the work reported in this paper

# Acknowledgements

This study was mainly supported by the Division of Materials Research (DMR) of the National Science Foundation (NSF) through award number NSF-DMR-1904245. Additional financial support was provided by the University of Maryland through the startup fund of Prof. J.-C. Zhao.

# Supplementary materials

Supplementary material associated with this article can be found, in the online version, at doi:10.1016/j.actamat.2021.117077.

# References

- [1] N. Saunders, A.P. Miodownik, CALPHAD, Pergamon, 1998.
- [2] H.L. Lukas, S.G. Fries, B. Sundman, Computational thermodynamics: the Calphad method, 2007. doi:10.1017/CBO9780511804137.
- [3] L. Kaufman, J. Ågren, CALPHAD, first and second generation Birth of the materials genome, Scr. Mater. 70 (2014) 3-6, doi:10.1016/j.scriptamat.2012.12. 003.
- [4] C.E. Campbell, U.R. Kattner, Z.K. Liu, The development of phase-based property data using the CALPHAD method and infrastructure needs, Integr. Mater. Manuf. Innov. 3 (2014) 158–180, doi:10.1186/2193-9772-3-12.
- [5] Z.-K. Liu, Computational thermodynamics and its applications, Acta Mater. 200 (2020) 745–792, doi:10.1016/j.actamat.2020.08.008.
   [6] Z.K. Liu, Y. Wang, Computational Thermodynamics of Materials, Computational T
- [6] Z.K. Liu, Y. Wang, Computational Thermodynamics of Materials, Computational Thermodynamics of Materials, Cambridge University Press, 2016.
- [7] J. Ågren, Diffusion in phases with several components and sublattices, J. Phys. Chem. Solids. 43 (1982) 421–430, doi:10.1016/0022-3697(82)90152-4.
- [8] J.O. Andersson, J. Ågren, Models for numerical treatment of multicomponent diffusion in simple phases, J. Appl. Phys. 72 (1992) 1350–1355, doi:10.1063/1. 351745.
- [9] H. Mehrer, Diffusion in Solid Metals and Alloys, Landolt-Börnstein Group III Condensed Matter, 26, Springer-Verlag, Berlin/Heidelberg, 1990, doi:10.1007/ b37801.

[10] L.S. Darken, Diffusion, mobility and their interrelation through free energy in binary metallic systems, Trans. AIME. (1948) 184–201, doi:10.1007/s11661-010-0177-7.

- [11] J. Ågren, Numerical treatment of diffusional reactions in multicomponent alloys, J. Phys. Chem. Solids. 43 (1982) 385–391, doi:10.1016/0022-3697(82)
- [12] O. Redlich, A.T. Kister, Algebraic representation of thermodynamic properties and the classification of solutions, Ind. Eng. Chem. (1948), doi:10.1021/je50458a036.
- [13] W.F. Gale, T.C. Totemeier, Smithells Metals Reference Book, 2003, doi:10.5860/ choice.42-1588.
- [14] G. Neumann, C. Tuijn, Self-Diffusion and Impurity Diffusion in Pure Metals: Handbook of Experimental Data, Elsevier, 2011.
- [15] A.A. Kodentsov, G.F. Bastin, F.J.J. Van Loo, The diffusion couple technique in phase diagram determination, J. Alloys Compd. 320 (2001) 207–217, doi:10. 1016/S0925-8388(00)01487-0.
- [16] G. Ghosh, Dissolution and interfacial reactions of thin-film Ti/Ni/Ag metallizations in solder joints, Acta Mater. 49 (2001) 2609–2624, doi:10.1016/ S1359-6454(01)00187-2.
- [17] C.E. Campbell, W.J. Boettinger, U.R. Kattner, Development of a diffusion mobility database for Ni-base superalloys, Acta Mater. 50 (2002) 775–792, doi:10.1016/S1359-6454(01)00383-4.
- [18] Y. Liu, L. Zhang, D. Yu, Y. Ge, Study of diffusion and marker movement in FCC Ag-Au alloys, J. Phase Equilibria Diffus. 29 (2008) 405–413, doi:10.1007/ s11669-008-9355-3.
- [19] H. Wu, T. Mayeshiba, D. Morgan, High-throughput ab-initio dilute solute diffusion database, Sci. Data. 3 (2016) 1–11, doi:10.1038/sdata.2016.54.
- [20] S.S. Naghavi, V.I. Hegde, C. Wolverton, Diffusion coefficients of transition metals in FCC cobalt, Acta Mater 132 (2017) 467–478, doi:10.1016/j.actamat.2017. 04.060
- [21] Y. Liu, J. Wang, Y. Du, L. Zhang, D. Liang, Mobilities and diffusivities in fcc Fe-X (X = Ag, Au, Cu, Pd and Pt) alloys, Calphad 34 (2010) 253–262, doi:10. 1016/j.calphad.2010.04.002.
- [22] Y.W. Cui, M. Jiang, I. Ohnuma, K. Oikawa, R. Kainuma, K. Ishida, Computational study of atomic mobility for fcc phase of Co-Fe and Co-Ni binaries, J. Phase Equilibria Diffus. 29 (2008) 2–10, doi:10.1007/s11669-007-9238-z.
- [23] Y. Liu, L. Zhang, D. Yu, Diffusion mobilities in fcc Cu-Au and fcc Cu-Pt alloys, J. Phase Equilibria Diffus. 30 (2009) 136–145, doi:10.1007/s11669-009-9469-2.
- [24] S.L. Cui, L.J. Zhang, W.B. Zhang, Y. Du, H.H. Xu, Computational study of diffusivities in diamond Ge-Si alloys, J. Min. Metall. Sect. B Metall. 48 (2012) 227–249, doi:10.2298/JMMB111102021C.
- [25] J. Wang, H.S. Liu, L.B. Liu, Z.P. Jin, Assessment of diffusion mobilities in FCC Cu-Ni alloys, Calphad 32 (2008) 94–100, doi:10.1016/j.calphad.2007.08.001.
- [26] Y. Liu, L. Zhang, Y. Du, J. Wang, D. Liang, Study of atomic mobilities and diffusion characteristics in bcc Ti-Ta and Ta-W alloys, Calphad 34 (2010) 310–316, doi:10.1016/j.calphad.2010.06.004.
- [27] Y. Liu, T. Pan, L. Zhang, D. Yu, Y. Ge, Kinetic modeling of diffusion mobilities in bcc Ti-Nb alloys, J. Alloys Compd. 476 (2009) 429–435, doi:10.1016/j.jallcom. 2008.09.019.
- [28] Y. Liu, Y. Ge, D. Yu, T. Pan, L. Zhang, Assessment of the diffusional mobilities in bcc Ti-V alloys, J. Alloys Compd. 470 (2009) 176–182, doi:10.1016/j.jallcom. 2008.02.111.
- [29] Y. Liu, L. Zhang, D. Yu, Computational study of mobilities and diffusivities in bcc Ti-Zr and bcc Ti-Mo alloys, J. Phase Equilibria Diffus. 30 (2009) 334–344, doi:10.1007/s11669-009-9557-3.
- [30] Y. Liu, L. Zhang, T. Pan, D. Yu, Y. Ge, Study of diffusion mobilities of Nb and Zr in bcc Nb-Zr alloys, Calphad 32 (2008) 455-461, doi:10.1016/j.calphad.2008. 06.008.
- [31] Y. Liu, D. Yu, L. Zhang, Y. Ge, Atomic mobilities and diffusional growth in solid phases of the V-Nb and V-Zr systems, Calphad 33 (2009) 425–432, doi:10. 1016/j.calphad.2008.12.008.
- [32] Thermo-Calc Software TCNI9 Ni-based alloys database, accessed March, 2021.
- [33] Thermo-Calc Software TCFE10 Steels/Fe-alloys database, accessed March, 2021.
- [34] Thermo-Calc Software TCTI2 Titanium/Titanium Aluminide-based alloys database, accessed March, 2021.
- [35] Thermo-Calc Software TCSLD3 Solder alloys database, accessed March, 2021.
- [36] Thermo-Calc Software TCCU3 Copper-based alloys database, accessed March, 2021.
- [37] J.O. Andersson, T. Helander, L. Höglund, P. Shi, B. Sundman, Thermo-Calc & DICTRA, computational tools for materials science, Calphad 26 (2002) 273–312, doi:10.1016/S0364-5916(02)00037-8.
- [38] A. Berche, J.C. Tédenac, P. Jund, Ab-initio calculations and CALPHAD description of Cr-Ge-Mn and Cr-Ge-Si, Calphad 49 (2015) 50-57, doi:10.1016/j.calphad.2015.02.004.
- [39] H.W. Mead, C.E. Birchenall, Diffusion in gold and Au-Ag alloys, JOM 9 (1957) 874–877, doi:10.1007/bf03397933.
- [40] W.C. Mallard, A.B. Gardner, R.F. Bass, L.M. Slifkin, Self-diffusion in silver-gold solid solutions, Phys. Rev. 129 (1963) 617–625, doi:10.1103/PhysRev.129.617.
- [41] W. Johnson, Diffusion experiments on a gold-silver alloy by chemical and radioactive tracer methods, Trans. Am. Inst. Min. Metall. Eng. 147 (1942) 331–346.
- [42] W. Seith, A. Kottmann, Diffusion in solid metals, Angew. Chemie. 64 (1952) 379–391.
- [43] R.W. Balluffi, L.L. Seigle, Diffusion in bimetal vapor-solid couples, J. Appl. Phys. 25 (1954) 607–614, doi:10.1063/1.1721698.

[44] H. Ebert, G. Trommsdorf, Die diffusion von silber in gold, Zeit. Elektrochem. Angew. Phys. Chemie. 54 (1950) 294–296, doi:10.1002/bbpc.19500540411.

- [45] J.P. Gomez, C. Remy, D. Calais, Diffusion chimique et effet Kirkendall dans le systeme fer-palladium, Mem Sci Rev Met 70 (1973) 597–605.
- [46] J. Fillon, D. Calais, Autodiffusion dans les alliages concentres fer-palladium, J. Phys. Chem. Solids. 38 (1977) 81–89, doi:10.1016/0022-3697(77)90150-0.
- [47] M.J.H. Van Dal, M.C.L.P. Pleumeekers, A.A. Kodentsov, F.J.J. Van Loo, Intrinsic diffusion and Kirkendall effect in Ni-Pd and Fe-Pd solid solutions, Acta Mater 48 (2000) 385–396, doi:10.1016/S1359-6454(99)00375-4.
- [48] R. Kube, H. Bracht, J.L. Hansen, A.N. Larsen, E.E. Haller, S. Paul, W. Lerch, Composition dependence of Si and Ge diffusion in relaxed Si<sub>1-x</sub>Ge<sub>x</sub> alloys, J. Appl. Phys. 107 (2010) 3–8, doi:10.1063/1.3380853.
- [49] N.R. Zangenberg, J. Lundsgaard Hansen, J. Fage-Pedersen, A. Nylandsted Larsen, Ge self-diffusion in epitaxial Si<sub>1-x</sub>Ge<sub>x</sub> layers, Phys. Rev. Lett. 87 (2001) 2–5. doi:10.1103/PhysRevLett.87.125901.
- [50] A. Strohm, T. Voss, W. Frank, L. Pauli, J. Raisanen, Self-diffusion of <sup>71</sup>Ge and <sup>31</sup>Si in Si-Ge alloys, Z. Met. 93 (2002) 737–744.
- [51] A. Strohm, T. Voss, W. Frank, J. Räisänen, M. Dietrich, Self-diffusion of <sup>71</sup>Ge in Si-Ge, Phys. B Condens. Matter. 308–310 (2001) 542–545, doi:10.1016/S0921-4526(01)00814-6.
- [52] P. Laitinen, A. Strohm, J. Huikari, A. Nieminen, T. Voss, C. Grodon, I. Riihimäki, M. Kummer, J. Äystö, P. Dendooven, J. Räisänen, W. Frank, Self-diffusion of <sup>31</sup>Si and <sup>71</sup>Ge in relaxed Si<sub>0.20</sub>Ge<sub>0.80</sub> layers, Phys. Rev. Lett. 89 (2002) 1–4, doi:10.1103/PhysRevLett.89.085902.
- [53] G. Xia, J.L. Hoyt, M. Canonico, Si-Ge interdiffusion in strained Si/strained SiGe heterostructures and implications for enhanced mobility metal-oxidesemiconductor field-effect transistors, J. Appl. Phys. 101 (2007) 044901, doi:10.1063/1.2430904.
- [54] M. Gavelle, E.M. Bazizi, E. Scheid, P.F. Fazzini, F. Cristiano, C. Armand, W. Lerch, S. Paul, Y. Campidelli, A. Halimaoui, Detailed investigation of Ge-Si interdiffusion in the full range of Si1-x Gex (0<x<1) composition, J. Appl. Phys. 104 (2008) 113524, doi:10.1063/1.3033378.</p>
- [55] D.B. Aubertine, P.C. McIntyre, Influence of Ge concentration and compressive biaxial stress on interdiffusion in Si-rich SiGe alloy heterostructures, J. Appl. Phys. 97 (2005) 013531, doi:10.1063/1.1828240.
- [56] N. Ozguven, P.C. McIntyre, Silicon-germanium interdiffusion in high-germanium-content epitaxial heterostructures, Appl. Phys. Lett. 92 (2008) 1–4, doi:10.1063/1.2917798.
- [57] Z. Chen, J.C. Zhao, Recommendation for reliable evaluation of diffusion coefficients from diffusion profiles with steep concentration gradients, Materialia 2 (2018) 63–67, doi:10.1016/j.mtla.2018.06.011.
- [58] R.F. Peart, D.H. Tomlin, Diffusion of solute elements in beta-titanium, Acta Metall 10 (1962) 123–134, doi:10.1016/0001-6160(62)90057-3.
- [59] G.B. Gibbs, D. Graham, D.H. Tomlin, Diffusion in titanium and titanium—niobium alloys, Philos. Mag 8 (1963) 1269–1282, doi:10.1080/ 14786436308207292.
- [60] A.E. Pontau, D. Lazarus, Diffusion of titanium and niobium in bcc Ti-Nb alloys, Phys. Rev. B. 19 (1979) 4027–4037, doi:10.1103/PhysRevB.19.4027.
- [61] F. Roux, A. Vignes, Diffusion dans les systèmes Ti-Nb, Zr-Nb, V-Nb, Mo-Nb, W-Nb, Rev. Phys. Appliquée. 5 (1970) 393–405, doi:10.1051/rphysap: 0197000503039300.
- [62] Y.E. Ugaste, Y.A. Zaykin, Investigation of mutual diffusion in titanium-vanadium and titanium-niobium systems, Phys. Met. Metallogr. 40 (1975) 567–575.
- [63] V.M. Polyanskii, B.N. Podgorskii, O.D. Makarovets, Diffusion processes in the Ti-Nb system, Svarochnoe Proizv 3 (1971) 9–10.
- [64] S.G. Fedotov, M.G. Chudinov, K.M. Konstantinov, Reciprocal diffusion in the systems Ti-V, Ti-Nb, Ti-Ta and Ti-Mo, Fiz. Met. Met. 27 (1969) 873–876.
- [65] V.I. Gryzunov, B.K. Aitbaev, G. Omasheva, T.I. Fryzunova, Interdiffusion in the titanium-niobium system, Seriya Khim 6 (1993) 29–33.
- [66] L.L. Vergasova, D.A. Prokoshkin, E.V. Vasi, Concentrational and temperature correlation of interdiffusion coefficients in binary Nb alloys, Izv. Akad. Nauk. SSSR, Met. 4 (1970) 198–204.
- [67] L. Zhu, Q. Zhang, Z. Chen, C. Wei, G.M. Cai, L. Jiang, Z. Jin, J.C. Zhao, Measurement of interdiffusion and impurity diffusion coefficients in the bcc phase of the Ti–X (X = Cr, Hf, Mo, Nb, V, Zr) binary systems using diffusion multiples, J. Mater. Sci. 52 (2017) 3255–3268, doi:10.1007/s10853-016-0614-0.
- [68] Z. Chen, Z.K. Liu, J.C. Zhao, Experimental Determination of Impurity and Interdiffusion Coefficients in Seven Ti and Zr Binary Systems Using Diffusion Multiples, Metall. Mater. Trans. A 49 (2018) 3108–3116, doi:10.1007/ s11661-018-4645-9.
- [69] S. Benci, G. Gasparrini, E. Germagnoli, G. Schianchi, Diffusion of gold in Cu<sub>3</sub>Au, J. Phys. Chem. Solids. 26 (1965) 687–690, doi:10.1016/0022-3697(65) 20020 Y
- [70] W.B. Alexander, Studies on Atomic Diffusion in Metals, University fo North Caralina, 1969.
- [71] T. Heumann, T. Rottwinkel, Measurement of the interdiffusion, intrinsic, and tracer diffusion coefficients in Cu-rich Cu-Au solid solutions, J. Nucl. Mater. 70 (1978) 567–570.
- [72] M. Badia, A. Vignes, Interdiffusion and the Kirkendall effect in binary alloys, Mem. Sci. Rev. Met. 66 (1969) 915–927.
- [73] I.B. Borovskii, N.P. Llin, E.L. Loseva, Study of mutual diffusion in Cu-Au system, Tr. Instituta Metall. Im. A.A. Baĭkova. 15 (1963) 32–40.
- [74] M.R. Pinnel, B. Laboratories, Mass Diffusion in Polycrystalline Copper /Electroplated Gold Planar Couples, Metall. Trans. 3 (1972) 1989–1997.

[75] R. Ravi, A. Paul, Diffusion mechanism in the gold-copper system, J. Mater. Sci. Mater. Electron. 23 (2012) 2152–2156, doi:10.1007/s10854-012-0729-2.

- [76] T. Ziebold, R.E. Ogilvie, Ternary diffusion in copper-silver-gold alloys, Trans. AIME. 239 (1967) 942–953.
- [77] A.E. Austin, N.A. Richard, Grain-boundary diffusion of gold in copper, J. Appl. Phys. 33 (1962) 3569–3574, doi:10.1063/1.1702448.
- [78] A.D. Kurtz, B.L. Averbach, M. Cohen, Self-diffusion of gold in gold-nickel alloys, Acta Metall 3 (1955) 442–446, doi:10.1016/0001-6160(55)90132-2.
- [79] J.E. Reynolds, B.L. Averbach, M. Cohen, Self-diffusion and interdiffusion in gold-nickel alloys, Acta Metall 5 (1957) 29–40, doi:10.1016/0001-6160(57) 90152-9
- [80] M.J.H. Van Dal, M.C.L.P. Pleumeekers, A.A. Kodentsov, F.J.J. Van Loo, Diffusion studies and re-examination of the Kirkendall effect in the Au-Ni system, J. Alloys Compd. 309 (2000) 132–140, doi:10.1016/S0925-8388(00)01056-2.
- [81] Y. Iijima, Y. Yamazaki, Interdiffusion between metals of widely different self-diffusion rates, Defect Diffus. Forum. 237–240 (2005) 62–73, doi:10.4028/www.scientific.net/ddf.237-240.62.
- [82] A. Kohn, J. Levasseur, J. Philibert, M. Wanin, Experimental study of the theories of the Kirkendall effect in the iron-nickel and iron-cobalt systems, Acta Metall 18 (1970) 163–173, doi:10.2307/2005321.
- [83] Y.E. Ugaste, A.A. Kodentsov, F. van Loo, Concentration dependence of diffusion coefficients in Co-Ni Fe-Ni and Co-Fe systems, Phys. Met. Met. 88 (1999) 88-94
- [84] S.G. Fishman, D. Gupta, D.S. Lieberman, Diffusivity and isotope-effect measurements in equiatomic Fe-Co, Phys. Rev. B. 2 (1970) 1451–1460, doi:10.1103/PhysRevB.2.1451.
- [85] K. ichi Hirano, M. Cohen, Diffusion of cobalt in iron-cobalt alloys, Trans. Japan Inst. Met. 13 (1972) 96–102, doi:10.2320/matertrans1960.13.96.
- [86] T. Ustad, H. Sørum, Interdiffusion in the Fe-Ni, Ni-Co, and Fe-Co systems, Phys. Status Solidi. 20 (1973) 285–294, doi:10.1002/pssa.2210200129.
- [87] K.-I. Hirano, Y. Iijima, K. Araki, H. Homma, B.K. Hirano, Y. Iijima, K. Araki, H. Homma, Interdiffusion in iron-cobalt alloys, Trans. Iron Steel Inst. Japan 17 (1977) 194–203, doi:10.2355/isijinternational1966.17.194.
- [88] B. Million, J. Kucĕra, Concentration dependence of diffusion of cobalt in nickel-cobalt alloys, Acta Metall 17 (1969) 339–344, doi:10.1016/ 0001-6160(69)90073-X.
- [89] B. Million, J. Kučera, Concentration dependence of nickel diffusion in nickelcobalt alloys, Czechoslov. J. Phys. 21 (1971) 161–171, doi:10.1007/BF01702804.
- [90] K. Hirano, R.P. Agarwala, B.L. Averbach, M. Cohen, Diffusion in cobalt-nickel alloys, J. Appl. Phys. 33 (1962) 3049–3054, doi:10.1063/1.1728564.
- [91] Y. Hirai, Y. Tasaki, M. Kosaka, Study on the Friction-Welded Diffusion Couples-Chemical Diffusion of Co-Ni Alloy at 1100 C, Rep. Gov. Ind. Res. Inst. 22 (1973) 125–131.
- [92] Q. Zhang, J.-C. Zhao, Extracting interdiffusion coefficients from binary diffusion couples using traditional methods and a forward-simulation method, Intermetallics 34 (2013) 132–141, doi:10.1016/j.intermet.2012.11.012.
- [93] V.T. Heumann, A. Kottmann, Uber den ablauf der diffusionsvorgange in substit, Zeit. Metall. 44 (1953) 139–154.
- [94] I.B. Borovskiy, I.D. Marchukova, Y.E. Ugaste, Local X-ray spectranalysis of mutual diffusion in binary systems forming a continuous series of solid solutions II the systems Fe-Ni, Ni-Co, Ni-Pt and Co-Pt, Phys. Met. Metallogr. 24 (1967) 51-56.
- [95] J. Kučera, K. Cíha, K. Stránský, Interdiffusion in the Co-Ni system-I concentration penetration curves and interdiffusion coefficients, Czechoslov. J. Phys. 27 (1977) 758–768, doi:10.1007/BF01589317.
- [96] Y. Iijima, K. Hirano, Interdiffusion in cobalt-nickel alloys, J. Japan Inst. Met. 35 (1971) 511–517.
- [97] Y. Iijima, K. ichi Hirano, Interdiffusion in Co-Pd alloys, Trans. Japan Inst. Met. 13 (1972) 419–424, doi:10.2320/matertrans1960.13.419.
- [98] K. Monma, H. Suto, H. Oikawa, Diffusion of Ni and Cu in nickel-copper alloys, J. Japan Institue Metall. 28 (1964) 192–196.
- [99] K.J. Anusavice, R.T. DeHoff, Diffusion of the tracers Cu67, Ni66, and Zn65 in copper-rich solid solutions in the system Cu-Ni-Zn, Metall. Trans. 3 (1972) 1279–1298, doi:10.1007/bf02642463.
- [100] R. Damköhler, T. Heumann, Experimentelle Untersuchungen zur Klärung des Diffusionsverhaltens kupferreicher Kupfer-Nickel Legierungen, Phys. Status Solidi. 73 (1982) 117–127, doi:10.1002/pssa.2210730115.
- [101] J. Levasseur, J. Philibert, Détermination des coefficients de diffusion intrinsèques par mesure de l'effet Kirkendall, Phys. Status Solidi. 21 (1967) K1–K4, doi:10.1002/pssb.19670210145.
- [102] Y. Iijima, K. Hirano, M. Kikuchi, Determination of intrinsic diffusion coefficients in a wide concentration range of a Cu-Ni couple by the multiple markers method, Trans. Japan Inst. Met. 23 (1982) 19–23, doi:10.2320/matertrans1960.23.19.
- [103] T. Heumann, K.J. Grundhoff, Diffusion and Kirkendall Effect in the Cu-Ni System, Zeit. Metall. 63 (1972) 173–180.
- [104] D.E. Thomas, C.E. Birchenall, Concentration Dependence of Diffusion Coefficients In Metallic Solid Solution, JOM 4 (1952) 867–873, doi:10.1007/ bf03398155.
- [105] I.D. Marchukova, M.I. Miroshkina, Diffusion in the system copper-nickel, Phys. Met. Metallogr. 32 (1971) 1254–1259.
- [106] G. Brunel, G. Cizeron, P. Lacombe, Study of chemical diffusion in copper-nickel couples between 800 and 1060C by the Matano and Hall methods: varaiation of activation energy as a function of concentration, COMPTES RENDUS Hebd. DES SEANCES L Acad. DES Sci. Ser. C. 269 (1969) 895–898.

[107] R.D. Johnson, B.H. Faulkenberry, Diffusion Coefficients of Copper and Platinum into Copper Platinum Alloys. 1963.

- [108] O. Kubaschewski, H. Ebert, Diffusion measurements in gold and platinum alloys, Zeit. Elektrochem. 50 (1944) 138–144.
- [109] B. Mishra, P. Kiruthika, A. Paul, Interdiffusion in the Cu-Pt system, J. Mater. Sci. Mater. Electron. 25 (2014) 1778–1782, doi:10.1007/s10854-014-1798-1.
  [110] V. Ganesan, V. Seetharaman, V.S. Raghunathan, Interdiffusion in the nickel-
- [110] V. Ganesan, V. Seetharaman, V.S. Raghunathan, Interdiffusion in the nickeliron system, Mater. Lett. 2 (1984) 257–262, doi:10.1016/0167-577X(84) 90125-3.
- [111] B. Million, J. Růžičková, J. Velíšek, J. Vřešrál, Diffusion processes in the Fe-Ni system, Mater. Sci. Eng. 50 (1981) 43–52, doi:10.1016/0025-5416(81)90084-7.
- [112] J. Levasseur, J Philibert, Determination des coefficients de diffusion intrinseques par mesure de leffet kirkendall dans le systeme fer-nickel, COMPTES RENDUS Hebd. DES SEANCES L Acad. DES Sci. Ser. C. 264 (1967) 380.
- [113] A.P. Babkin, E.M. Slyusarenko, S.F. Dunaev, Determination of mutual diffusion coefficients in Nb-V system using method of finite thickness interlayers, Vestn. Mosk. Univ. Seriya 2, Khimiya 31 (1990) 361–364 https://inis.iaea.org/search/search.aspx?orig\_q=RN:22033616. accessed March 29, 2020.
- [114] Y.E. Ugaste, E.M. Lazarev, V.N. Pimenov, Investigation of self-diffusion in the systems Nb-V, V-Pd, and Pb-Nb, Izv. Akad. Nauk. SSSR, Met. 2 (1971) 211–215.
- [115] R.C. Geiss, C.S. Hartley, J.E. Steedly, Interdiffusion in niobium-vanadium alloys, J. Less-Common Met. 9 (1965) 309–320, doi:10.1016/0022-5088(65)90114-1.
- [116] A.P. Mokrov, V.M. Zharkov, No Title, Diffuzion Protsessy Met. 1 (1974) 39.
- [117] C. Herzig, U. Köhler, S.V. Divinski, Tracer diffusion and mechanism of non-Arrhenius diffusion behavior of Zr and Nb in body-centered cubic Zr-Nb alloys, J. Appl. Phys. 85 (1999) 8119–8130, doi:10.1063/1.370650.
- [118] G.P. Tiwari, B.D. Sharma, V.S. Raghunathan, R.V. Patil, Self- and solute-diffusion in dilute zirconium-niobium alloys in  $\beta$ -phase, J. Nucl. Mater. 46 (1973) 35–40, doi:10.1016/0022-3115(73)90119-0.
- [119] H. Zou, G.M. Hood, R.J. Schultz, N. Matsuura, J.A. Roy, J.A. Jackman, Diffusion of Hf and Nb in Zr-19%Nb, J. Nucl. Mater. 230 (1996) 36–40, doi:10.1016/0022-3115(96)00024-4.
- [120] R.V. Patil, G.B. Kale, S.P. Garg, Chemical diffusion in Zr-Nb system, J. Nucl. Mater. 223 (1995) 169–173.
- [121] E.A. Balakir, Y.P. Zotov, E.B. Malysheva, V.I. Panchishnyj, Investigation of mutual diffusion in the Zr-Nb system, Izv. Vyss. Uchebnykh Zaved. Tsvetnaya Metall. 4 (1975) 126–128.
- [122] S. Prasad, A. Paul, Interdiffusion in Nb-Mo, Nb-Ti and Nb-Zr systems, Defect Diffus. Forum. 323–325 (2012) 491–496, doi:10.4028/www.scientific.net/DDF. 323-325.491.
- [123] D. Ansel, I. Thibon, M. Boliveau, J. Debuigne, Interdiffusion in the body cubic centered β-phase of Ta-Ti alloys, Acta Mater 46 (1998) 423–430, doi:10.1016/ S1359-6454(97)00272-3.
- [124] J.F. Murdock, C.J. McHargue, Self-diffusion in body-centered cubic titanium-vanadium alloys, Acta Metall 16 (1968) 493–500, doi:10.1016/0001-6160(68)
- [125] P.T. Carlson, Interdiffusion and intrinsic diffusion in binary vanadiumtitanium solid solutions at 1350°C, Metall. Trans. A. 7 (1976) 199–208, doi:10. 1007/BF02644457.
- [126] G.B. Kale, S.K. Khera, G.P. Tiwari, Interdiffusion studies in titanium-vanadium system, Trans. Indian Inst. Met. 29 (1976) 422–425 https://inis.iaea.org/search/search.aspx?orig\_q=RN:8315065. accessed March 292020.
- [127] C. Herzig, U. Köhler, M. Büscher, Temperature Dependence of <sup>44</sup>Ti and <sup>95</sup>Zr Diffusion and of <sup>88</sup>Zr/<sup>95</sup>Zr Isotope Effect in the Equiatomic BCC TiZr-Alloy, Defect Diffus. Forum. 95–98 (1993) 793–798, doi:10.4028/www.scientific.net/ddf.95–98.793.

- [128] I. Thibon, D. Ansel, T. Gloriant, Interdiffusion in  $\beta$ -Ti-Zr binary alloys, J. Alloys Compd. 470 (2009) 127–133, doi:10.1016/j.jallcom.2008.02.082.
- [129] K. Bhanumurthy, A. Laik, G.B. Kale, Novel method of evaluation of diffusion coefficients in Ti-Zr system, Defect Diffus. Forum. 279 (2008) 53–62, doi:10. 4028/www.scientific.net/ddf.279.53.
- [130] A. Brunsch, S. Steeb, Diffusionsuntersuchungen im system Ti-Zr mittels mikrosonde, Zeitschrift Fur Naturforsch.Ung - Sect. A J. Phys. Sci. 29 (1974) 1319–1324, doi:10.1515/zna-1974-0912.
- [131] V.S. Raghunathan, G.P. Tiwari, B.D. Sharma, Chemical diffusion in the  $\beta$  phase of the Zr-Ti alloy system, Metall. Mater. Trans. B. 3 (1972) 783–788, doi:10. 1007/bf02647649.
- [132] S. Hassam, J. Ägren, M. Gaune-Escard, J.P. Bros, The Ag-Au-Si system: experimental and calculated phase diagram, Metall. Trans. A. 21 (1990) 1877–1884 A. doi:10.1007/BF02647235.
- [133] B. Sundman, S.G. Fries, W.A. Oates, A thermodynamic assessment of the Au-Cu system, Calphad 22 (1998) 335–354, doi:10.1016/S0364-5916(98)00034-0.
- [134] J. Wang, X.G. Lu, B. Sundman, X. Su, Thermodynamic assessment of the Au-Ni system, Calphad 29 (2005) 263–268, doi:10.1016/j.calphad.2005.09.004.
- [135] J. Wang, L.B. Liu, H.S. Liu, Z.P. Jin, Assessment of the diffusional mobilities in the face-centred cubic Au-Ni alloys, Calphad 31 (2007) 249–255, doi:10.1016/ j.calphad.2006.11.006.
- [136] A.F. Guillermet, Critical evaluation of the thermodynamic properties of the iron-cobalt system, High Temp. High Press. 19 (1987) 477–499.
- [137] A.F. Guillermet, Assessment of the thermodynamic properties of the Ni-Co system, Zeit. Metall. 78 (1987) 639–647, doi:10.1515/ijmr-1987-780905.
- [138] G. Ghosh, C. Kantner, G.B. Oison, Thermodynamic modeling of the Pd-X(X=Ag, Co, Fe, Ni) systems, J. Phase Equilibria. 20 (1999) 295–308, doi:10.1361/105497199770335811.
- [139] Y. Liu, D. Liang, Y. Du, L. Zhang, D. Yu, Mobilities and diffusivities in fcc Co-X (X=Ag, Au, Cu, Pd and Pt) alloys, Calphad 33 (2009) 695–703, doi:10.1016/j. calphad.2009.09.001.
- [140] S. an Mey, Thermodynamic re-evaluation of the Cu-Ni system, Calphad 16 (1992) 255–260, doi:10.1016/0364-5916(92)90022-P.
- [141] T. Abe, B. Sundman, H. Onodera, Thermodynamic assessment of the Cu-Pt system, J. Phase Equilibria Diffus 27 (2006) 5–13, doi:10.1361/ 105497196X92736.
- [142] A.F. Guillermet, Assessing the thermodynamics of the Fe-Co-Ni system using a calphad predictive technique, Calphad 13 (1989) 1–22, doi:10.1016/0364-5916(89)90034-5.
- [143] Y.W. Cui, M. Jiang, I. Ohnuma, K. Oikawa, R. Kainuma, K. Ishida, Computational study of atomic mobility in Co-Fe-Ni ternary fcc alloys, J. Phase Equilibria Diffus. 29 (2008) 312–321, doi:10.1007/s11669-008-9341-9.
- [144] Y. Zhang, H. Liu, Z. Jin, Thermodynamic assessment of the Nb-Ti system, Calphad 25 (2001) 305–317, doi:10.1016/S0364-5916(01)00051-7.
- [145] K.C.H. Kumar, P. Wollants, L. Delaey, Thermodynamic calculation of Nb-Ti-V phase diagram, Calphad 18 (1994) 71–79, doi:10.1016/0364-5916(94)90008-6.
- [146] A.Fernandez Guillermet, Thermodynamic analysis of the stable phases in the Zr-Nb system and calculation of the phase diagram, Zeit. Metall. 82 (1991) 478-487.
- [147] L. Höglund, J. Ågren, Analysis of the Kirkendall effect, marker migration and pore formation, Acta Mater 49 (2001) 1311–1317, doi:10.1016/S1359-6454(01) 00054-4
- [148] I. Ansara, A.T. Dinsdale, M.H. Rand, Cost 507: thermochemical database for light metal alloys, 1998.
- [149] M.A. Turchanin, P.G. Agraval, A.R. Abdulov, Thermodynamic assessment of the Cu-Ti-Zr system. II, Powder Metall. Metal Ceram. 47 (2008) 428–446, doi:10. 1007/s11106-008-9039-x.

# Supplementary Information

for

# A simple yet general model of binary diffusion coefficients emerged from a comprehensive assessment of 18 binary systems

( https://doi.org/10.1016/j.actamat.2021.117077 )

Wei Zhong<sup>1</sup>, Qiaofu Zhang<sup>2</sup>, Ji-Cheng Zhao<sup>1,\*</sup>

# Conversion between diffusion coefficients and atomic mobility:

Atomic mobility  $M_i$  is defined by Einstein's relation  $M_i = D_i^*/RT = D_{0i}^* \exp(-Q_i/RT)/RT$  where  $D_{0i}^*$  and  $Q_i$  are the pre-factor and the activation energy of the Arrhenius equation of the tracer diffusion coefficient  $D_i^*$  of element i. Thus,

$$M_i = \frac{D_{0i}^*}{RT} \exp\left(\frac{-Q_i}{RT}\right) = \frac{1}{RT} \exp\left(\frac{RT \ln D_{0i}^* - Q_i}{RT}\right) = \frac{1}{RT} \exp\left(\frac{\Phi_i}{RT}\right)$$
 (S1)

Where the *atomic mobility parameter*  $\Phi_i$  widely used by the CALPHAD community is:  $\Phi_i = RT \ln D_{0i}^* - Q_i = RT \ln D_i^*$ . For a binary A-B solution where i = A or B,  $\Phi_i$  is further expressed as [1]:

$$\Phi_i = x_A \Phi_i^A + x_B \Phi_i^B + x_A x_B \left[ \sum_{r=0,1} r \Phi_i^{A,B} (x_A - x_B)^r \right]$$
 (S2)

Where  ${}^r\Phi_i^{A,B}$  values are the atomic mobility interaction parameters to be fitted. Since  $\Phi_i = RT \ln D_i^*$ , Equation (S2) can be converted into Equation (S3) which is the same as Equation (6) in the article.

$$\ln D_i^* = x_A \ln D_i^A + x_B \ln D_i^B + x_A x_B \sum_{r=0,1,\dots} {^r\Phi_i^{A,B}(x_A - x_B)^r} / RT$$
 (S3)

Therefore, one can convert back and forth between tracer diffusion coefficient  $D_i^*$  and atomic mobility parameter  $\Phi_i$  via the simple relation:  $\Phi_i = RT \ln D_i^*$ .

**Table S1**. Summary of experimental interdiffusion, intrinsic and tracer diffusion coefficients in the literature for the 18 binary systems ( $\bullet$ : used for parameter optimization;  $\bullet$ : partially used;  $\bigcirc$ : not used).

System	Literature	Diffusion data	Method	Note	Ref
	Seith & Kottmann	$\widetilde{D}$	Diffusion couple	•	[2]
	Balluffi & Seigle	$\widetilde{D},D^I$	Diffusion couple	•	[3]
Ag-Au	Mead & Birchenall	$D_{Ag}^*$	Tracer		[4]
	Mallard et al.	$D^*$	Tracer		[5]
	Johnson	$\widetilde{D}, D^*$	Diffusion couple, Tracer	•	[6]
	Ebert & Trommsdorf	$\widetilde{D}$	Diffusion couple		[7]
	Badia & Vignes	$\widetilde{D}$	Diffusion couple	•	[8]
	Ziebold & Ogilvie	$\widetilde{D}$	Diffusion couple	•	[9]
	Pinnel & Bennett	$\widetilde{D}$	Diffusion couple	•	[10]

<sup>&</sup>lt;sup>1</sup> Department of Materials Science and Engineering, University of Maryland, 4418 Stadium Drive, College Park, Maryland 20742 USA

<sup>&</sup>lt;sup>2</sup> QuesTek Innovations LLC, 1820 Ridge Avenue, Evanston, Illinois 60201 USA

<sup>\*</sup> Corresponding author. Email address: jczhao@umd.edu (J.-C. Zhao)

	Heumann & Rottwinkel	$\widetilde{D}, D^*, D^I$	Diffusion couple, Tracer	•	[11]
Au-Cu	Ravi & Paul	$\widetilde{D}$	Diffusion couple	0	[12]
	Borovskii	$\widetilde{D}$	Diffusion couple	0	[13]
	Austin & Richard	$\widetilde{D}$	Electroplating	0	[14]
	Benci et al.	$D_{Au}^*$	Tracer		[15]
	Alexander	$D_{Au}^*$	Tracer		[16]
	Reynolds et al.	$\widetilde{D}, D_{Ni}^*$	Diffusion couple, Tracer	•	[17]
Au-Ni	van Dal et al.	$\widetilde{D}, D^I$	Diffusion couple	•	[18]
	Iijima & Yamazaki	$\widetilde{D}$	Diffusion couple	•	[19]
	Kurtz et al.	$D_{Au}^*$	Tracer		[20]
	Badia & Vignes	$\widetilde{\widetilde{D}}$	Diffusion couple	•	[8]
	Ustad & Sorum	$\widetilde{D}$	Diffusion couple	0	[21]
	Hirano et al.	$\widetilde{D}$	Diffusion couple	0	[22]
Co-Fe	Kohn et al.	$D^*$	Tracer		[23]
	Ugaste et al.	$D^*$	Tracer		[24]
	Hirano & Cohen	$D_{Co}^*$	Tracer		[25]
	Fishman et al.	$D^*$	Tracer		[26]
	Hirai et al.	$\widetilde{D}$	Diffusion couple	•	[27]
	Zhang & Zhao	$\widetilde{D}$	Diffusion multiple	•	[28]
	Heumann & Kottmann	$\widetilde{D}$	Diffusion couple	•	[29]
	Ugaste et al.	$\widetilde{\widetilde{D}}$	Diffusion couple	•	[24]
~	Borovskiy et al.	$\widetilde{D}$	Diffusion couple	•	[30]
Co-Ni	Ustad & Sorum	$\widetilde{D}$	Diffusion couple	•	[21]
	Kucera et al.	$\widetilde{D}$	Diffusion couple	•	[31]
	Iijima & Hirano	$\widetilde{D}$	Diffusion couple	•	[32]
	Hirano et al.	$D^*$	Tracer		[33]
	Million & Kucera	$D_{Co}^*$	Tracer		[34]
	Million & Kucera	$D_{Ni}^*$	Tracer		[35]
Co-Pd	Iijima & Hirano	$\widetilde{D}, D^I$	Diffusion couple	•	[36]
	Levasseur & Philibert	$\widetilde{D}, D^I$	Diffusion couple	•	[37]
	Iijima et al.	$\widetilde{D}, D^I$	Diffusion couple	•	[38]
	Thomas & Birchenall	$\widetilde{\widetilde{D}}$	Diffusion couple	0	[39]
	Heumann & Grundhoff	$\widetilde{D}, D^I$	Foil	•	[40]
Cu-Ni	Marchukova & Miroshkina	$\widetilde{\widetilde{D}}$	Diffusion couple	0	[41]
	Brunel et al.	$\widetilde{\widetilde{D}}$	Diffusion couple		[42]
	Anusavice & DeHoff	$D^*$	Tracer		[43]
	Monma et al.	$D^*$	Tracer		[44]
	Damkohler & Heumann	$D^*, D^I$	Tracer, Diffusion couple		[45]
	Mishra et al.	$\widetilde{\widetilde{D}}$	Diffusion couple	0	[46]
Cu-Pt	Johnson & Faulkenberry	$D^*$	Tracer		[47]
	Kubaschewski & Ebert	$\widetilde{D}$	Diffusion couple	•	[48]
	Levasseur & Philibert	$\widetilde{D}, D^I$	Diffusion couple	•	[49]
	Ustad & Sorum	/	Diffusion couple	•	[21]
	Borovskiy et al.	$\widetilde{D}$ $\widetilde{D}$	Diffusion couple	0	[30]
Fe-Ni	Million et al.	$\widetilde{D}, D^*$	Diffusion couple, Tracer	•	[50]
	Badia & Vignes	$\widetilde{D}$	Diffusion couple	•	[8]
	Kohn et al.	$\widetilde{D}, D^*, D^I$	Diffusion couple, Tracer	•	[23]
	Ganesan et al.	$\widetilde{D}$	Diffusion couple	0	[51]
	van Dal et al.	$\widetilde{D}, D^I$	Diffusion couple	•	[52]
Fe-Pd	Gomez et al.	$\widetilde{D}$	Diffusion couple	•	[53]
	Fillon & Calais	$D^*$	Tracer		[54]
	I mon & Julius		114001		ا ای

	Xia et al.	$\widetilde{D}$	Diffusion couple	•	[55]
	Gavelle et al.	$\widetilde{D}$	Diffusion couple	0	[56]
	Aubertine & McIntyre	$\widetilde{D}$	Diffusion couple	•	[57]
	Ozguven & McIntyre	$\widetilde{D}$	Diffusion couple	•	[58]
Ge-Si	Kube et al.	$D^*$	SIMS		[59]
	Strohm et al.	$D^*$	Tracer		[60]
	Strohm et al.	D*	Tracer		[61]
	Zangenberg et al.	$D_{Ge}^*$	SIMS		[62]
	Latinen et al.	$D^*$	Tracer		[63]
	Roux & Vignes	$\widetilde{D}$	Diffusion couple	•	[64]
	Ugaste & Zajkin	$\widetilde{D}$	Diffusion couple	•	[65]
	Polyanskii et al.	$\widetilde{D}$	Diffusion couple	0	[66]
	Gryzunov et al.	$\widetilde{D}$	Diffusion couple	0	[67]
NH 75°	Fedotov et al.	$\widetilde{D}$	Diffusion couple	0	[68]
Nb-Ti	Vergasova et al.	$\widetilde{D}$	Diffusion couple	0	[69]
	Chen et al.	$\widetilde{D}$	Diffusion multiple	•	[70]
	Zhu et al.	$\widetilde{\widetilde{D}}$	Diffusion multiple	•	[71]
	Peart & Tomlin	$D_{Nb}^*$	Tracer		[72]
	Gibbs et al.	$D_{Nb}^*$	Tracer		[73]
	Pontau & Lazarus	$D^*$	Tracer		[74]
	Geiss et al.	$\widetilde{D}, D^I$	Diffusion couple	•	[75]
	Mokrov & Zharkov	$\widetilde{D}, D^I$	Diffusion couple	•	[76]
	Vergasova et al.	$\widetilde{\widetilde{D}}$	Diffusion couple	0	[69]
Nb-V	Babkin et al.	$\widetilde{D}$	Diffusion couple	•	[77]
	Ugaste et al.	$\widetilde{D}$	Diffusion couple	0	[78]
	Roux & Vignes	$\widetilde{D}$	Diffusion couple	0	[64]
	Patil et al.	$\widetilde{D}$	Diffusion couple	0	[79]
	Chen et al.	$\widetilde{D}$	Diffusion multiple	•	[70]
	Vergasova et al.	$\widetilde{\widetilde{D}}$	Diffusion couple	0	[69]
	Balakir et al.	$\widetilde{D}$	Diffusion couple	0	[80]
Nb-Zr	Prasad & Paul	$\widetilde{D}$	Diffusion couple	0	[81]
	Herzig et al.	D*	Tracer		[82]
	Tiwari et al.	D*	Tracer		[83]
	Zou et al.	$D_{Nb}^*$	Tracer		[84]
Ni-Pd	van Dal et al.	$\widetilde{D}, D^I$	Diffusion couple	•	[52]
	Fedetov et al.	$\widetilde{\widetilde{D}}$	Diffusion couple	0	[68]
Ta-Ti	Chen et al.	$\widetilde{D}$	Diffusion couple	•	[70]
	Ansel et al.	$\widetilde{D}, D^I$	Diffusion couple	0	[85]
	Ugaste & Zajkin	$\widetilde{D}$	Diffusion couple	•	[65]
	Zhu et al.	$\widetilde{D}$	Diffusion multiple	0	[71]
Ti-V	Fedotov et al.	$\widetilde{\widetilde{D}}$	Diffusion couple	0	[68]
	Carlson	$\widetilde{D}, D^I$	Diffusion couple	•	[86]
	Kale et al.	$\widetilde{D}$	Diffusion couple	0	[87]
	Murdock et al.	$D^*$	Tracer		[88]
	Thibon et al.	$\widetilde{D}$	Diffusion couple	•	[89]
	Bhanumurthy et al.	$\widetilde{D}$	Diffusion couple	0	[90]
	Chen et al.	$\widetilde{D}$	Diffusion couple	•	[70]
Ti-Zr	Brunsch & Steeb	$\widetilde{D}$	Diffusion couple	•	[91]
	Zhu et al.	$\widetilde{D}$	Diffusion couple	•	[71]
	Raghunathan et al.	$\widetilde{\widetilde{D}}$	Diffusion couple	•	[92]
	Herzig et al.	$D^*$	Tracer	+ -	[93]
	TICIZIE CI al.	υ	Tracci	1	

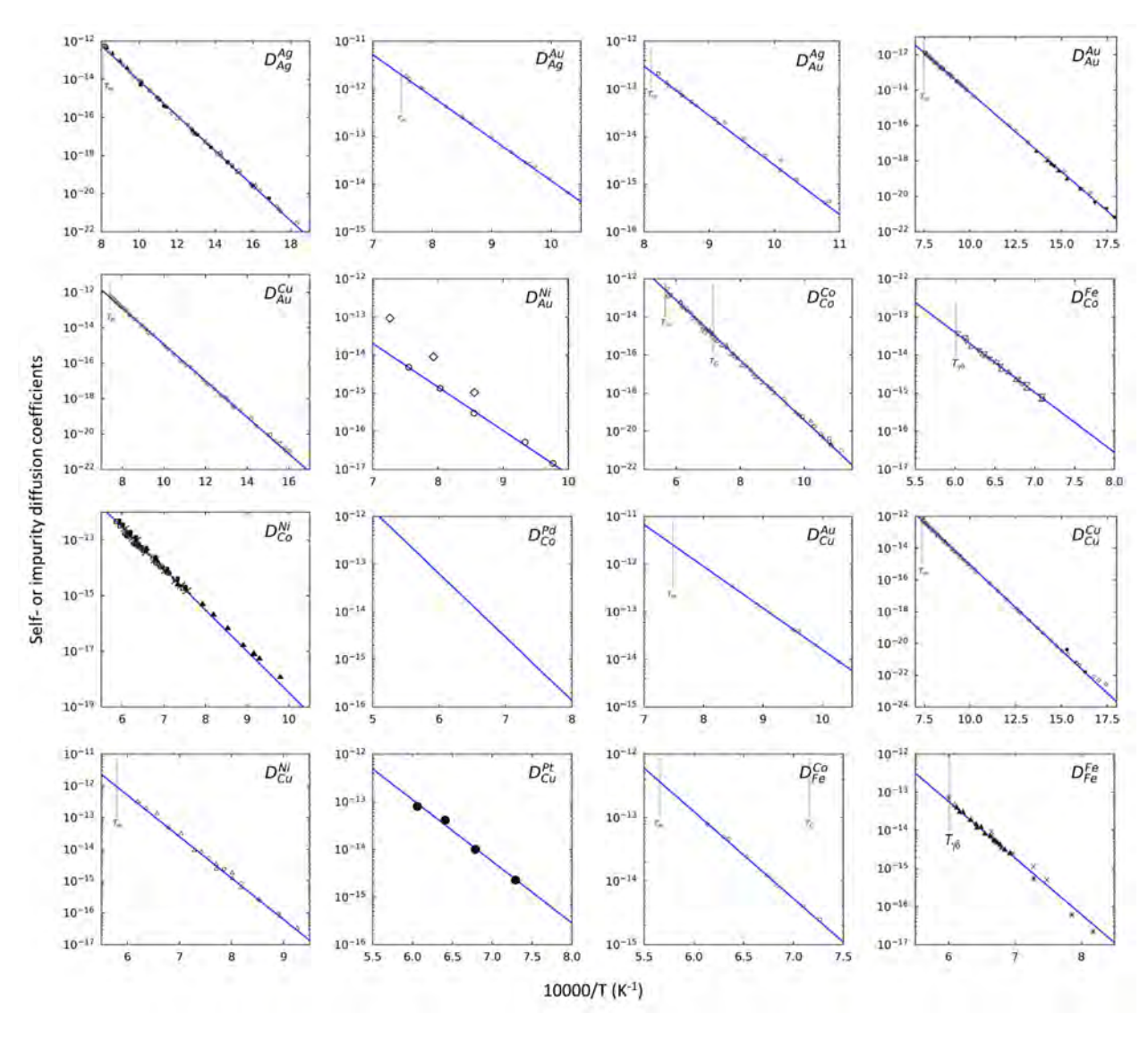
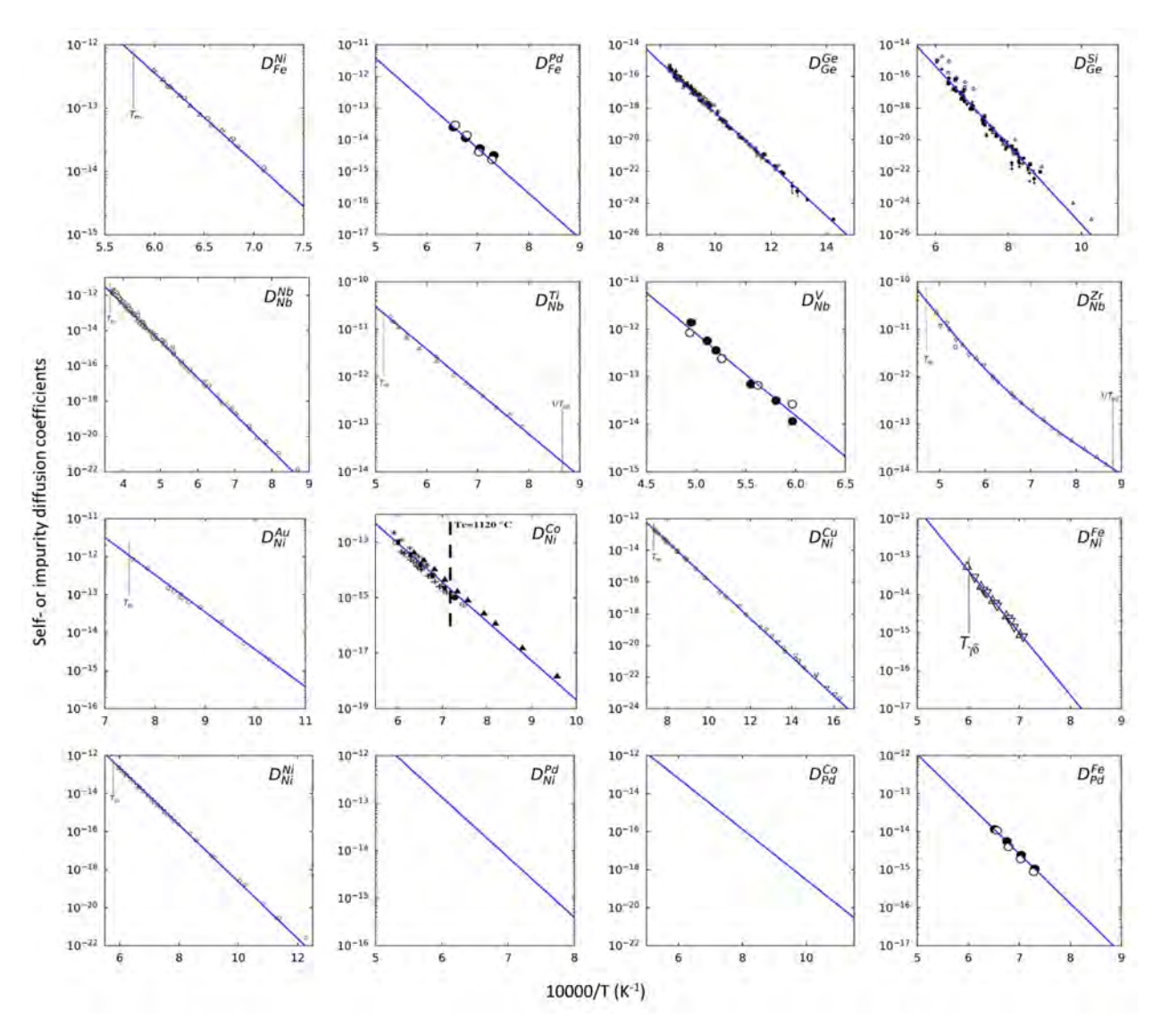
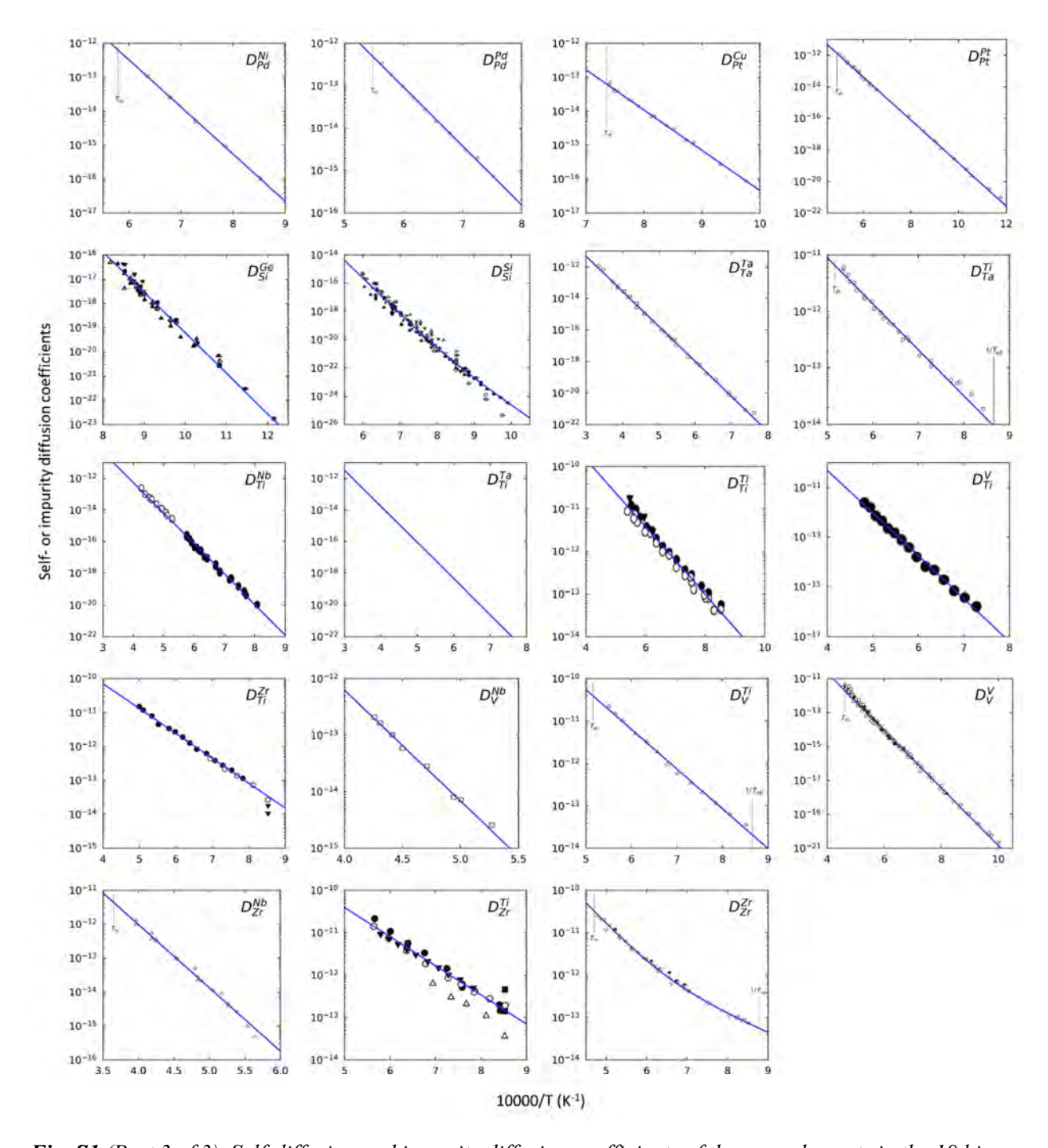


Fig. S1 (Part 1 of 3). Self-diffusion and impurity diffusion coefficients of the pure elements in the 18 binary systems from the literature and the current assessment (See Table 2 in the main text for reference details).



*Fig. S1* (Part 2 of 3). Self-diffusion and impurity diffusion coefficients of the pure elements in the 18 binary systems from the literature and the current assessment (See *Table 2* in the main text for reference details).



*Fig. S1* (Part 3 of 3). Self-diffusion and impurity diffusion coefficients of the pure elements in the 18 binary systems from the literature and the current assessment (See *Table 2* in the main text for reference details).

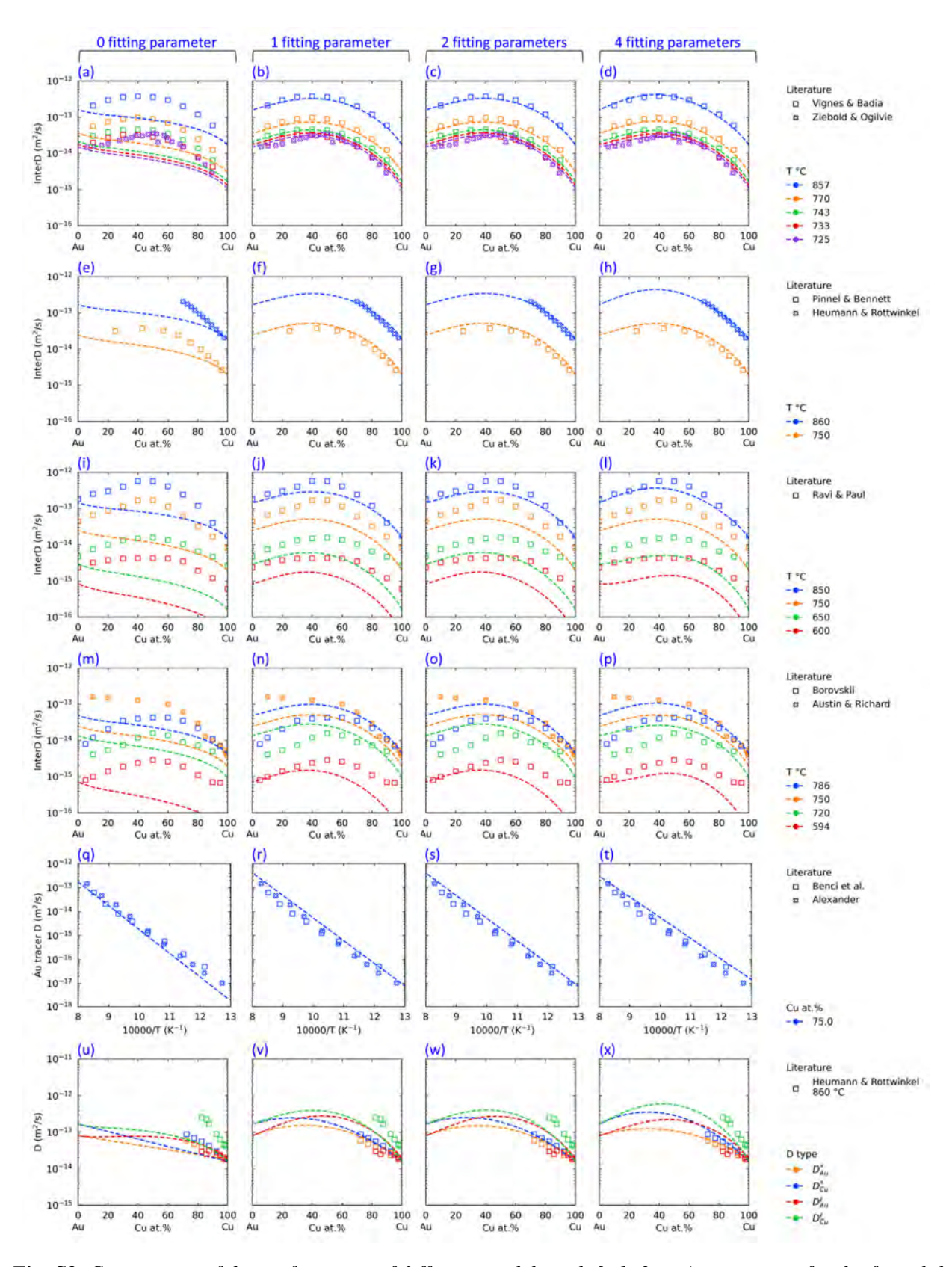


**Fig. S2**. Comparison of the performance of diffusion models with 0, 1, 2 or 4 parameters for the fcc solid solution of the Au-Cu binary system.

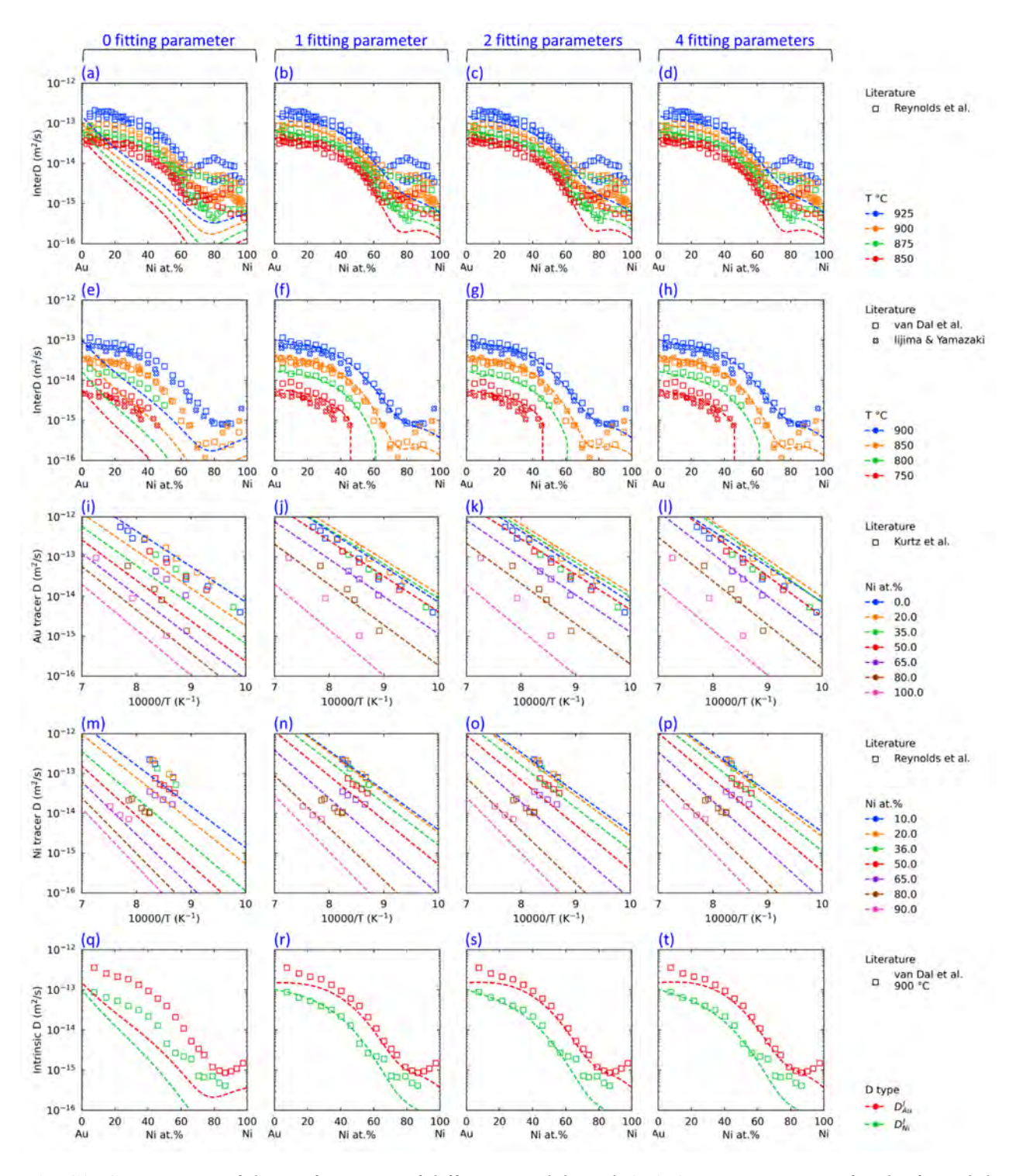


**Fig. S3**. Comparison of the performance of diffusion models with 0, 1, 2 or 4 parameters for the fcc solid solution of the Au-Ni binary system.

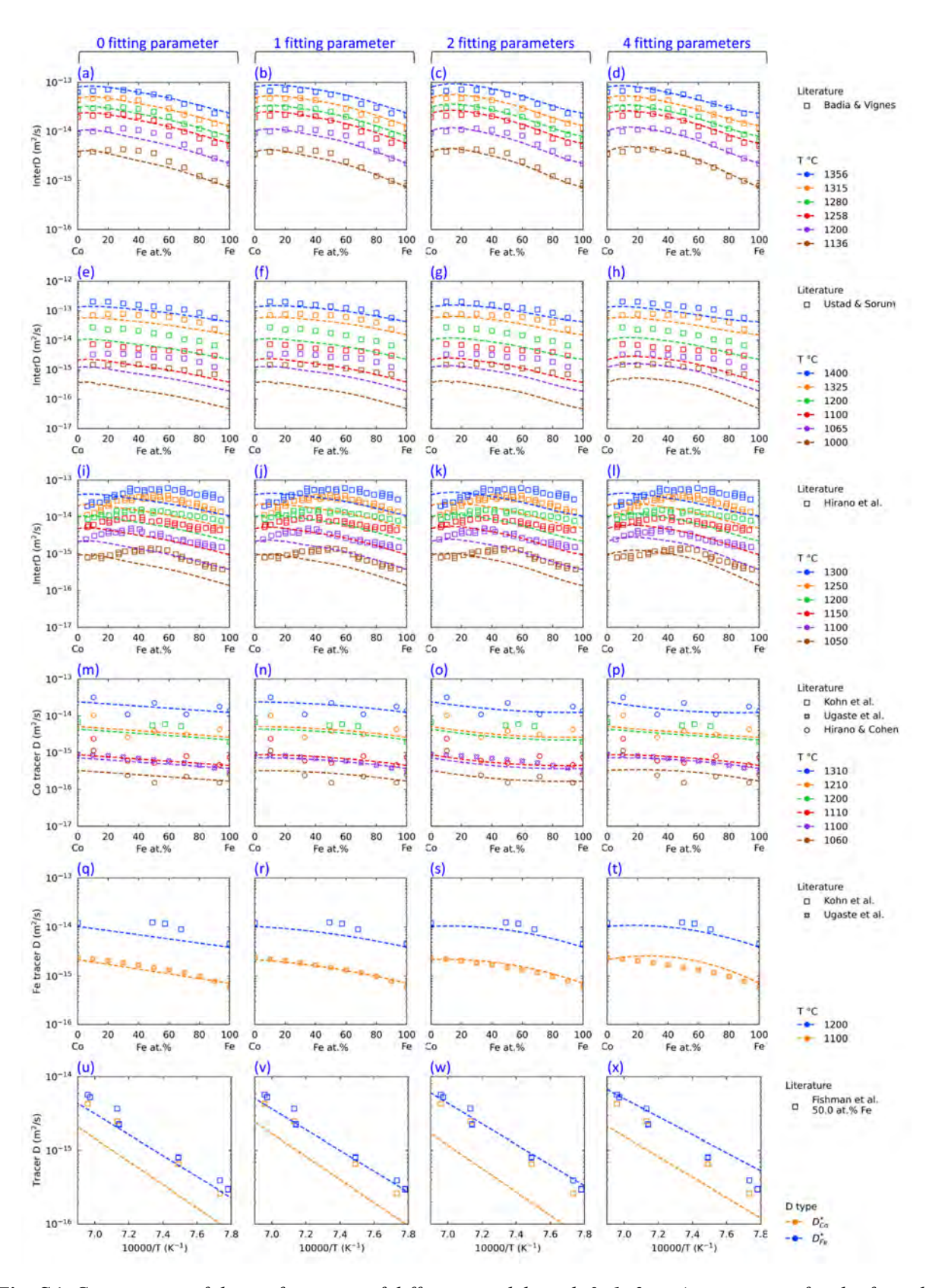


**Fig. S4**. Comparison of the performance of diffusion models with 0, 1, 2 or 4 parameters for the fcc solid solution of the Co-Fe binary system.

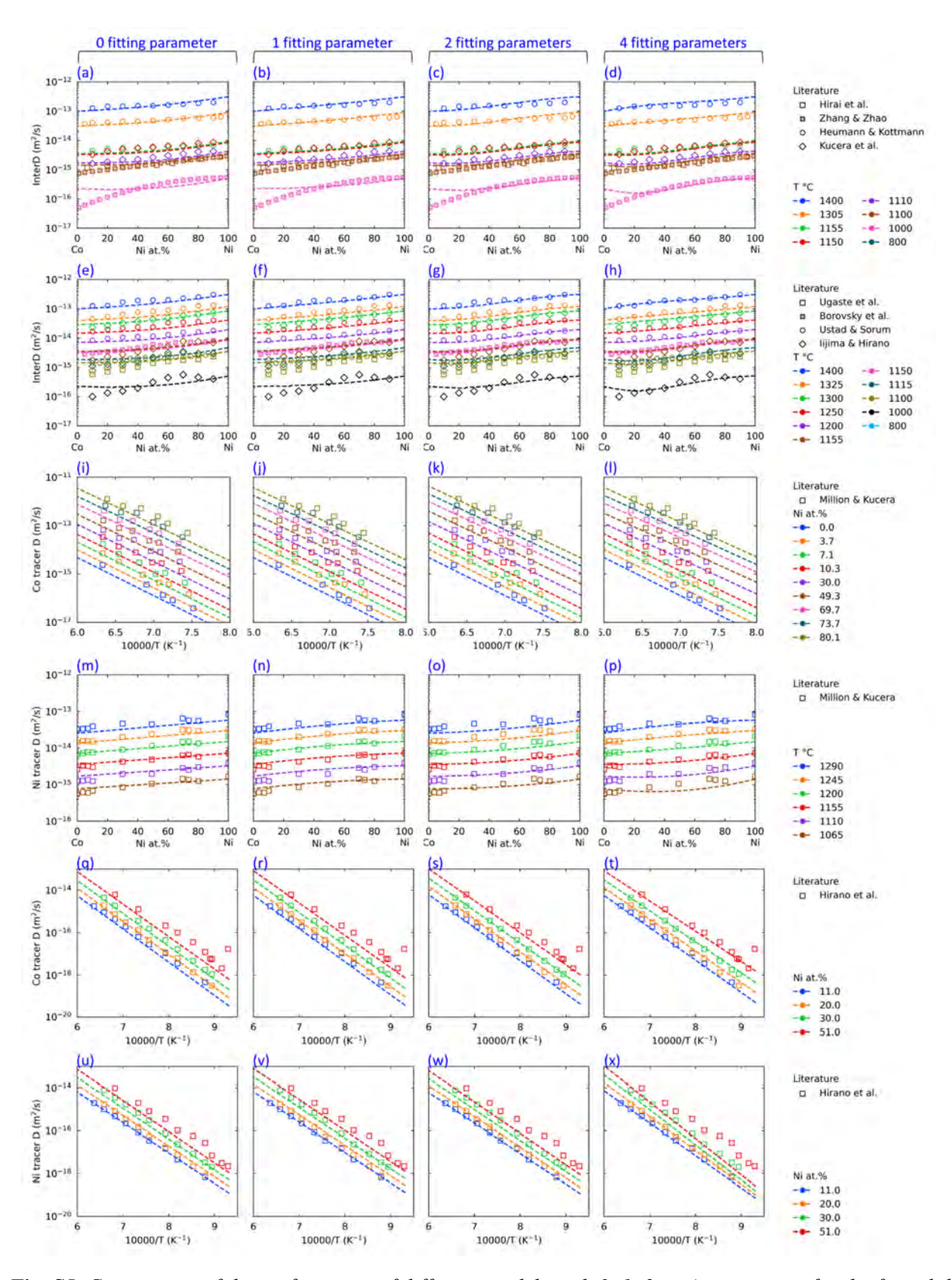


**Fig. S5**. Comparison of the performance of diffusion models with 0, 1, 2 or 4 parameters for the fcc solid solution of the Co-Ni binary system.

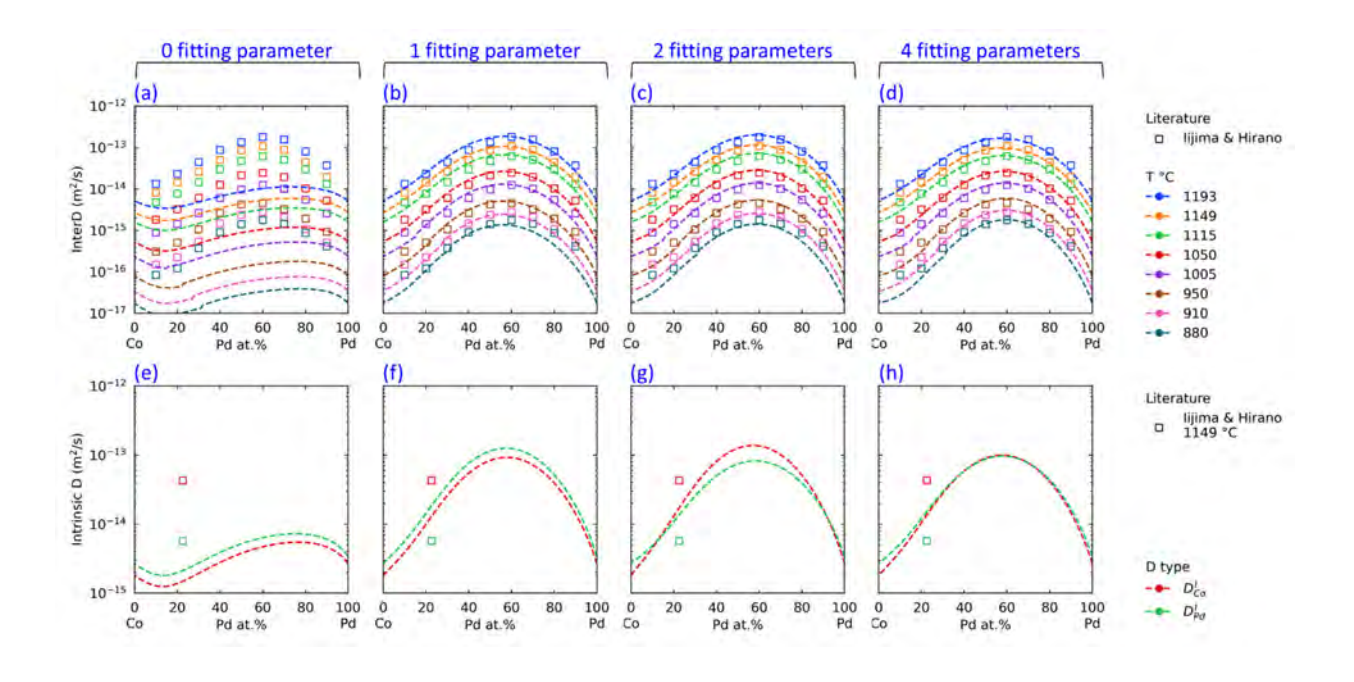


**Fig. S6**. Comparison of the performance of diffusion models with 0, 1, 2 or 4 parameters for the fcc solid solution of the Co-Pd binary system.

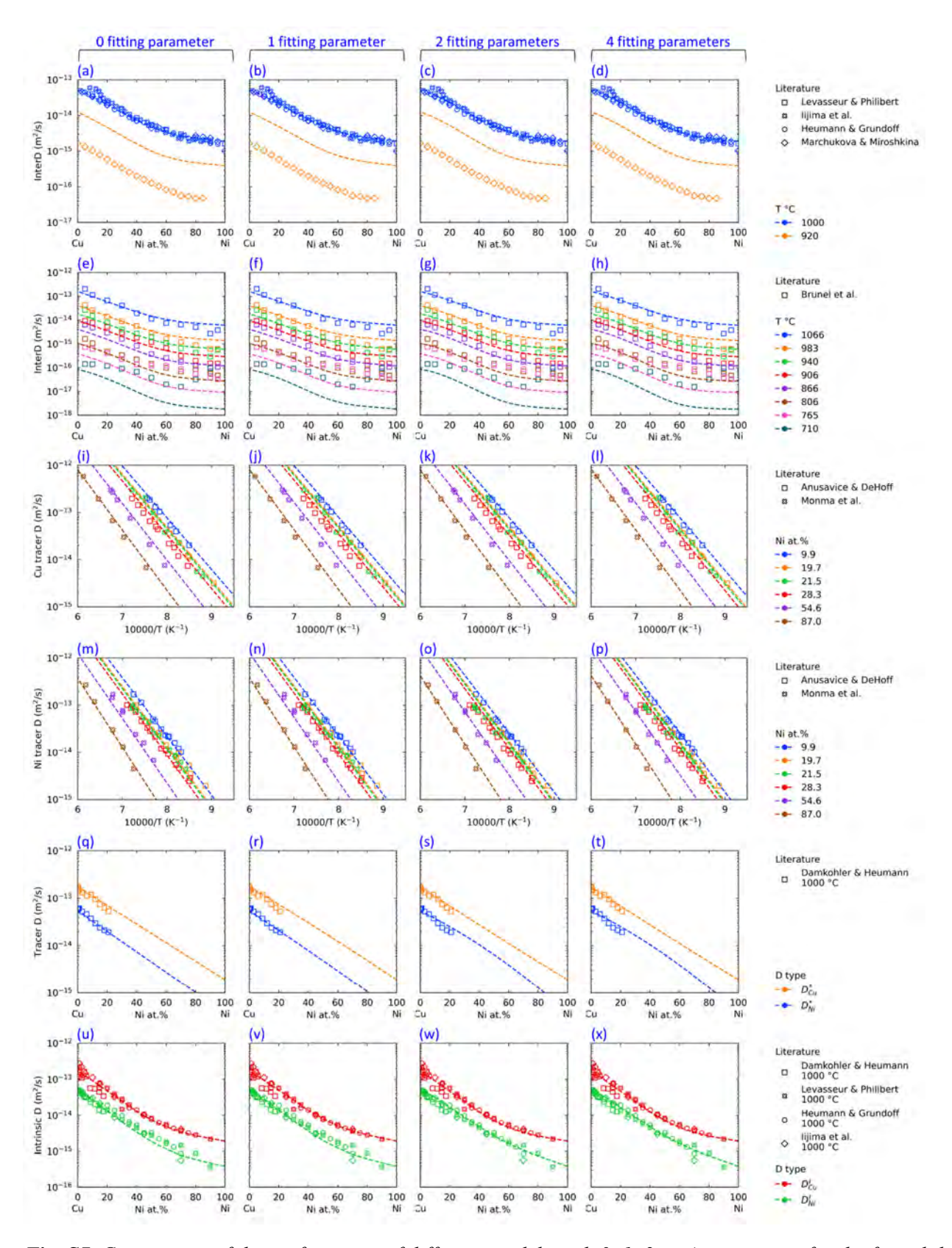


**Fig. S7**. Comparison of the performance of diffusion models with 0, 1, 2 or 4 parameters for the fcc solid solution of the Cu-Ni binary system.

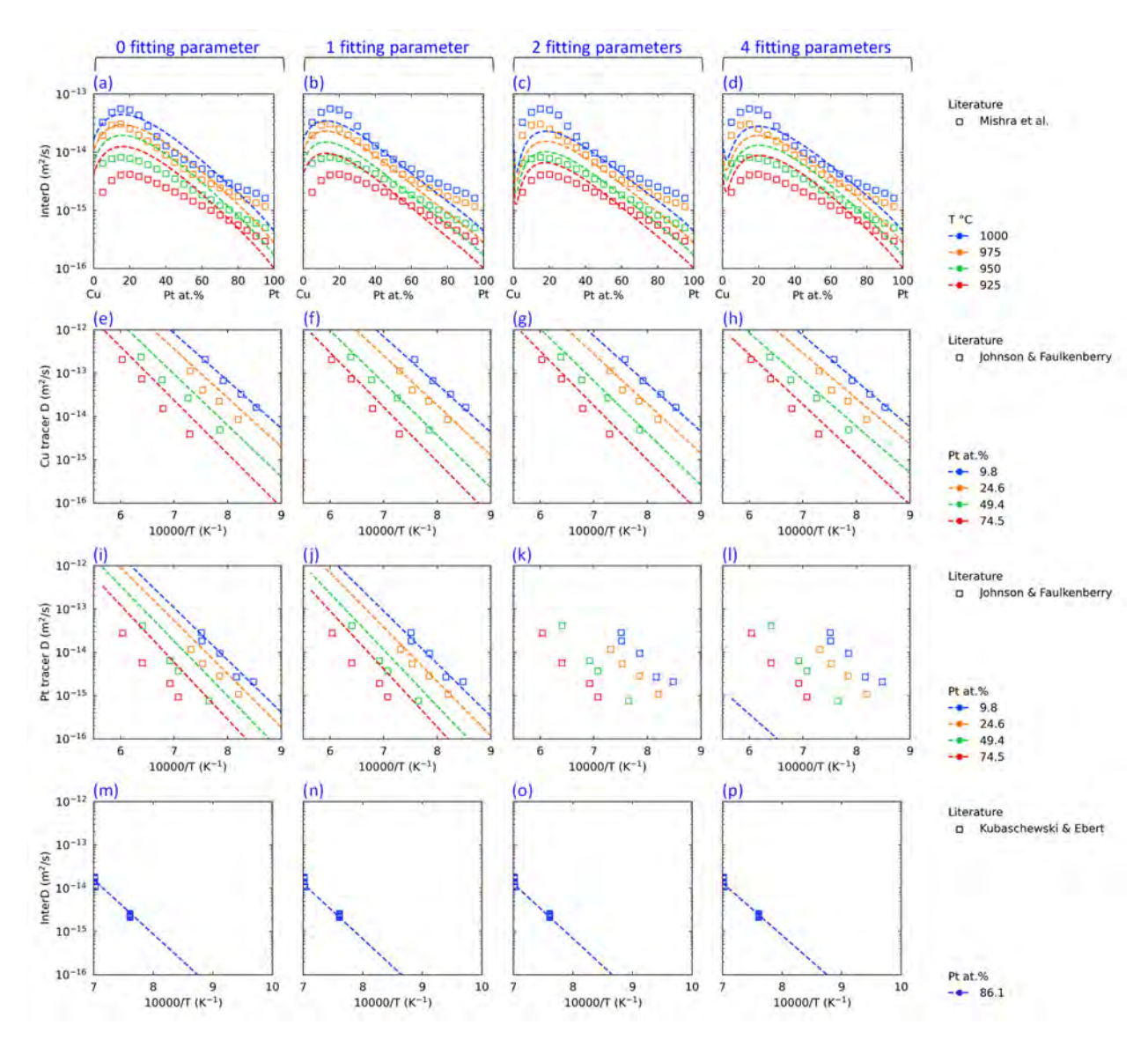


**Fig. S8**. Comparison of the performance of diffusion models with 0, 1, 2 or 4 parameters for the fcc solid solution of the Cu-Pt binary system. The lines in subfigures (k) and (l) are mostly below/outside the bottom of these sub-figures and thus are substantially below the experimental results, showing substantial deviation.

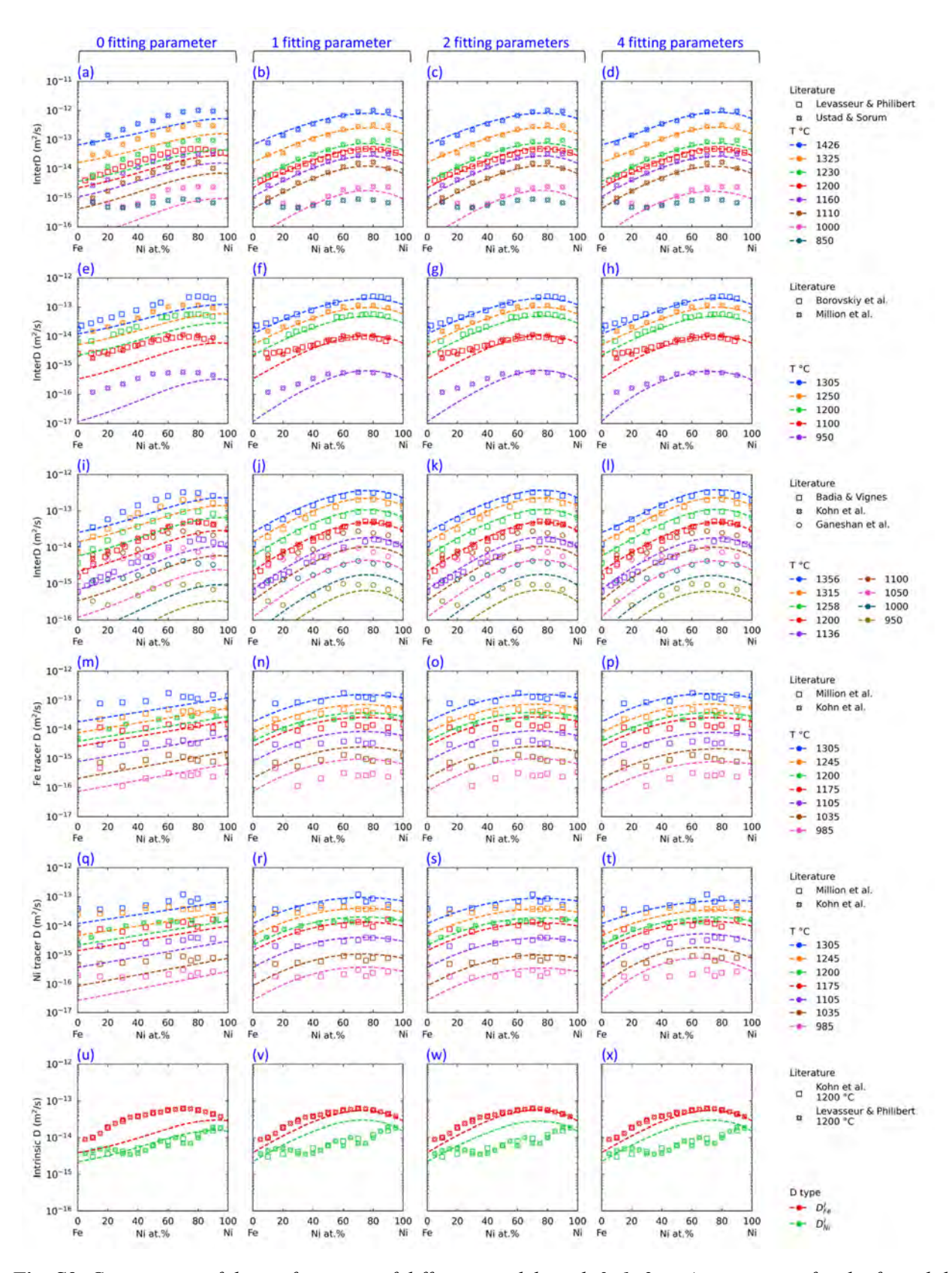


**Fig. S9**. Comparison of the performance of diffusion models with 0, 1, 2 or 4 parameters for the fcc solid solution of the Fe-Ni binary system.

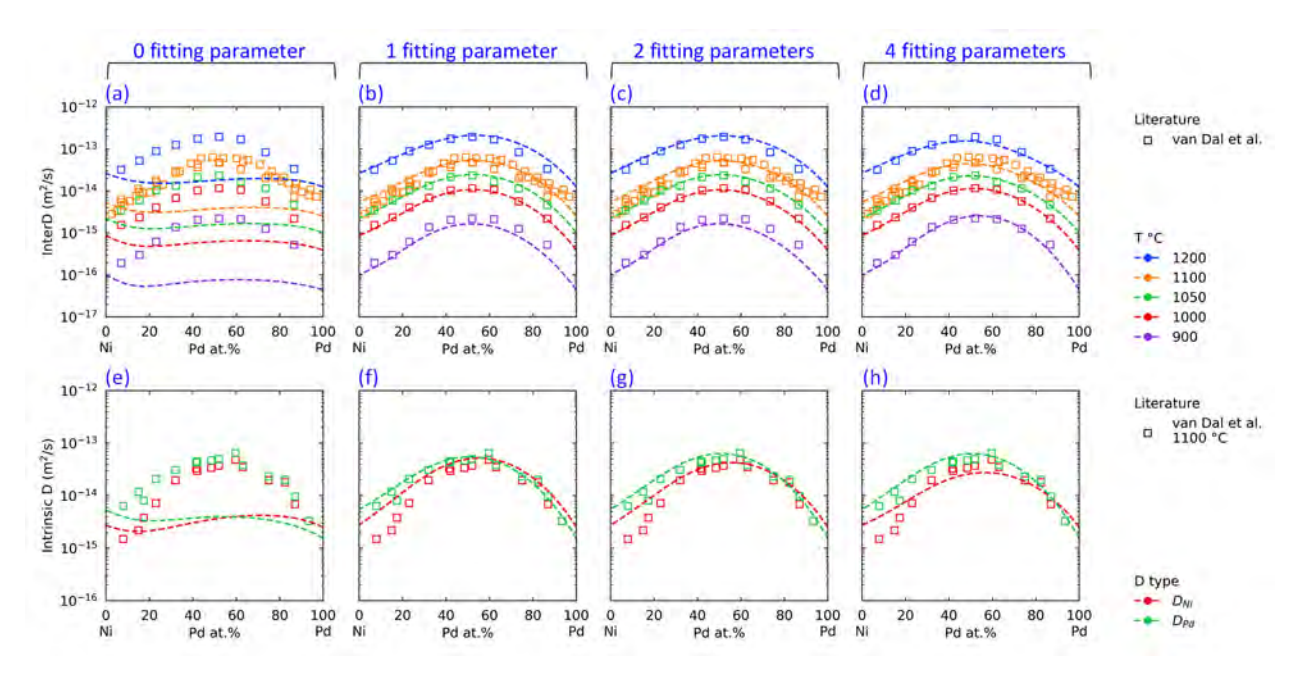


*Fig. S10.* Comparison of the performance of diffusion models with 0, 1, 2 or 4 parameters for the fcc solid solution of the Ni-Pd binary system.

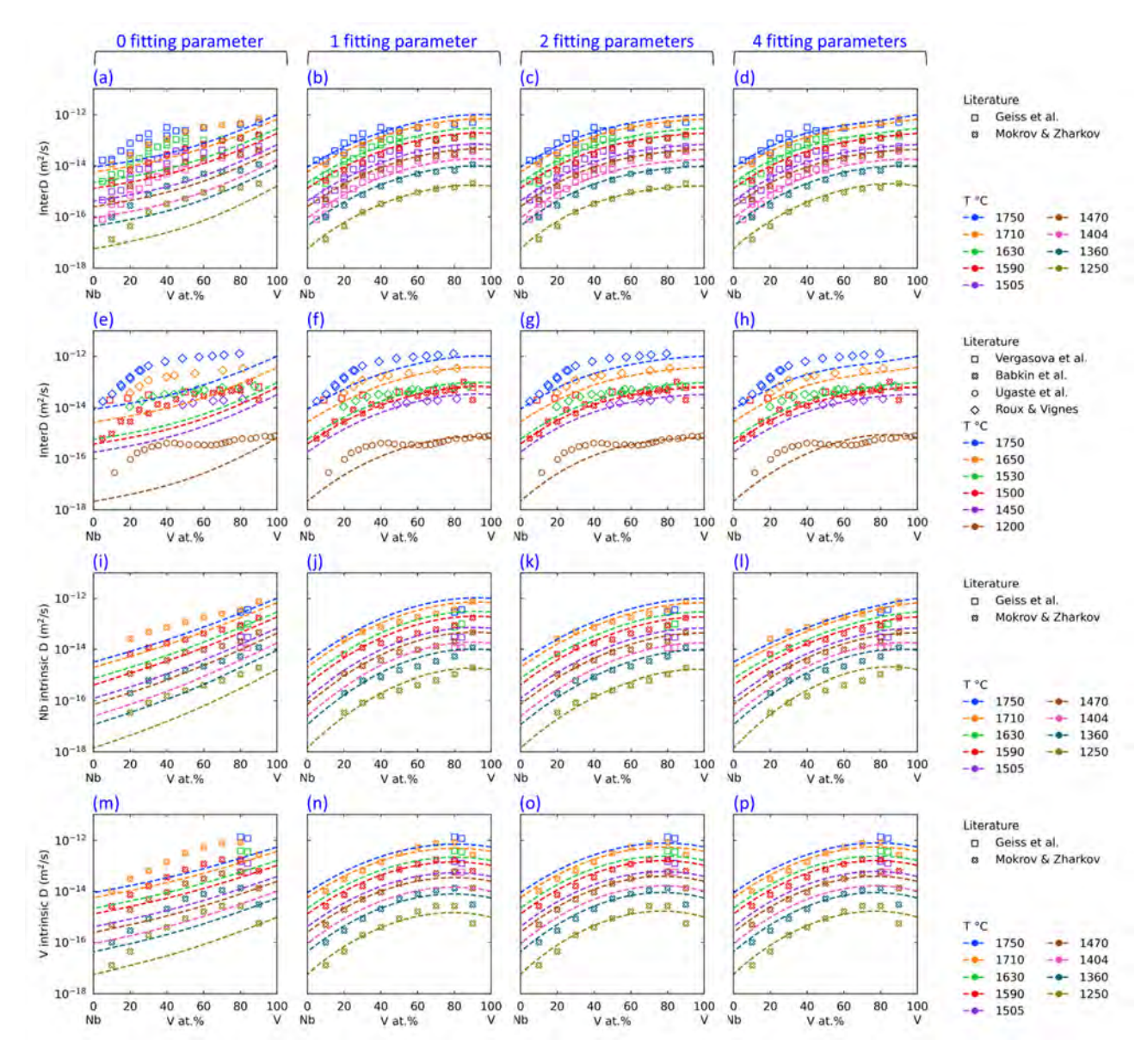


*Fig. S11.* Comparison of the performance of diffusion models with 0, 1, 2 or 4 parameters for the bcc solid solution of the Nb-V binary system.

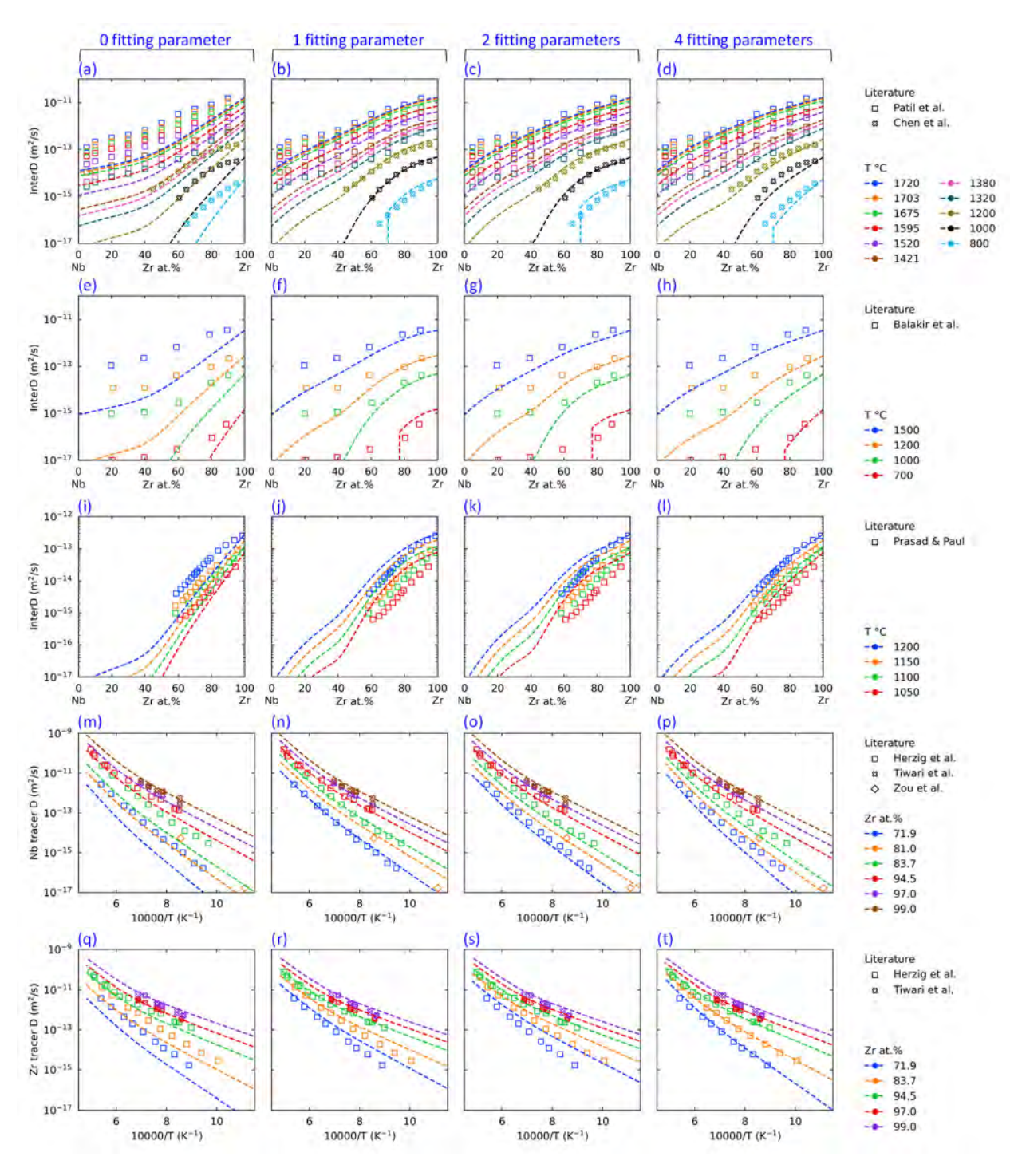
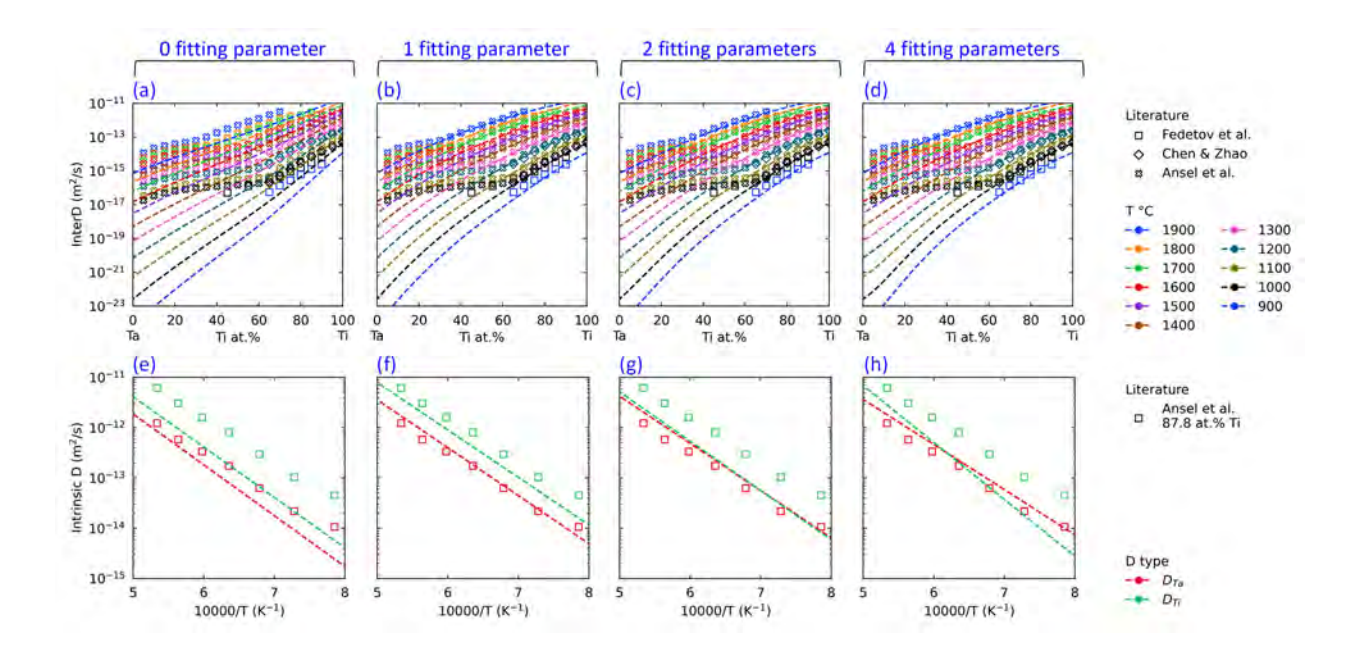


Fig. S12. Comparison of the performance of diffusion models with 0, 1, 2 or 4 parameters for the bcc solid solution of the Nb-Zr binary system.



*Fig. S13.* Comparison of the performance of diffusion models with 0, 1, 2 or 4 parameters for the bcc solid solution of the Ta-Ti binary system.

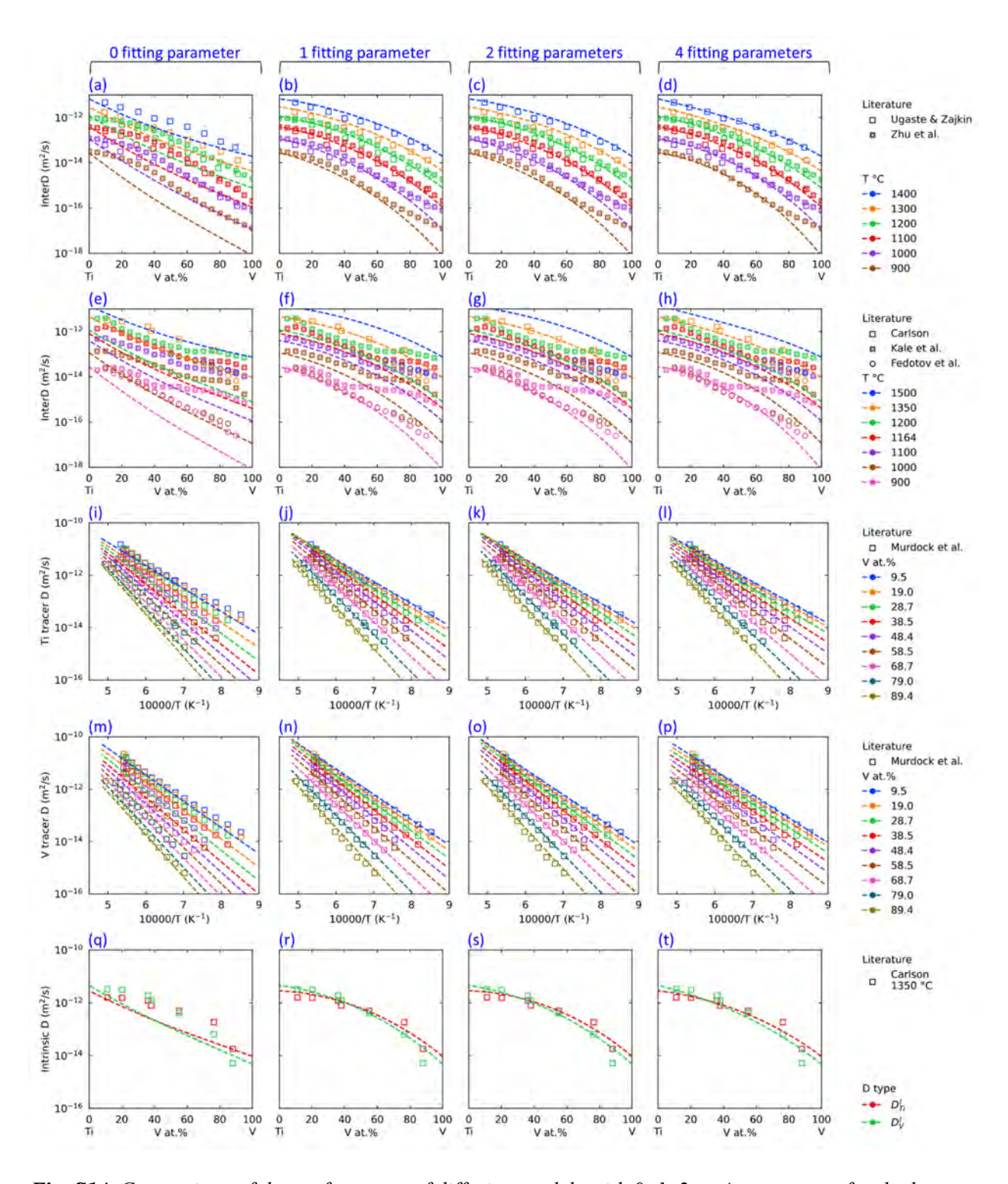
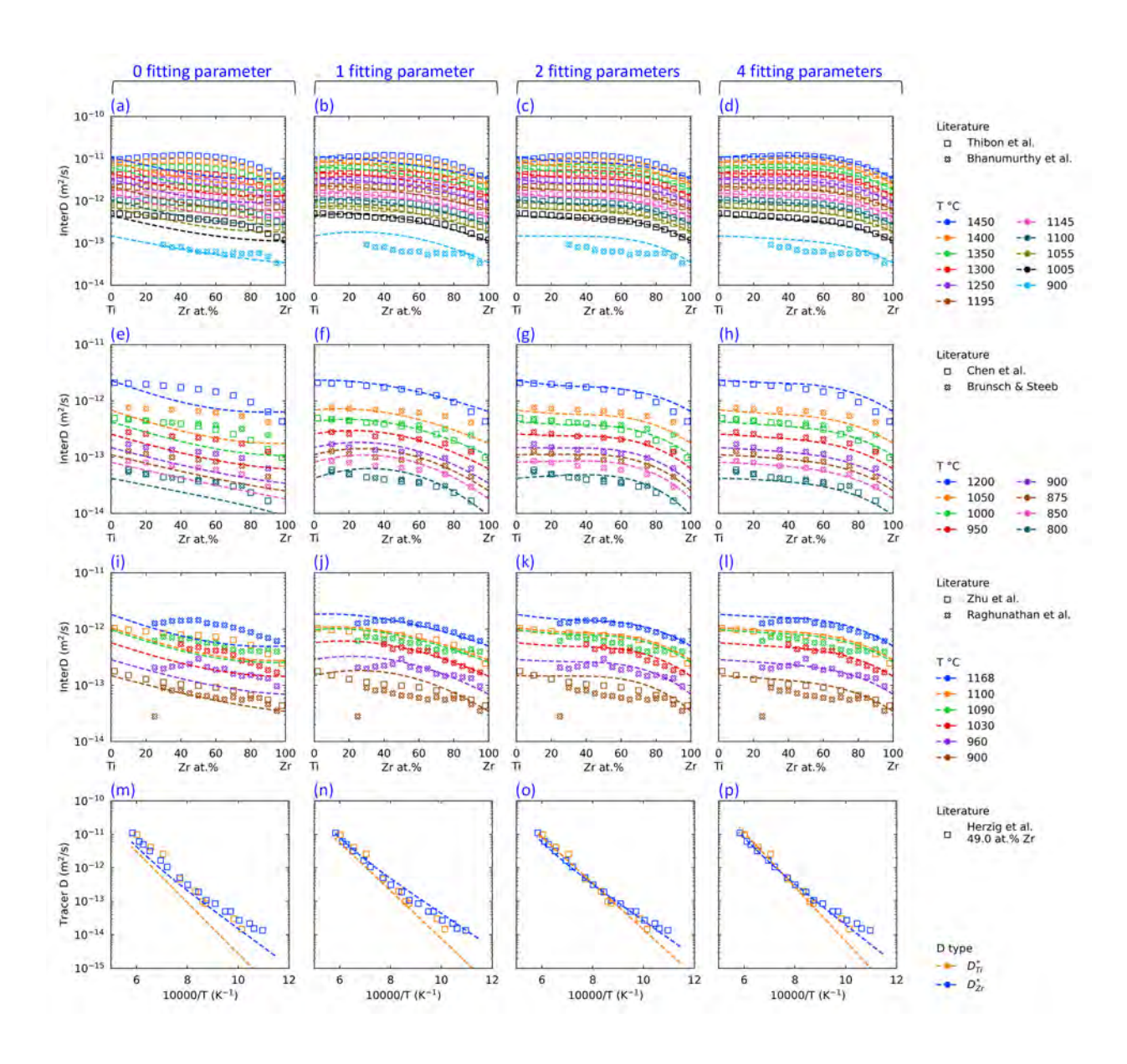


Fig. S14. Comparison of the performance of diffusion models with 0, 1, 2 or 4 parameters for the bcc solid solution of the Ti-V binary system.



*Fig. S15.* Comparison of the performance of diffusion models with 0, 1, 2 or 4 parameters for the bcc solid solution of the Ti-Zr binary system.

# References

- [1] J.O. Andersson, J. Ågren, Models for numerical treatment of multicomponent diffusion in simple phases, J. Appl. Phys. 72 (1992) 1350–1355. https://doi.org/10.1063/1.351745.
- [2] W. Seith, A. Kottmann, Diffusion in solid metals, Angew. Chemie. 64 (1952) 379–391.
- [3] R.W. Balluffi, L.L. Seigle, Diffusion in bimetal vapor-solid couples, J. Appl. Phys. 25 (1954) 607–614. https://doi.org/10.1063/1.1721698.
- [4] H.W. Mead, C.E. Birchenall, Diffusion in gold and Au-Ag alloys, Jom. 9 (1957) 874–877. https://doi.org/10.1007/bf03397933.
- [5] W.C. Mallard, A.B. Gardner, R.F. Bass, L.M. Slifkin, Self-diffusion in silver-gold solid solutions, Phys. Rev. 129 (1963) 617–625. https://doi.org/10.1103/PhysRev.129.617.
- [6] W. Johnson, Diffusion experiments on a gold-silver alloy by chemical and radioactive tracer methods, Trans. Am. Inst. Min. Metall. Eng. 147 (1942) 331–346.
- [7] H. Ebert, G. Trommsdorf, Die Diffusion von Silber in Gold, Zeitschrift Für Elektrochemie Und Angew. Phys. Chemie. 54 (1950) 294–296. https://doi.org/10.1002/bbpc.19500540411.
- [8] M. Badia, A. Vignes, Interdiffusion and the Kirkendall Effect in Binary Alloys, MEM SCI REV MET. 66 (1969) 915–927.
- [9] T.. Ziebold, R.E. Ogilvie, Ternary diffusion in copper-silver-gold alloys, Trans. AIME. 239 (1967) 942–953.
- [10] M.R. Pinnel, B. Laboratories, Mass Diffusion in Polycrystalline Copper / Electroplated Gold Planar Couples, Metall. Trans. 3 (1972) 1989–1997.
- [11] T. Heumann, T. Rottwinkel, Measurement of the interdiffusion, intrinsic, and tracer diffusion coefficients in Cu-rich Cu-Au solid solutions, J. Nucl. Mater. 70 (1978) 567–570.
- [12] R. Ravi, A. Paul, Diffusion mechanism in the gold-copper system, J. Mater. Sci. Mater. Electron. 23 (2012) 2152–2156. https://doi.org/10.1007/s10854-012-0729-2.
- [13] I.B. Borovskii, N.P. Llin, E.L. Loseva, Study of mutual diffusion in Cu-Au system, Tr. Instituta Metall. Im. A.A. Baĭkova. 15 (1963) 32–40.
- [14] A.E. Austin, N.A. Richard, Grain-boundary diffusion of gold in copper, J. Appl. Phys. 33 (1962) 3569–3574. https://doi.org/10.1063/1.1702448.
- [15] S. Benci, G. Gasparrini, E. Germagnoli, G. Schianchi, Diffusion of gold in Cu3Au, J. Phys. Chem. Solids. 26 (1965) 687–690. https://doi.org/10.1016/0022-3697(65)90020-X.
- [16] W.B. Alexander, Studies on atomic diffusion in metals, University fo North Caralina, 1969.
- [17] J.E. Reynolds, B.L. Averbach, M. Cohen, Self-diffusion and interdiffusion in gold-nickel alloys, Acta Metall. 5 (1957) 29–40. https://doi.org/10.1016/0001-6160(57)90152-9.
- [18] M.J.H. Van Dal, M.C.L.P. Pleumeekers, A.A. Kodentsov, F.J.J. Van Loo, Diffusion studies and reexamination of the Kirkendall effect in the Au-Ni system, J. Alloys Compd. 309 (2000) 132–140. https://doi.org/10.1016/S0925-8388(00)01056-2.
- [19] Y. Iijima, Y. Yamazaki, Interdiffusion between metals of widely different self-diffusion rates, Defect Diffus. Forum. 237–240 (2005) 62–73. https://doi.org/10.4028/www.scientific.net/ddf.237-240.62.
- [20] A., Kurtz, B., Averbach, M. Cohen, Self-diffusion of gold in gold-nickel alloys, Acta Metall. 3 (1955) 442–446. https://doi.org/10.1016/0001-6160(55)90132-2.
- [21] T. Ustad, H. Sørum, Interdiffusion in the Fe-Ni, Ni-Co, and Fe-Co systems, Phys. Status Solidi. 20 (1973) 285–294. https://doi.org/10.1002/pssa.2210200129.
- [22] K.-I. Hirano, Y. Iijima, K. Araki, H. Homma, B.K. Hirano, Y. Iijima, K. Araki, H. Homma, Interdiffusion in Iron- Cobalt Alloys, Trans. Iron Steel Inst. Japan. 17 (1977) 194–203. https://doi.org/10.2355/isijinternational1966.17.194.
- [23] A. Kohn, J. Levasseur, J. Philibert, M. Wanin, Experimental study of the theories of the Kirkendall effect in the iron-nickel and iron- cobalt systems, Acta Metall. 18 (1970) 163–173. https://doi.org/10.2307/2005321.
- [24] Y.E. Ugaste, A.A. Kodentsov, F. van Loo, Concentration dependence of diffusion coefficients in Co-Ni Fe-Ni and Co-Fe systems, Phys. Met. Met. 88 (1999) 88–94.
- [25] K. ichi Hirano, M. Cohen, Diffusion of Cobalt in Iron-Cobalt Alloys., Trans Jap Inst Met. 13 (1972) 96–102. https://doi.org/10.2320/matertrans1960.13.96.
- [26] S.G. Fishman, D. Gupta, D.S. Lieberman, Diffusivity and isotope-effect measurements in equiatomic Fe-Co, Phys. Rev. B. 2 (1970) 1451–1460. https://doi.org/10.1103/PhysRevB.2.1451.
- [27] Y. Hirai, Y. Tasaki, M. Kosaka, Study on the Friction-Welded Diffusion Couples--Chemical Diffusion of Co-Ni Alloy at 1100 C, Rep. Gov. Ind. Res. Inst. 22 (1973) 125–131.
- [28] Q. Zhang, J.-C. Zhao, Extracting interdiffusion coefficients from binary diffusion couples using traditional

- methods and a forward-simulation method, Intermetallics. 34 (2013) 132–141. https://doi.org/10.1016/j.intermet.2012.11.012.
- [29] V.T. Heumann, A. Kottmann, Uber den ablauf der diffusionsvorgange in substitutionsmischkristallen, Z. Met. 44 (1953) 139–154.
- [30] I.B. Borovskiy, I.D. Marchukova, Y.E. Ugaste, Local X-ray spectranalysis of mutual diffusion in binary systems forming a continuous series of solid solutions II the systems Fe-Ni, Ni-Co, Ni-Pt and Co-Pt, Phys. Met. Metallogr. 24 (1967) 51–56.
- [31] J. Kučera, K. Cíha, K. Stránský, Interdiffusion in the Co-Ni system-I concentration penetration curves and interdiffusion coefficients, Czechoslov. J. Phys. 27 (1977) 758–768. https://doi.org/10.1007/BF01589317.
- [32] Y. Iijima, K. Hirano, Interdiffusion in cobalt-nickel alloys, JAPAN Inst. Met. 35 (1971) 511–517.
- [33] K. Hirano, R.P. Agarwala, B.L. Averbach, M. Cohen, Diffusion in cobalt-nickel alloys, J. Appl. Phys. 33 (1962) 3049–3054. https://doi.org/10.1063/1.1728564.
- [34] B. Million, J. Kučera, Concentration dependence of diffusion of cobalt in nickel-cobalt alloys, Acta Metall. 17 (1969) 339–344. https://doi.org/10.1016/0001-6160(69)90073-X.
- [35] B. Million, J. Kučera, Concentration dependence of nickel diffusion in nickel-cobalt alloys, Czechoslov. J. Phys. 21 (1971) 161–171. https://doi.org/10.1007/BF01702804.
- [36] Y. Iijima, K. ichi Hirano, Interdiffusion in Co-Pd alloys, Trans Jap Inst Met. 13 (1972) 419–424. https://doi.org/10.2320/matertrans1960.13.419.
- [37] J. Levasseur, J. Philibert, Détermination des coefficients de diffusion intrinsèques par mesure de l'effet Kirkendall, Phys. Status Solidi. 21 (1967) K1–K4. https://doi.org/10.1002/pssb.19670210145.
- [38] Y. Iijima, K. Hirano, M. Kikuchi, Determination of intrinsic diffusion coefficients in a wide concentration range of a Cu-Ni couple by the multiple markers method, Trans. Japan Inst. Met. 23 (1982) 19–23. https://doi.org/10.2320/matertrans1960.23.19.
- [39] D.E. Thomas, C.E. Birchenall, Concentration Dependence of Diffusion Coefficients In Metallic Solid Solution, Jom. 4 (1952) 867–873. https://doi.org/10.1007/bf03398155.
- [40] T. Heumann, K.J. Grundhoff, Diffusion and Kirkendall Effect in the Cu-Ni System, Zeitschrift Für Met. 63 (1972) 173–180.
- [41] I.D. Marchukova, M.I. Miroshkina, Diffusion in the system copper-nickel, Phys. Met. Metallogr. 32 (1971) 1254–1259.
- [42] G. Brunel, G. Cizeron, P. Lacombe, Study of chemical diffusion in copper-nickel couples between 800 and 1060C by the Matano and Hall methods: varaiation of activation energy as a function of concentration, COMPTES RENDUS Hebd. DES SEANCES L Acad. DES Sci. Ser. C. 269 (1969) 895–898.
- [43] K.J. Anusavice, R.T. DeHoff, Diffusion of the tracers Cu67, Ni66, and Zn65 in copper-rich solid solutions in the system Cu-Ni-Zn, Metall. Trans. 3 (1972) 1279–1298. https://doi.org/10.1007/bf02642463.
- [44] K. Monma, H. Suto, H. Oikawa, Diffusion of Ni and Cu in nickel-copper alloys, J. Japan Institue Metall. 28 (1964) 192–196.
- [45] R. Damköhler, T. Heumann, Experimentelle Untersuchungen zur Klärung des Diffusionsverhaltens kupferreicher Kupfer–Nickel Legierungen, Phys. Status Solidi. 73 (1982) 117–127. https://doi.org/10.1002/pssa.2210730115.
- [46] B. Mishra, P. Kiruthika, A. Paul, Interdiffusion in the Cu-Pt system, J. Mater. Sci. Mater. Electron. 25 (2014) 1778–1782. https://doi.org/10.1007/s10854-014-1798-1.
- [47] R.D. Johnson, B.H. Faulkenberry, Diffusion Coefficients of Copper and Platinum into Copper Platinum Alloys, 1963.
- [48] O. Kubaschewski, H. Ebert, Diffusion measurements in gold and platinum alloys, Ztschr Elektrochem. 50 (1944) 138–144.
- [49] J. Levasseur, Philibert. J, Determination des coefficients de diffusion intrinseques par mesure de leffet kirkendall dans le systeme fer-nickel, COMPTES RENDUS Hebd. DES SEANCES L Acad. DES Sci. Ser. C. 264 (1967) 380.
- [50] B. Million, J. Růžičková, J. Velíšek, J. Vřešťál, Diffusion processes in the Fe-Ni system, Mater. Sci. Eng. 50 (1981) 43–52. https://doi.org/10.1016/0025-5416(81)90084-7.
- [51] V. Ganesan, V. Seetharaman, V.S. Raghunathan, Interdiffusion in the nickel-iron system, Mater. Lett. 2 (1984) 257–262. https://doi.org/10.1016/0167-577X(84)90125-3.
- [52] M.J.H. Van Dal, M.C.L.P. Pleumeekers, A.A. Kodentsov, F.J.J. Van Loo, Intrinsic diffusion and Kirkendall effect in Ni-Pd and Fe-Pd solid solutions, Acta Mater. 48 (2000) 385–396. https://doi.org/10.1016/S1359-6454(99)00375-4.
- [53] J.P. Gomez, C. Remy, D. Calais, Diffusion chimique et effet Kirkendall dans le systeme fer-palladium, Mem

- Sci Rev Met. 70 (1973) 597-605.
- [54] J. Fillon, D. Calais, Autodiffusion dans les alliages concentres fer-palladium, J. Phys. Chem. Solids. 38 (1977) 81–89. https://doi.org/10.1016/0022-3697(77)90150-0.
- [55] G. Xia, J.L. Hoyt, M. Canonico, Si-Ge interdiffusion in strained Si/strained SiGe heterostructures and implications for enhanced mobility metal-oxide-semiconductor field-effect transistors, J. Appl. Phys. 101 (2007). https://doi.org/10.1063/1.2430904.
- [56] M. Gavelle, E.M. Bazizi, E. Scheid, P.F. Fazzini, F. Cristiano, C. Armand, W. Lerch, S. Paul, Y. Campidelli, A. Halimaoui, Detailed investigation of Ge-Si interdiffusion in the full range of Si1-x Gex (0<x<1) composition, J. Appl. Phys. 104 (2008). https://doi.org/10.1063/1.3033378.
- [57] D.B. Aubertine, P.C. McIntyre, Influence of Ge concentration and compressive biaxial stress on interdiffusion in Si-rich SiGe alloy heterostructures, J. Appl. Phys. 97 (2005). https://doi.org/10.1063/1.1828240.
- [58] N. Ozguven, P.C. McIntyre, Silicon-germanium interdiffusion in high-germanium-content epitaxial heterostructures, Appl. Phys. Lett. 92 (2008) 1–4. https://doi.org/10.1063/1.2917798.
- [59] R. Kube, H. Bracht, J.L. Hansen, A.N. Larsen, E.E. Haller, S. Paul, W. Lerch, Composition dependence of Si and Ge diffusion in relaxed Si1-x Gex alloys, J. Appl. Phys. 107 (2010) 3–8. https://doi.org/10.1063/1.3380853.
- [60] A. Strohm, T. Voss, W. Frank, J. Räisänen, M. Dietrich, Self-diffusion of 71Ge in Si-Ge, Phys. B Condens. Matter. 308–310 (2001) 542–545. https://doi.org/10.1016/S0921-4526(01)00814-6.
- [61] A. Strohm, T. Voss, W. Frank, L. Pauli, J. Raisanen, Self-diffusion of 71Ge and 31Si in Si-Ge alloys, ZEITSCHRIFT FUR Met. 93 (2002) 737–744.
- [62] N.R. Zangenberg, J. Lundsgaard Hansen, J. Fage-Pedersen, A. Nylandsted Larsen, Ge Self-Diffusion in Epitaxial Si1-xGex Layers, Phys. Rev. Lett. 87 (2001) 2–5. https://doi.org/10.1103/PhysRevLett.87.125901.
- [63] P. Laitinen, A. Strohm, J. Huikari, A. Nieminen, T. Voss, C. Grodon, I. Riihimäki, M. Kummer, J. Äystö, P. Dendooven, J. Räisänen, W. Frank, Self-Diffusion of 31Si and 71Ge in Relaxed Si0.20Ge0.80 Layers, Phys. Rev. Lett. 89 (2002) 1–4. https://doi.org/10.1103/PhysRevLett.89.085902.
- [64] F. Roux, A. Vignes, Diffusion dans les systèmes Ti-Nb, Zr-Nb, V-Nb, Mo-Nb, W-Nb, Rev. Phys. Appliquée. 5 (1970) 393–405. https://doi.org/10.1051/rphysap:0197000503039300.
- [65] Y.E. Ugaste, Y.A. Zaykin, Investigation of mutual diffusion in titanium-vanadium and titanium-niobium systems, Phys. Met. Metallogr. 40 (1975) 567–575.
- [66] V.M. Polyanskii, B.N. Podgorskii, O.D. Makarovets, Diffusion processes in the Ti-Nb system, Svarochnoe Proizv. 3 (1971) 9–10.
- [67] V.I. Gryzunov, B.K. Aitbaev, G. Omasheva, T.I. Fryzunova, Interdiffusion in the titanium–niobium system, Seriya Khimicheskaya. 6 (1993) 29.
- [68] S.G. Fedotov, M.G. Chudinov, K.M. Konstantinov, Reciprocal diffusion in the systems Ti-V, Ti-Nb, Ti-Ta and Ti-Mo, Fiz. Met. Met. 27 (1969) 873–876.
- [69] L.L. Vergasova, D.A. Prokoshkin, E.V. Vasi, Concentrational and temperature correlation of interdiffusion coefficients in binary Nb alloys, Izv. Akad. Nauk. SSSR, Met. 4 (1970) 198–204.
- [70] Z. Chen, Z.K. Liu, J.C. Zhao, Experimental Determination of Impurity and Interdiffusion Coefficients in Seven Ti and Zr Binary Systems Using Diffusion Multiples, Metall. Mater. Trans. A Phys. Metall. Mater. Sci. 49 (2018) 3108–3116. https://doi.org/10.1007/s11661-018-4645-9.
- [71] L. Zhu, Q. Zhang, Z. Chen, C. Wei, G.M. Cai, L. Jiang, Z. Jin, J.-C. Zhao, Measurement of interdiffusion and impurity diffusion coefficients in the bcc phase of the Ti–X (X = Cr, Hf, Mo, Nb, V, Zr) binary systems using diffusion multiples, J. Mater. Sci. 52 (2017) 3255–3268. https://doi.org/10.1007/s10853-016-0614-0.
- [72] R.F. Peart, D. H. Tomlin, Diffusion of solute elements in beta-titanium, Acta Metall. 10 (1962) 123–134. https://doi.org/10.1016/0001-6160(62)90057-3.
- [73] G.B. Gibbs, D. Graham, D.H. Tomlin, Diffusion in titanium and titanium—niobium alloys, Philos. Mag. 8 (1963) 1269–1282. https://doi.org/10.1080/14786436308207292.
- [74] A.E. Pontau, D. Lazarus, Diffusion of titanium and niobium in bcc Ti-Nb alloys, Phys. Rev. B. 19 (1979) 4027–4037. https://doi.org/10.1103/PhysRevB.19.4027.
- [75] R.C. Geiss, C.S. Hartley, J.E. Steedly, Interdiffusion in niobium-vanadium alloys, J. Less-Common Met. 9 (1965) 309–320. https://doi.org/10.1016/0022-5088(65)90114-1.
- [76] A.P. Mokrov, V.M. Zharkov, No Title, Diffuzion Protsessy Met. 1 (1974) 39.
- [77] A.P. Babkin, E.M. Slyusarenko, S.F. Dunaev, Determination of mutual diffusion coefficients in Nb-V system using method of finite thickness interlayers, Vestn. Mosk. Univ. Seriya 2. Khimiya. 31 (1990) 361–364.

- [78] Y.E. Ugaste, E.M. Lazarev, V.N. Pimenov, Investigation of self-diffusion in the systems Nb-V, V-Pd, and Pb-Nb, Izv. Akad. Nauk. SSSR, Met. 2 (1971) 211–215.
- [79] R.V. Patil, G.B. Kale, S.P. Garg, Chemical diffusion in Zr-Nb system, J. Nucl. Mater. 223 (1995) 169–173.
- [80] E.A. Balakir, Y.P. Zotov, E.B. Malysheva, V.I. Panchishnyj, Investigation of mutual diffusion in the Zr-Nb system, Izv. Vyss. Uchebnykh Zaved. Tsvetnaya Metall. 4 (1975) 126–128.
- [81] S. Prasad, A. Paul, Interdiffusion in Nb-Mo, Nb-Ti and Nb-Zr systems, Defect Diffus. Forum. 323–325 (2012) 491–496. https://doi.org/10.4028/www.scientific.net/DDF.323-325.491.
- [82] C. Herzig, U. Köhler, S. V. Divinski, Tracer diffusion and mechanism of non-Arrhenius diffusion behavior of Zr and Nb in body-centered cubic Zr-Nb alloys, J. Appl. Phys. 85 (1999) 8119–8130. https://doi.org/10.1063/1.370650.
- [83] G.P. Tiwari, B.D. Sharma, V.S. Raghunathan, R. V. Patil, Self- and solute-diffusion in dilute zirconium-niobium alloys in β-phase, J. Nucl. Mater. 46 (1973) 35–40. https://doi.org/10.1016/0022-3115(73)90119-0.
- [84] H. Zou, G.M. Hood, R.J. Schultz, N. Matsuura, J.A. Roy, J.A. Jackman, Diffusion of Hf and Nb in Zr-19%Nb, J. Nucl. Mater. 230 (1996) 36–40. https://doi.org/10.1016/0022-3115(96)00024-4.
- [85] D. Ansel, I. Thibon, M. Boliveau, J. Debuigne, Interdiffusion in the body cubic centered β-phase of Ta-Ti alloys, Acta Mater. 46 (1998) 423–430. https://doi.org/10.1016/S1359-6454(97)00272-3.
- [86] P.T. Carlson, Interdiffusion and intrinsic diffusion in binary vanadium-titanium solid solutions at 1350°C, Metall. Trans. A. 7 (1976) 199–208. https://doi.org/10.1007/BF02644457.
- [87] G.B. Kale, S.K. Khera, G.P. Tiwari, Interdiffusion studies in titanium-vanadium system, Trans. Indian Inst. Met. 29 (1976) 422–425.
- [88] J.. Murdock, C.. McHargue, Self-diffusion in body-centered cubic titanium-vanadium alloys, Acta Metall. 16 (1968) 493–500. https://doi.org/10.1016/0001-6160(68)90123-5.
- [89] I. Thibon, D. Ansel, T. Gloriant, Interdiffusion in β-Ti-Zr binary alloys, J. Alloys Compd. 470 (2009) 127–133. https://doi.org/10.1016/j.jallcom.2008.02.082.
- [90] K. Bhanumurthy, A. Laik, G.B. Kale, Novel Method of Evaluation of Diffusion Coefficients in Ti-Zr System, Defect Diffus. Forum. 279 (2008) 53–62. https://doi.org/10.4028/www.scientific.net/ddf.279.53.
- [91] A. Brunsch, S. Steeb, Diffusionsuntersuchungen im System Ti-Zr mittels Mikrosonde, Zeitschrift Fur Naturforsch.Ung Sect. A J. Phys. Sci. 29 (1974) 1319–1324. https://doi.org/10.1515/zna-1974-0912.
- [92] V.S. Raghunathan, G.P. Tiwari, B.D. Sharma, Chemical diffusion in the β phase of the Zr-Ti alloy system, Metall. Mater. Trans. B. 3 (1972) 783–788. https://doi.org/10.1007/bf02647649.
- [93] C. Herzig, U. Köhler, M. Büscher, Temperature Dependence of <sup>44</sup>Ti and <sup>95</sup>Zr Diffusion and of <sup>88</sup>Zr/<sup>95</sup>Zr Isotope Effect in the Equiatomic BCC TiZr-Alloy, Defect Diffus. Forum. 95–98 (1993) 793–798. https://doi.org/10.4028/www.scientific.net/ddf.95-98.793.